Supramolecular coordination polymers in water: rings, chains and networks

Promotor
Prof. dr. E. J. R. Sudhölter, hoogleraar in de organische chemie,
Wageningen Universiteit

Co-promotor
Dr. A. T. M. Marcelis, universitair hoofd docent, Laboratorium voor Organische Chemie, Wageningen Universiteit

Promotiecommissie

Prof. dr E. W. Meijer	Technische Universiteit Eindhoven
Prof dr. ir. W. E. Hennink	Universiteit Utrecht
Dr. ir. N. A. M. Besseling	Wageningen Universiteit
Prof. dr. M. A. Cohen Stuart	Wageningen Universiteit

Tina Vermonden

Supramolecular coordination polymers in water: rings, chains and networks

Proefschrift
ter verkrijging van de graad van doctor
op gezag van de rector magnificus
van Wageningen Universiteit,
Prof. dr. ir. L. Speelman,
in het openbaar te verdedigen op
woensdag 30 maart 2005
des namiddags te vier uur in de Aula.

ISBN 90-8504-148-1

Contents

From supramolecular chemistry towards reversible coordination polymers **1**

1.1 Introduction **2**
1.2 From supramolecular chemistry towards (metallo) supramolecular polymers **3**
1.3 Strength of association between monomers in reversible polymers **7**
1.4 Ring-chain equilibrium in reversible polymers **10**
1.4.1 Concentration dependence 11
1.4.2 Temperature dependence 12
1.4.3 Dependence on the structure of the monomers 12
1.5 Viscoelasticity **14**
1.6 Aim and outline of this thesis **16**
1.7 References **18**

Water-soluble reversible coordination polymers: chains and rings **21**

2.1 Introduction **22**
2.2 Ring-chain equilibrium: model calculations **23**
2.2.1 Model 23
2.2.2 General trends 27
2.3 Experimental results and discussion **31**
2.3.1 Molar ratio dependence 32
2.3.2 Concentration dependence 35
2.3.3 Temperature dependence 40
2.3.4 Spacer length dependence 44
2.4 Concluding remarks **46**
2.5 Experimental section **46**
2.6 References **48**

Three-dimensional water-soluble reversible neodymium(III) and lanthanum(III) coordination polymers **51**

3.1 Introduction **52**
3.2 Results and discussion **53**
3.3 Conclusions **62**
3.4 Experimental section **63**
3.5 References **64**

Linear rheology of water-soluble reversible neodymium (III) coordination polymers **65**

4.1 Introduction **66**
4.1.1 Reversible coordination polymers 66
4.1.2 Linear rheology of equilibrium polymers 67
4.2 Results and discussion **69**
4.2.1 Concentration dependence 71
4.2.2 Temperature dependence 77
4.3 Concluding remarks **80**
4.4 Experimental section **80**
4.5 References **80**

Synthesis of 4-functionalized terdendate pyridine-based ligands **83**

5.1 Introduction **84**
5.2 Results and discussion **85**
5.3 Experimental section **88**
5.4 References **95**

Solvent effects on the reversibility of coordination polymers **97**

6.1 Introduction **98**

6.2 Results and discussion **99**

6.2.1 Viscosity measurements 100

6.2.2 NMR measurements 102

6.3 Concluding remarks **104**

6.4 Experimental section **105**

6.5 References **105**

Trifunctional ligands in coordination polymers **107**

7.1 Introduction **108**

7.2 Results and discussion **109**

7.3 Conclusions and recommendations **111**

7.4 Experimental section **112**

7.5 References **113**

Summary **115**

Samenvatting **118**

Dankwoord **122**

Curriculum vitae **125**

List of publications **126**

From supramolecular chemistry towards reversible coordination polymers

Chapter 1

1.1 Introduction

Inspired by nature, scientists are using non-covalent bonds between molecules more and more as a tool to construct large supramolecular systems. Extensive studies of biological systems led to a better understanding of intramolecular interactions and acknowledgment of their importance. A well-known example from nature is the hydrogen bonding between DNA strands that has inspired chemists for many decades now. Hydrogen bonding is of crucial importance for the functioning of biomolecules in biological systems, as seen for instance in DNA replication and in the structure and function of proteins. However, hydrogen bonding is not the only way to form non-covalent bonds. Another important interaction in biological systems is the metal ion-ligand interaction. A famous example from nature is the binding of oxygen by iron in hemoglobin, which is responsible for transport of oxygen in blood. Furthermore, many other metalloproteins are known that perform specific tasks, like electron transfer and oxidation catalysis. These and many more examples of non-covalent interactions from nature motivated chemists and led to the beginning of supramolecular chemistry about three decades ago. Supramolecular chemistry may be defined as 'chemistry beyond the molecule', bearing on the organized entities of higher complexity that result from the association of two or more chemical species held together by intermolecular forces. This is stated by one of the pioneers in this field: Jean-Marie Lehn. The goal of the field of supramolecular chemistry is to gain control over the intermolecular bond.[1]

The intermolecular bonds can originate from various interactions, which correspond to different degrees of strength, directionality, dependence on distances and angles: metal ion coordination, electrostatic forces, hydrogen bonding, Van der Waals interactions, π–π stacking, donor-acceptor interactions, etc. The metal ion coordination interactions range from strong to very strong, while single hydrogen bonds are much weaker interactions. Because all these intermolecular interactions are generally weaker than covalent bonds, they are kinetically more labile and dynamically more flexible. In the field of supramolecular chemistry the molecules should be designed, such that they find each other by molecular recognition. This process of spontaneous association is called self-assembly or self-organization.

In the beginning of the supramolecular chemistry era, most scientists tried to synthesize well-defined structures. In the last decade, they also try to create less defined aggregates, such as supramolecular polymers.[2] These structures have varying degrees of polymerization, with only an average chain length. The term "supramolecular polymers" is quite popular and is used for various systems in which supramolecular forces play a role. However, we use the definition posed by

Brunsveld et al.[3]: a supramolecular polymer is a polymer that is made of repeating units held together by only non-covalent bonds and the bonding within the chain should be significantly stronger than the interactions between chains.

Synthetic polymers are one of the most important inventions of the 20th century leading to numerous new materials. Their applications can be found in for example construction, electronic and biomedical fields. The many applications of conventional polymers only show that there can be many more applications when the field of polymers expands. By the introduction of supramolecular polymers, the field of polymer chemistry has become much broader. Polymer chemists are no longer restricted to macromolecules with repeating units linked by covalent bonds. When reversible intermolecular bonds replace covalent bonds between repeating units in a polymer, a supramolecular polymer is obtained. These kinds of polymers are expected to have some of the properties of covalently bound polymers, but also some new properties can be expected due to the reversibility of the bonds. How these new properties translate themselves into applications is hard to tell at this point, but they might be found in nature-mimicking applications, like self-healing or responsive materials.

The design of supramolecular polymers with reversible intermolecular bonds, which are strong enough to form long polymers, is a field of research that is recently emerging. Sijbesma et al. reported some mechanical properties of materials formed by hydrogen bonded reversible polymers that are strongly temperature dependent.[4-6] So, the first material properties of supramolecular polymers have been reported and the characterization of the material properties proceeds rapidly, possibly leading to applications in the near future.

1.2 From supramolecular chemistry towards (metallo) supramolecular polymers

The two main groups of supramolecular polymers nowadays are the hydrogen-bonded polymers and the coordination polymers. However, recently a few papers appeared describing soluble supramolecular polymers based on host-guest interactions using cyclodextrin or crown ethers as hosts.[7,8] A short overview of the history of hydrogen-bonded and coordination polymers will be given, starting with the hydrogen-bonded polymers.

Jean-Marie Lehn is the key person when supramolecular chemistry is involved. He published the first hydrogen-bonded supramolecular aggregates. Triple hydrogen bonds between 2,4,6-triaminopyrimidine and barbituric acid derivatives led to the formation of ordered supramolecular strands, when the compounds were mixed in a

1:1 ratio (see figure 1).[9] Not much later he published similar strands, but now build up from self-complementary molecules.[10]

Nowadays many groups work on self-assembled polymers based on multiple hydrogen bonds.[11-14] Also oligonucleotides as connecting groups between monomers are used, making DNA-resembling reversible polymers.[15-17] One of the most successful groups in this field is probably the group of Bert Meijer. They use self-complementary units that can bind to each other via quadrupole hydrogen bonds. Their most successful hydrogen-bonding moiety is the ureidopyrimidinone (Upy) group displayed in figure 2. This group forms quadrupole hydrogen bonds with a very high binding constant of $6 \cdot 10^7$ M^{-1} in chloroform. Using this group some molecules have been synthesized that self-assemble into polymers with rubber-like properties.[4,6]

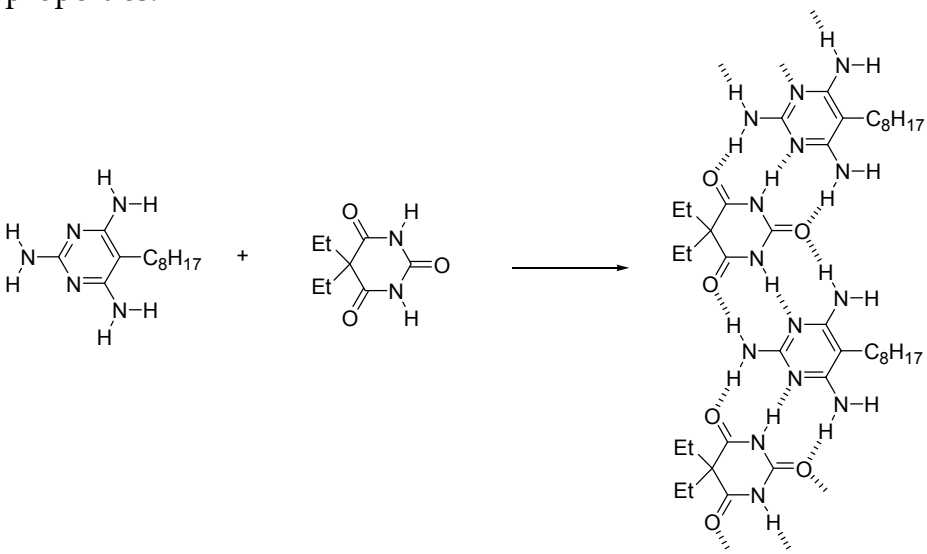

Figure 1: *Lehn's barbituric acid/2,4,6-triaminopyrimidine motif.*

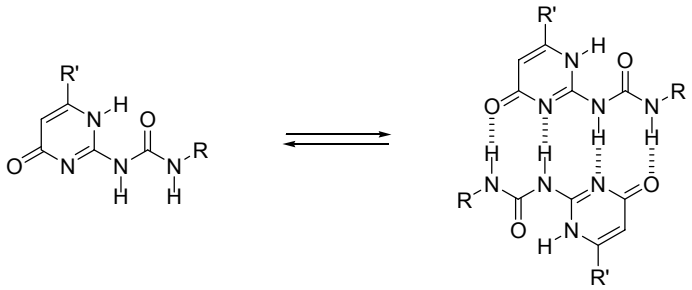

Figure 2: *Dimerization of ureidopyrimidinone for the use in hydrogen bonded polymers.*

Jean-Marie Lehn also made the first steps towards the synthesis of metallo-supramolecular polymers. In the early nineties, he reported the self-assembly of oligo-2,2′-bipyridines around Cu^+ and Ni^{2+} ions into helical strands.[18-20] Cu^+ ions have a tetrahedral complexation geometry and in combination with the oligobipyridines double-stranded helices are formed in an organic solvent (figure 3). When mixtures of oligobipyridines with different lengths are used, the system arranges itself to form

only helices with strands of the same length. Around the octahedrally coordinated Ni^{2+} ions triple stranded helices are formed. This system is very sophisticated because when mixtures of Cu^{+} and Ni^{2+} are used, the helices formed contain only either Cu^{+} or only Ni^{2+} ions. No mixture helices are formed, due to self-recognition of the system. Hence, the process of self-assembly involves the preferential binding of like metal ions by like ligand strands, indicating a subtlety that can be realized in supramolecular coordination chemistry.

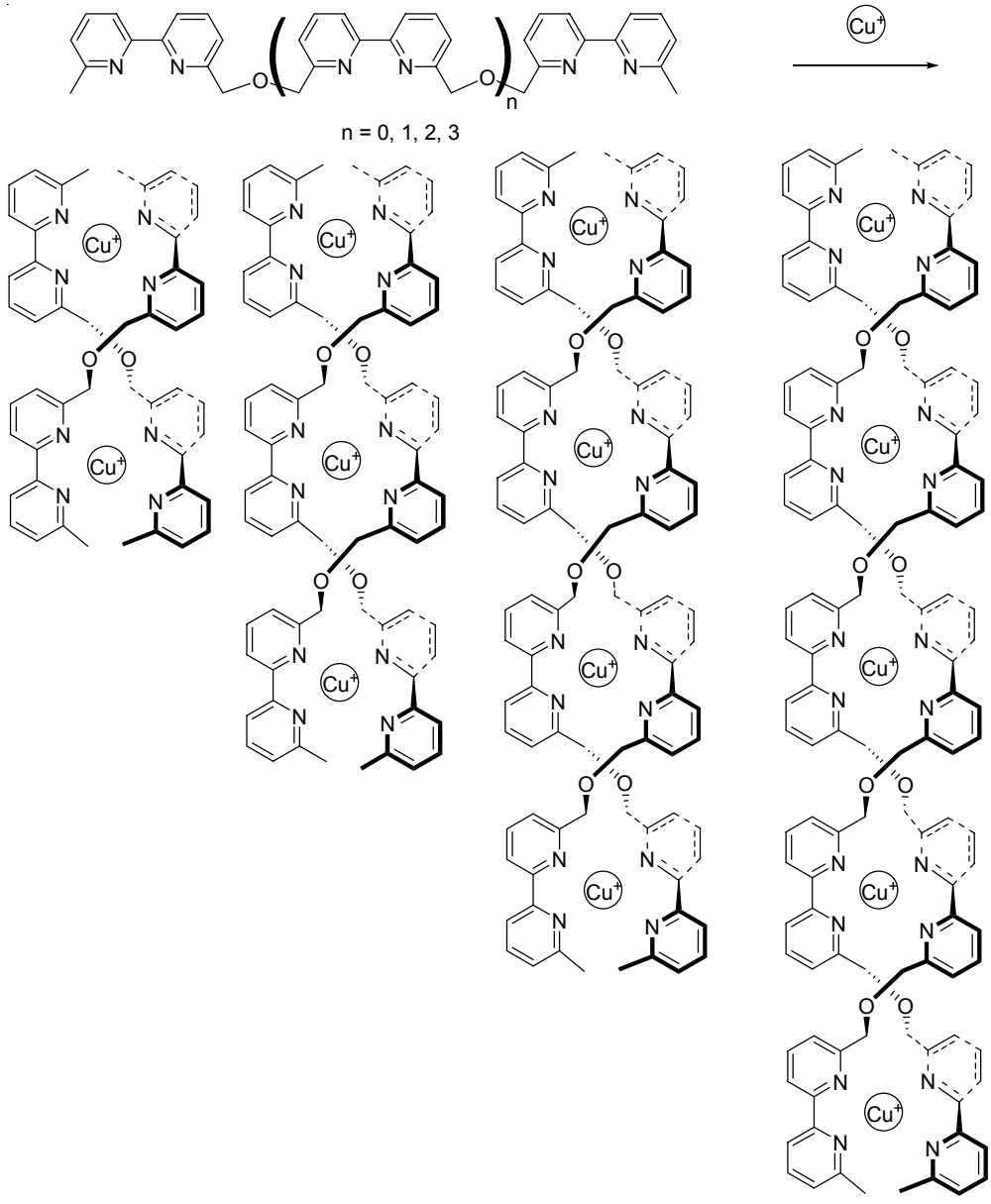

Figure 3: *Self-recognition in the self-assembly of double helicates from a mixture of oligobipyridine strands and Cu^{+} ions.*

Although the above-mentioned example shows the potential of metallo-supramolecular chemistry, no supramolecular coordination polymers are formed.

Rehahn is credited for studying the first soluble supramolecular polymers based on metal-ligand interactions.[21-23] His polymers are based on the coordination of derivatives of bipyridines with ruthenium(II) ions (figure 4). Although the polymers are soluble in a variety of solvents including water, the formation of the polymers is not reversible, since no ligand exchange could be detected.

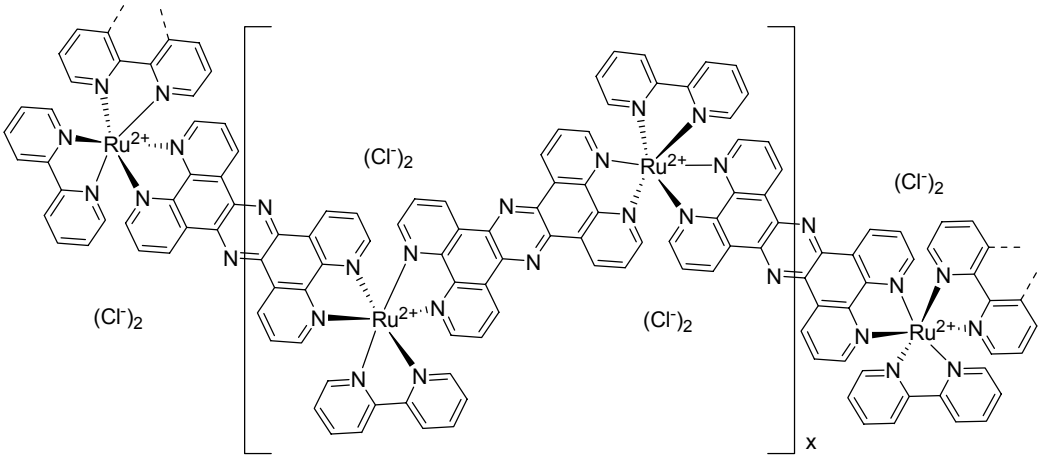

***Figure 4**: Rehahn's soluble ruthenium(II) coordination polymers.*

Not much later the possibilities of 2,2',6',2''-terpyridine ligands as complexing groups were recognized by several scientists.[24-27] In figure 5, an example of the formation of coordination polymers using terpyridines is given, which was investigated in the group of Schubert.[28] For the formation of supramolecular coordination polymers bipyridine and terpyridines are nowadays the most frequently used ligand groups. They have advantages like easy synthesis and strong complexing abilities to a broad range of metal ions.[29,30] Nevertheless, some other complexing groups such as for example porphyrins are known to be useful complexing groups for the formation of supramolecular coordination polymers.[31,32]

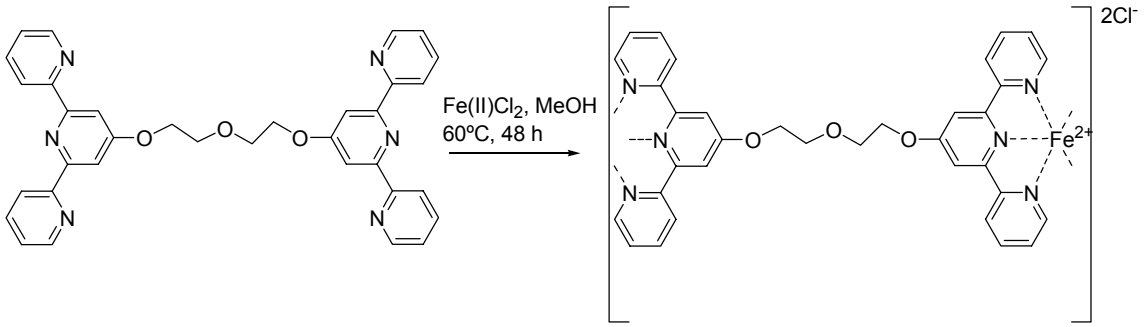

***Figure 5**: Schematic representation of polymer formation using bifunctional terpyridinemonomers.[28]*

Finally, some polymers[33] or polymer-like structures[34] have been reported in which both hydrogen bonds and coordination bonds are used in the main chain. The monomers in the polymers described by Schubert et al. are based on both an ureidopyrimidinone group and a terpyridine group (figure 6). The polymers are formed in chloroform, but at this moment the solubility of the polymers is a limiting factor in studying the properties of these polymers.[33]

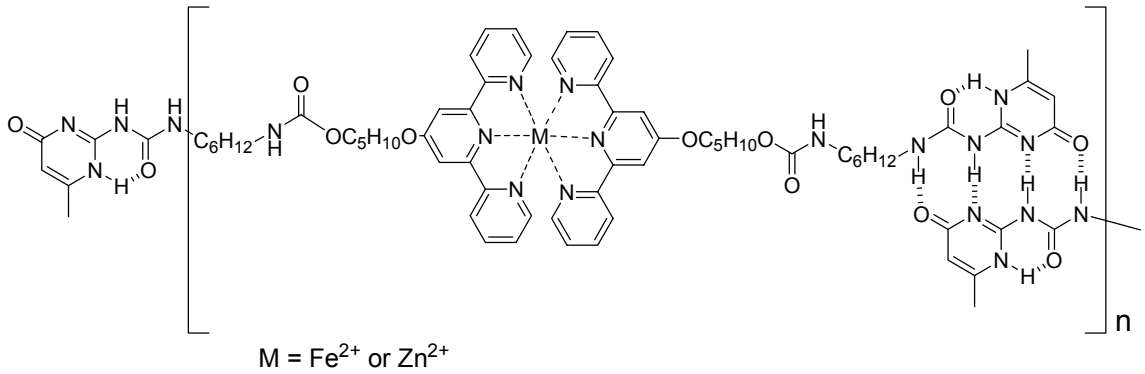

***Figure 6**: Hydrogen-bonded metallo-supramolecular polymer.*[33]

1.3 Strength of association between monomers in reversible polymers

The strength of the bonds between monomers in supramolecular polymers determines the average length of the polymers, and is therefore an important parameter. The solvent has a distinct influence on the strength of the interactions and thus the average chain length. For example, in hydrogen-bonded polymers the strength of the bonding is strong enough to form chains with a substantial length when multiple hydrogen bonds per monomer are used in a non-hydrogen bond forming organic solvent. However, when water or another polar solvent is added to the system, the solvent competes and breaks down the hydrogen bonds between the monomers and as a result the average chain length drops rapidly. So, the polarity and hydrogen bonding ability of an organic solvent influence the average chain length and therefore also the viscosity of the polymer solutions.[35,36] In the case of coordination polymers, the association between monomers and metal ions in water can be high enough to form reversible polymers. This also means that when coordination polymers are formed in an organic solvent without any water present, the bonds are not as reversible as in water and can even approach the strength of covalent bonds.[37,38] Recently, it was shown that metal-ligand bonds of coordination polymers in organic solvents can be broken by mechanical forces such as ultrasonication.[39] After ultrasonication the polymers reform to the former average chain length in 23 hours. Nevertheless, the ideal solvent to form fast-equilibrating

coordination polymers is water or another solvent that can coordinate metal ions like for example methanol.

Besides the solvent, the geometry of the monomers plays an important role in the strength of the binding.[36,40] In hydrogen bonded systems the strength of the interaction increases enormously when multiple hydrogen bonds per monomer are used instead of only one.[41] When the monomers can form only one hydrogen bond with another monomer, the strength is not nearly high enough to form polymers even at very high concentrations. The association constants go up to 10^7 M^{-1} for quadrupole hydrogen bonded monomers in an organic solvent like chloroform.[42] Association constants in the order of 10^5 - 10^7 M^{-1} are high enough to form reversible polymers.

The same analogue is found for the geometry of monomers and the complexation of metal ions. The more groups capable of binding to one metal ion, the stronger the interaction is. For coordination complexes this is called the chelate effect. When transition metal ions are used that can accommodate 6-coordination, the ideal binding group in a monomer has three binding sites for the metal ion. Such a ligand group is called a terdendate ligand group. To build coordination polymers, the monomers require two of those terdendate ligand groups. Further on, these monomers are also called bifunctional terdendate ligands.

The association constants between terdendate ligands and transition metal ions in water can be in the same order as quadrupole hydrogen bonds in an organic solvent. However, for the formation of coordination polymers actually two different complexation constants play a role. First one ligand group L, will form a complex with a metal ion M, and then the second ligand group will associate to the ML complex. The reactions and complexation constants (K) involved are:

$$M + L \rightleftharpoons LM \qquad K_1 = \frac{[LM]}{[M].[L]}$$

$$LM + L \rightleftharpoons L_2M \qquad K_2 = \frac{[L_2M]}{[LM].[L]}$$

The overall complexation constant β is equal to: $\beta = \frac{[L_2M]}{[L]^2.[M]}$

For example the binding constants of dipicolinic acid (figure 7) in water to different transition metal ions are given in table 1.[43]

***Table 1**: Complexation constants of dipicolinic acid and a few transition metal ions in water.*[43]

	log K_1	log K_2	log β
Ni^{2+}	6.95	6.55	13.50
Zn^{2+}	6.35	5.53	11.88
Cd^{2+}	6.75	4.40	11.15

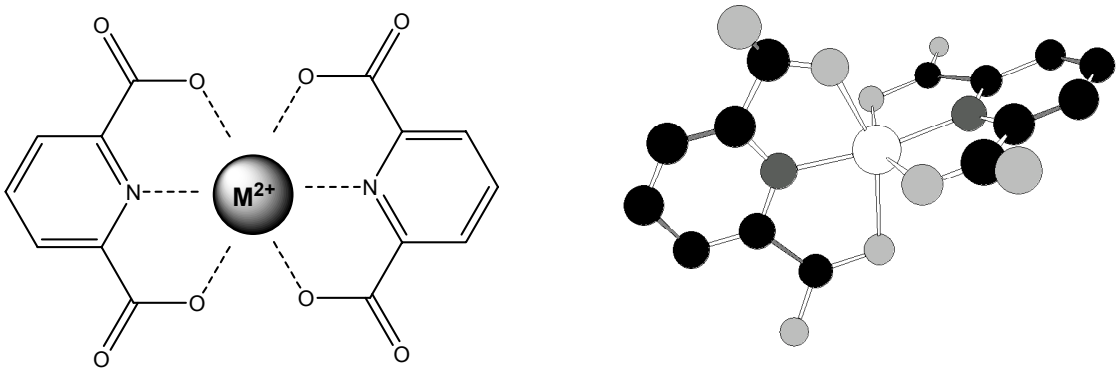

***Figure 7**: Two dipicolinic acid molecules complexed to a divalent transition metal ion, schematic and 3-D representation.*

The use of lanthanide ions instead of first row transition metal ions leads to a different stoichiometry of binding. Lanthanide ions are much larger than first row transition metal ions and some can accommodate 9-coordination. The charge of many lanthanide ions is 3+, but this is not the reason why they are capable of binding three terdendate ligands. The size of the ions is responsible for the additional binding place (figure 8). A third complexation reaction is involved with a third complexation constant:

$L_2M + L \rightleftharpoons L_3M$ $\qquad K_3 = \dfrac{[L_3M]}{[L_2M].[L]}$

And the overall complexation constant β is defined now as: $\beta = \dfrac{[L_3M]}{[L]^3.[M]}$

For the complexation of dipicolinic acid the complexation constants to a few lanthanide ions is given in table 2.[44]

***Table 2**: Complexation constants of dipicolinic acid and a few lanthanide ions in water.*[44]

	log K_1	log K_2	log K_3	log β
La^{3+}	7.98	5.81	4.27	18.06
Nd^{3+}	8.78	6.72	5.06	20.56
Eu^{3+}	8.84	7.14	5.51	21.49

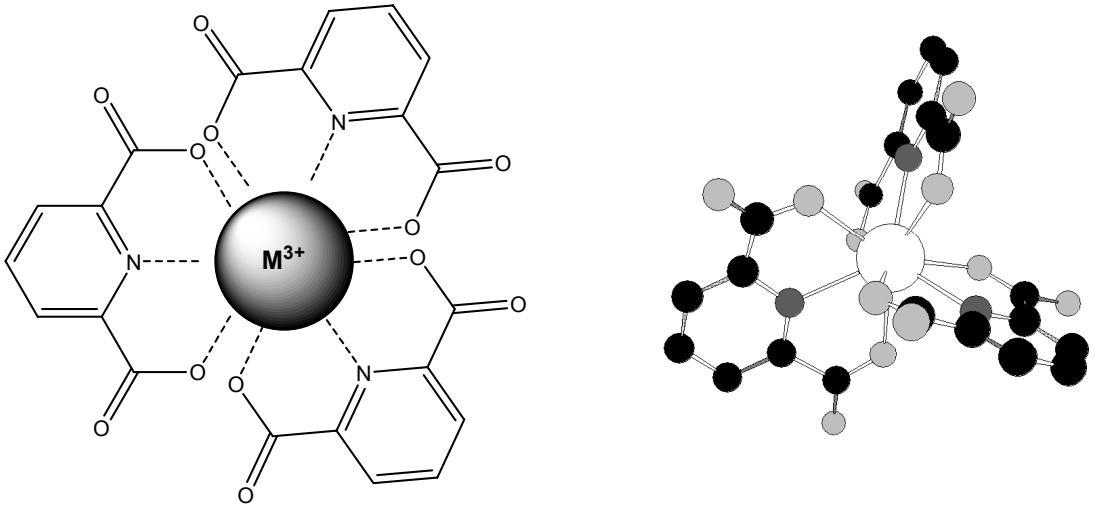

***Figure 8**: Three dipicolinic acid molecules bound to a trivalent lanthanide ion, schematic and 3-D representation.*

1.4 Ring-chain equilibrium in reversible polymers

Cyclization is a common side reaction in all polymerization reactions. The presence of rings besides linear chains influences the properties of polymer solutions and polymers in bulk. For covalently bonded polymers, it was even shown that the physical properties of large rings differ slightly from their linear analogues of the same length.[45] In the formation of reversible polymers the cyclization reaction can also not be prevented.[46,47] However, in reversible systems it is difficult to determine the exact contributions of rings and chains because most measuring techniques influence the equilibrium. Concentration dependent viscosity measurements can give information about the contribution of rings as will be described in the next paragraph. Another technique that can identify rings and chains separately, if they differ sufficiently in size, is diffusion ordered nuclear magnetic resonance spectroscopy (DOSY NMR).[48,49] This technique can identify molecular components of mixtures and simultaneously characterize the sizes of the structures. In a typical 2D DOSY spectrum the chemical shifts of the protons in the sample are plotted in one direction and the corresponding diffusion coefficients in the other direction. Since rings are usually much smaller than the chains, they will have much higher diffusion coefficients and can be detected separately.[50]

The equilibrium between rings and linear chains can be influenced by different factors. Up till now the ring-chain equilibrium in reversible polymers has been studied mainly for hydrogen-bonded polymers.[51] The general influence of concentration, temperature and structural changes on the ring-chain equilibrium will be discussed below.

1.4.1 Concentration dependence

One of the first theoretical studies of polymeric systems, which took in account the presence of rings, was done by Jacobsen and Stockmayer on polycondensation reactions.[52] They calculated the average molecular weights and amounts of ring and chain fractions as a function of concentration. Upon dilution the ring fraction increases due to decreasing probabilities to form a bond with another molecule. It is even possible to obtain a 100 percent fraction of rings beyond a critical dilution. This is called the critical concentration; below this concentration only rings exist and above this concentration the ring concentration remains constant while all additional molecules arrange in chains.[53,54] This definition for the critical concentration is only valid when the binding constant between the monomers becomes close to infinity.

Jacobson and Stockmayer also made predictions about the size of the rings and their relative amounts.[52] The larger the size of the rings, the smaller the fractions of these rings will be, because the probability of meeting of two ends becomes smaller with increasing length of the chain. According to Jacobson and Stockmayer the probability that a chain is in a ring conformation scales with an exponent of -5/2 with the polymerization degree. The consequence is that almost all rings are very small and large rings are only sporadically present.

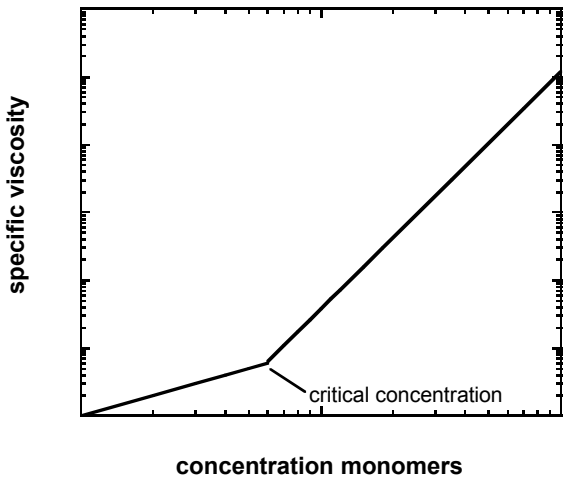

***Figure 9**: Specific viscosity as a function of concentration of monomers in a reversible polymer system that is able to form rings and linear chains.*

The critical concentration can be determined with viscosity measurements, since the molecular weight of the structures that are present influences the viscosity of the solution. The average size of rings is barely dependent on the concentration and therefore their effect on the viscosity is proportional to the concentration. For linear chains the molecular weight increases upon increasing concentration yielding a

steeper slope than for rings when viscosity is plotted against concentration. In reversible polymers the length of the chains depends on the concentration and Cates et al. predicted the increase in viscosity as a function of concentration for these kinds of polymers. The viscosity for flexible reversible polymers and worm-like micelles should increase with concentration with an exponent of approximately 3.5 above the overlap concentration.[55,56] When the viscosity of a solution of reversible polymers is measured as a function of concentration, this will lead to two regimes.[57,58] Below the critical concentration the slope of the curve will be approximately one due to the contribution of only the rings. Above the critical concentration the slope will go up to about 3.5 due to the contribution of the linear chains as shown in figure 9.

1.4.2 Temperature dependence

Temperature is also known to have an effect on the viscosity of polymer solutions. The viscosity decreases with increasing temperature due to the increased mobility of the molecules. Only very few exceptions are reported and they all belong to entropy driven ring-opening polymerization reactions[59,60], while most polymerization reactions are enthalpy driven. For reversible polymers however, the viscosity can increase with increasing temperature as well.[50] This is only the case when the solution consists of a considerable fraction of rings (and therefore not at high concentrations where the fraction of rings is small compared to the chain fraction). A higher temperature leads to a decrease of the binding constant. This means that the chains and rings break more easily than at lower temperature. Since chains always have two chain ends and rings do not, rings are favored over chains. The higher the binding constants, the stronger this effect will be. When the binding constant decreases due to an increase of temperature, ring opening will become more favorable. In this way an increase in viscosity can be found. However, after a certain increment of the temperature, the viscosity will go down again, because the chain breaking becomes the dominant process, which cannot be compensated anymore by ring opening.

1.4.3 Dependence on the structure of the monomers

Introducing small changes in the structure of the monomers can also influence the ring-chain equilibrium in reversible polymers. Because most researchers are interested in polymer properties, they try to prevent the ring formation as much as possible. However, to gain more insight in the ring-chain equilibrium in hydrogen-bonded polymers Ten Cate et al. looked at the effect of small changes in the structure of the monomers. Introducing only one or more methyl groups into the spacer of the

bifunctional monomers influences the preferred conformation of the molecules and as a result favors the equilibrium towards the formation of rings.[58]

Another way to influence the ring-chain equilibrium by small structural changes was done in the group of Bouteiller.[46] They compared monomers that differ in spacer length and their influence on the formation of hydrogen-bonded polymers in organic solvents. The cyclic content increases with decreasing length of the monomers, due to a higher probability for ring closure. However, after a certain reduction of the length of the monomer spacer the amount of rings will decrease because of the higher strain in the cyclic monomers. Consequently, the flexibility of the spacer also influences the amount of rings that will be formed.[32]

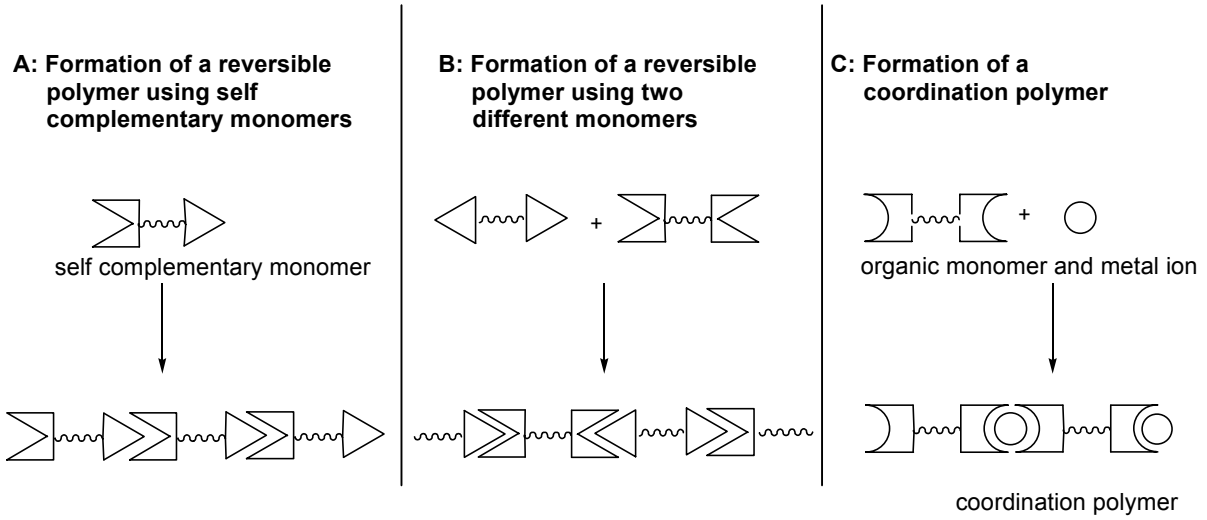

***Figure 10**: Schematic representation of the formation of reversible polymers builds up from self-complementary monomers (A) from two different kinds of monomers (B) and formation of coordination polymers (C).*

Some reported reversible polymers are not self-complementary. So, in that case two different kinds of monomers are present, which can form reversible bonds with each other (figure 10). For coordination polymers this is always the case, because organic monomers and metal ions are needed to build up the polymers.[28,61-64] In order to obtain long polymers in these systems, the molar ratio between the two species is very important. When either one kind of monomers is present in excess, the polymers cannot become very long, due to the formation of chain ends.[65-67] However, the molar ratio also influences the formation of rings.[61,68-70] The closer the molar ratio approaches unity, the larger the ring fraction will be.

1.5 Viscoelasticity

Materials can be classified in three categories: viscous, elastic and viscoelastic. In which category a material belongs depends on the time you are prepared to make observations. Consider for example glass, which is a solid when the observation time is an hour, a week or even months. However, in very old churches some flow in glass of windows can be observed under the influence of gravity. The glass has become thicker at the bottom and thinner at the top of the windows over the years. On the other hand, when a liquid such as water is subjected to short timescale ultrasonic pulses it displays elastic behavior. When a material displays both elastic and viscous behavior within the experimental time it is classified as viscoelastic. Many polymer solutions exhibit viscoelastic properties.[71] The first rheological properties of polymers containing reversible hydrogen bonds were described in the early nineties.[72,73] Nevertheless, most rheological properties of reversible polymers are studied in bulk and not in solution.[74-76]

In dynamical experiments linear and non-linear viscoelasticity can be distinguished. The material behaves only linearly when the applied strains (γ) or stresses (σ) are small. It means that when the applied stress is doubled the resulting strain will also double. Since many materials behave similar upon applied strains or stresses, even when they have totally different molecular structures, a few models have been developed to describe the dynamical properties. The simplest model that often can be used for polymer solutions is the Maxwell model. A mechanical analogue used to represent the viscoelastic properties in the Maxwell model is displayed in figure 11 and consists of a spring and a dashpot in series. The spring represents the elastic component because the force is linearly related to the displacement. The dashpot consists of a cup filled with a Newtonian fluid with viscosity η, with a piston placed in the fluid. The dashpot represents the viscous component of the material.[77]

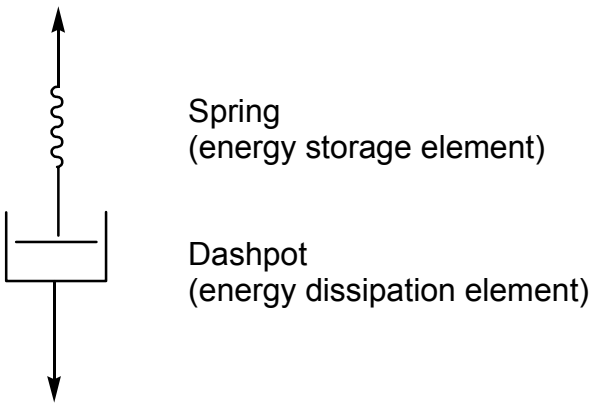

***Figure 11**: The Maxwell element.*

To show a few properties of materials that display Maxwellian behavior one can envisage a simple experiment in which a small strain is applied and then maintained at constant level. If the material behaves according to the Maxwell model, the stress will follow the strain to a maximum value and then reduces with time due to the dissipation of energy of the viscous element (dashpot). The time required for the stress to reduce to 1/e of the initial value is called the relaxation time, τ, of the material.

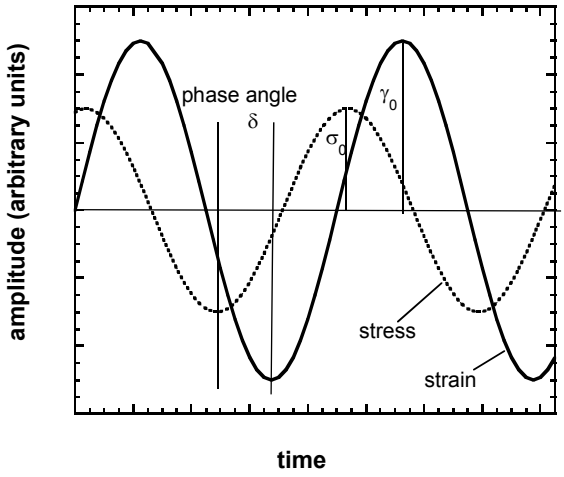

***Figure 12**: Stress response of a viscoelastic material to an oscillating strain.*

In many rheological experiments the response of viscoelastic materials to an oscillating stress or strain is measured. The sample is usually placed in a cone and plate geometry and an oscillating strain at a given radial frequency (ω) is applied. The stress responds to the applied strain and oscillates also with time. The oscillating strain and stress will be out of phase with a phase angle δ. When an elastic solid is placed between the cone and plate, the applied strain will result in a stress in the sample directly. The oscillating stress is in phase with the oscillating strain and δ will be zero. When however, a Newtonian fluid is measured, the stress in the sample will be out of phase by $\pi/2$, because the peak stress is proportional to the rate of strain. So for a viscoelastic material the oscillating stress will be out of phase with the oscillating strain, since the elastic component is in phase and the viscous component is out of phase (figure 12). To characterize a viscoelastic material also the ratio between the amplitudes of the maximum stress (σ_0) and the maximum strain (γ_0) as a function of the frequency (ω) is important. This ratio is called the complex modulus (G^*). Both the values for G^* and δ characterize the viscoelastic material. The complex modulus G^* can be separated in a real component and an imaginary component:

$$G^*(\omega) = \frac{\sigma_0}{\gamma_0} = G'(\omega) + iG''(\omega) \quad (1)$$

$G'(\omega)$ is the storage modulus, a measure for the elastic response and equals $(\sigma_0/\gamma_0)\cos\delta$. $G''(\omega)$ is the loss modulus, which is a measure for the viscous response and equals $(\sigma_0/\gamma_0)\sin\delta$. In the Maxwell model tan δ equals $1/\omega\tau$. If a viscoelastic material displays Maxwell behavior $G'(\omega)$ and $G''(\omega)$ are defined as:

$$G'(\omega) = \frac{G_0(\omega\tau)^2}{1+(\omega\tau)^2} \quad (2)$$

$$G''(\omega) = \frac{G_0\omega\tau}{1+(\omega\tau)^2} \quad (3)$$

G_0 is the plateau modulus and corresponds to the high frequency plateau of G' (see figure 13).

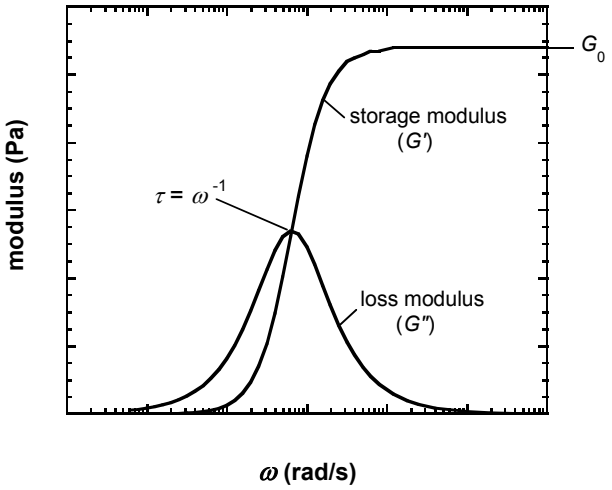

***Figure 13**: G′ and G″ as a function of the angular frequency (ω) according to the Maxwell model.*

1.6 Aim and outline of this thesis

The aim of the research described in this thesis is to prepare and characterize bifunctional ligands with the intention of gaining understanding about the properties of self-assembled coordination polymers in solution. In order to obtain water-soluble coordination polymers the bifunctional ligands should also be very well water-soluble. Water as a solvent has its obvious advantages with respect to applications in medical purposes and of course it is more environmental friendly than any organic solvent. Water also enhances the reversibility of the coordination bonds, since it can coordinate metal ions. Therefore, high complexation constants

between the metal ions and ligands are necessary in water to obtain polymers with a sufficient average chain length. Some organic solvents can also coordinate to metal ions, like for example methanol, ethanol and acetonitrile. In those solvents the coordination bonds can still be reversible. Upon going to organic solvents like chloroform and hexane, the reversibility of the bonds decreases considerably. In this thesis mainly water-soluble systems are described, but also one example of a coordination polymer in an organic solvent will be discussed.

In *chapter 2*, we describe the formation of water-soluble coordination polymers using Zn^{2+} ions and two bifunctional ligand molecules differing in spacer length. The influence of the spacer length on the equilibrium between ring and chain formation is studied using concentration en temperature dependent viscosity measurements. ^{1}H NMR and DOSY NMR are used to gain information on the relative amounts of rings and chains. To explain the experimental results a theoretical model is developed that confirms the relation between the flexibility and length of the spacer and the relative amount of rings and chains in solution.

In *chapter 3*, lanthanide metal ions are used with the same bifunctional ligands in water. Nd^{3+} and La^{3+} are metal ions that belong to the lanthanides and they are larger than the more common metal ions like Zn^{2+}, Ni^{2+} or Fe^{3+}. Due to the larger size they can bind three terdendate ligand groups instead of two. The binding of a third ligand group to the metal ions leads to the formation of cross-links besides linear chains and rings. The relative contributions of chains, rings and cross-links are investigated by measuring the viscosity of the polymer solutions as a function of concentration and molar ratio. Because ring-like structures give separate signals in ^{1}H NMR spectra, this technique is used to show the ring formation as a function of concentration and molar ratio. La^{3+} ions were used for these measurements, since Nd^{3+} ions broaden the peaks in the NMR spectra too much.

In *chapter 4* again neodymium ions are used in combination with water-soluble bifunctional ligands, but now at much higher concentrations. The solutions become visco-elastic at high concentration and the rheological behavior of the coordination polymers is studied. The concentration dependence of the linear rheological properties is compared to a theoretical model developed by Cates.[55,78] Temperature dependent measurements are performed to gain insight into the relaxation of the polymer chains and the activation energy related to this relaxation. Also visco-elastic properties of gels with a mixture of Zn^{2+} and Nd^{3+} and bifunctional ligands are investigated.

In *chapter 5*, the syntheses of four different types of mono and bifunctional ligands are described. All the chelating groups are based on pyridine moieties and they differ in the groups at the 2 and 6 positions of the pyridine. These groups are

aminomethyl, oxazolinyl, pyrazolyl and methylimidazolyl. Only the ligands with the aminomethyl groups are water-soluble. The other ligands only dissolve in organic solvents.

In *chapter 6*, the solvent effect on the complexation behavior of the aminomethyl and the methylimidazolyl ligands is studied using viscosity and ^{1}H NMR measurements. The aminomethyl ligands are studied with Zn^{2+} ions in water, while the methylimidazolyl ligands are studied with Zn^{2+} ions in a mixture of chloroform and acetonitrile (1:1).

In *chapter 7*, the syntheses of two trifunctional ligands are described. The influence on the solution viscosity of addition of these cross-linkers to bifunctional ligands and Zn^{2+} ions is studied.

1.7 References

1. Lehn, J.-M. *Supramolecular Chemistry, Concepts and Perspectives*,VCH Weinheim, **1995**.
2. Ciferri, A. *Supramolecular Polymers*, Marcel Dekker, New York, **2000**.
3. Brunsveld, L.; Folmer, B. J. B.; Meijer, E. W. *MRS Bulletin* **2000,** 49-53.
4. Folmer, B. J. B.; Sijbesma, R. P.; Versteegen, R. M.; Van der Rijt, J. A. J.; Meijer, E. W. *Adv. Mater.* **2000**, 874-878.
5. Brunsveld, L.; Folmer, B. J. B.; Meijer, E. W.; Sijbesma, R. P. *Chem. Rev.* **2001,** *101*, 4071-4097.
6. Keijzer, H. M.; Van Kessel, R.; Sijbesma, R. P.; Meijer, E. W. *Polymer* **2003**, *44*, 5505-5511.
7. Miyauchi, M.; Harada, A. *J. Am. Chem. Soc.* **2004**, *126*, 11418-11419.
8. Huang, F.; Gibson, H. W. *J. Am. Chem. Soc.* **2004**, *126*, 14738-14739..
9. Lehn, J.-M.; Mascal, M.; DeCian, A.; Fischer, J. *J. Chem. Soc., Chem. Commun.* **1990**, 479-481.
10. Lehn, J.-M.; Mascal, M.; DeCian, A.; Fischer, J. *J. Chem. Soc., Perkin Trans 2* **1992**, 461-467.
11. Castellano, R. K.; Rudvevich, D. M.; Rebek Jr., J. *Proc. Natl. Acad. Sci. USA* **1997**, *94*, 7132-7137.
12. Aggeli, A.; Bell, M.; Boden, N.; Keen, J. N.; Knowles, P. F.; McLeish, T. C. B.; Pitkeathly, M.; Radford, S. E. *Nature* **1997**, *386*, 259-262.
13. Shikata, T.; Ogata, D.; Hanabusa, K. *J. Phys. Chem. B* **2004**, *108*, 508-514.
14. Bong, D. T.; Clark, T. D.; Granja, J. R.; Ghadiri, M. R. *Angew. Chem. Int. Ed.* **2001**, *40*, 988-1011.
15. Fogleman, E. A.; Yount, W. C.; Xu, J.; Craig, S. L. *Angew. Chem. Int. Ed.* **2002**, *41*, 4026-4028.
16. Xu, J.; Fogleman, E. A.; Craig, S. L. *Macromolecules* **2004**, *37*, 1863-1870.
17. Kersey, F. R.; Lee, G.; Marszalek, P.; Craig, S. L. *J. Am. Chem. Soc.* **2004**, *126*, 3038-3039.

18. Lehn, J.-M.; Rigault, A.; Siegel, J.; Harrowfield, J.; Chevrier, B.; Moras, D. *Proc. Natl. Acad. Sci. USA* **1987**, *84*, 2565-2569.
19. Pfeil, A.; Lehn, J.-M. *J. Chem. Soc., Chem. Commun.* **1992**, 838-840.
20. Krämer, K.; Lehn, J.-M.; Marquis-Rigault, A. *Proc. Natl. Acad. Sci. USA* **1993**, *90*, 5394-5398.
21. Knapp, R.; Schott, A.; Rehahn, M. *Macromolecules* **1996**, *29*, 478-480.
22. Kelch, S.; Rehahn, M. *Macromolecules* **1997**, *30*, 6185-6193.
23. Kelch, S.; Rehahn, M. *Macromolecules* **1998**, *31*, 4102-4106.
24. Kelch, S.; Rehahn, M. *Macromolecules* **1999**, *32*, 5818-5828.
25. Schubert, U. S.; Eschbaumer, C. *Angew. Chem. Int. Ed.* **2002**, *41*, 2892-2926.
26. Schütte, M.; Kurth, D. G.; Linford, M. R.; Cölfen, H.; Möhwald H. *Angew. Chem. Int. Ed.* **1998,** *37*, 2891-2893.
27. Lehmann, P.; Kurth, D. G.; Brezesinski, G.; Symietz, C. *Chem. Eur. J.* **2001**, *7*, 1646-1651.
28. Schmatloch, S.; Fernández González, M.; Schubert, U. S. *Macromol. Rapid. Commun.* **2002**, *23*, 957-961.
29. Constable, E. C. *Macromol. Symp.* **1995**, *98*, 503-5024.
30. Swiegers, G. F.; Malefetse, T. J. *Chem. Rev.* **2000**, *100*, 3483-3537.
31. Michelsen, U.; Hunter, C. A. *Angew. Chem. Int. Ed.* **2000**, *39*, 764-767.
32. Twyman, L. J.; King, A. S. H. *Chem. Commun.* **2002**, 910-911.
33. Hofmeier, H.; El-ghayoury, A.; Schenning, A. P. H. J.; Schubert, U. S. *Chem. Commun.* **2004**, 318-319.
34. Choi, J. S.; Kang, C. W.; Jung, K.; Yang, J. W.; Kim, Y.-G.; Han, H. *J. Am. Chem. Soc.* **2004**, *126*, 8606-8607.
35. Castellano, R. K.; Clark, R.; Craig, S. L.; Nuckolls, C.; Rebek Jr., J. *Proc. Natl. Acad. Sci. USA* **2000**, *97*, 12418-12421.
36. Simic, V.; Bouteiller, L.; Jalabert, M. *J. Am. Chem. Soc.* **2003**, *125*, 13148-13154.
37. Lahn, B.; Rehahn, M. *e-Polymers* **2002**, *1*, 1-33.
38. Velten, U.; Rehahn, M. *Chem. Commun.* **1996**, 2639-2640.
39. Paulusse, J. M. J.; Sijbesma, R. P. *Angew. Chem. Int. Ed.* **2004**, *43*, 4460-4462.
40. Yount, W. C.; Juwarker, H.; Craig, S. L. *J. Am. Chem. Soc.* **2003**, *125*, 15302-15303.
41. Söntjens, S. H. M.; Sijbesma, R. P.; Van Genderen, M. H. P.; Meijer, E. W. *J. Am Chem. Soc.* **2000**, *122*, 7487-7493.
42. Bosman, A. W.; Brunsveld, L.; Folmer, B. J. B.; Sijbesma, R. P.; Meijer, E. W. *Macromol. Symp.* **2003**, *201*, 143-154.
43. Anderegg, G. *Helv. Chim. Acta* **1960**, *43*, 414-424.
44. Grenthe, I. *J. Am. Chem. Soc.* **1961**, *83*, 360-364.
45. Bielawski, C. W.; Benitez, D.; Grubbs, R. H. *Science* **2002**, *297*, 2041-2044.
46. Abed, S.; Boileau, S.; Bouteiller, L. *Macromolecules* **2000**, *33*, 8479-8487.
47. Gibson, H. W.; Yamaguchi, N.; Jones, J. W. *J. Am. Chem. Soc.* **2003**, *125*, 3522-3533.
48. Johnson Jr., C. S. *Prog. Nucl. Magn. Spectrosc.* **1999**, *34*, 203-256.
49. Morris, K. F.; Johnson Jr., C. S. *J. Am. Chem. Soc.* **1992**, *114*, 3139-3141.
50. Folmer, B. J. B.; Sijbesma, R. P.; Meijer, E. W. *J. Am. Chem. Soc.* **2001**, *123*, 2093-2094.

51. Sijbesma, R. P.; Beijer, F. H.; Brunsveld, L.; Folmer, B. J. B.; Hirschberg, J. H. K. K.; Lange, R. F. M.; Lowe, J. K. L.; Meijer, E. W. *Science* **1997**, *278*, 1601-1604.
52. Jacobson, H.; Stockmayer, W. H. *J. Chem. Phys.* **1950**,) *18*, 1600-1606.
53. Ercolani, G.; Luigi, M.; Mencarelli, P.; Roelens, S. *J. Am. Chem. Soc.* **1993**, *115*, 3901-3908.
54. Paulusse, J. M. J; Sijbesma, R. P. *Chem. Commun*. **2003**, 1494-1495.
55. Cates, M. E.; Candau, S. J. *J. Phys. Condens. Matter* **1990**, *2*, 6869-6892.
56. Turner, M. S.; Marques, C.; Cates, M. E. *Langmuir* **1993**, *9*, 695-701.
57. Ten Cate, A. T.; Sijbesma, R. P. *Macromol. Rapid Commun.* **2002**, *23*, 1094-1112.
58. Ten Cate, A. T.; Kooijman, H.; Spek, A. L.; Sijbesma, R. P.; Meijer, E. W. *J. Am. Chem. Soc.* **2004**, *126*, 3801-3808.
59. Greer, S. C. *J. Phys. Chem. B* **1998**, *102*, 5413-5422.
60. Tobolsky, A. V.; Eisenberg, A. *J. Am. Chem. Soc.* **1959**, *81*, 780-782.
61. Van der Gucht, J.; Besseling, N. A. M.; Van Leeuwen, H. P. *J. Phys. Chem. B* **2004**, *108*, 2531-2539.
62. Kimura, M.; Horai, T.; Muto, T.; Hanabusa, K.; Shirai, H. *Chem. Lett.* **1999**, 1129-1130.
63. Kimura, M.; Sano, M.; Muto, T.; Hanabusa, K.; Shirai, H. *Macromolecules* **1999**, *32*, 7951-7953.
64. Zapata, L.; Bathany, K.; Schmitter, J.-M.; Moreau, S. *Eur. J. Org. Chem.* **2003**, 1022-1028.
65. Velten, U.; Lahn, B.; Rehahn, M. *Macromol. Chem. Phys.* **1997**, *198*, 2789-2816.
66. Swiegers, G. F.; Malefetse, T. J. *Chem. Rev.* **2000**, *100*, 3483-3537.
67. Fogleman, E. A.; Yount, W. C.; Xu, J.; Craig, S. L. *Angew. Chem. Int. Ed.* **2002**, *41*, 4026-4028.
68. Choi, J. S.; Kang, C. W.; Jung, K.; Yang, J. W.; Kim, Y.-G.; Han, H. *J. Am. Chem. Soc.* **2004**, *126*, 8606-8607.
69. Chen, C.-C.; Dormidontova, E. E. *Polymer Preprints* **2004**, *45*, 391-392.
70. Chen, C.-C.; Dormidontova, E. E. *J. Am. Chem. Soc.* **2004**, *126*, 14972-14978.
71. Ferry, J. D. *Viscoelastic Properties of Polymers*, third edition, Wiley, New York, **1980**.
72. Hilger, C.; Stadler, R.; De Lucca Freitas, L. *Polymer* **1990**, *31*, 818-823.
73. Hilger, C.; Stadler, R. *Makromol. Chem.* **1990**, *191*, 1347-1361.
74. Hirschberg, J. H. K. K.; Beijer, F. H.; Van Aert, H. A.; Magusin, P. C. M. M.; Sijbesma, R. P.; Meijer, E. W. *Macromolecules* **1999**, *32*, 2696-2705.
75. Wübbenhorst, M.; Van Turnhout, J.; Folmer, J. B. J.; Sijbesma, R. P.; Meijer, E. W. *IEEE Trans. Dielectr. Electr. Insul.* **2001**, *8*, 365-372.
76. Bosman, A. W.; Sijbesma, R. P.; Meijer, E. W. *Materials Today* **2004**, *7*, 34-39.
77. Goodwin, J. W.; Hughes, R.W. *Rheology for Chemists, An Introduction*, The Royal Society of Chemistry, Cambridge, **2000**.
78. Cates, M. E. *Macromolecules* **1987**, *20*, 2289-2296.

Water-soluble reversible coordination polymers: chains and rings

Chapter 2

The formation of soluble reversible coordination polymers with Zn^{2+} ions in aqueous solution was studied for four bifunctional ligands, differing in spacer length. Viscosity measurements were used to follow the formation of polymers as a function of the ratio between metal ions and ligands, the total ligand concentration, and the temperature. All the experimental findings could be reproduced and interpreted with a theoretical model that accounts for the formation of chains and rings. At low concentrations and at a 1:1 metal to ligand ratio, a large fraction of the ligand monomers is incorporated in small rings, with a small contribution to the viscosity. Rings are less important at higher concentrations, or if one of the two components is in excess. The fraction of monomers in chains and rings could be estimated from ^1H NMR measurements, which were in good agreement with the model predictions. With increasing temperature, the fraction of monomers in rings decreases. As a result, the reduced viscosity increases with increasing temperature.

This chapter was published in slightly modified form: Vermonden, T.; Van der Gucht, J.; De Waard, P.; Marcelis, A. T. M.; Besseling, N. A. M.; Sudhölter, E. J. R.; Fleer, G. J.; Cohen Stuart, M. A. *Macromolecules* **2003**, 7035-7044.

2.1 Introduction

In recent years there has been an enormous progress in the field of supramolecular chemistry.[1,2] One of the most interesting developments is the design of supramolecular equilibrium polymers. These are linear chains of small molecules held together by non-covalent, reversible interactions.[3-6] They reproduce many of the properties of traditional polymers but introduce also distinctly new features. For example, their molar mass distribution is not fixed but responds to variable conditions such as the monomer concentration, the temperature, and the presence of external fields, such as shear. An important class of supramolecular polymers is that of so-called coordination polymers.[7-15] In a coordination polymer the bonds between monomers are based on metal-ligand interactions. The associating molecules each have two ligand groups (*L*) that can form 1:2 complexes (ML_2) with metal ions (*M*). Addition of metal ions to a solution of these bifunctional monomers results in the formation of polymers as depicted schematically in scheme 1. There is extensive literature about coordination polymers in the solid state, but the number of coordination polymers that has been characterized in solution is surprisingly small. Most soluble coordination polymers developed so far are based on kinetically stable metal-ligand interactions in non-coordinating solvents.[7-9] The exchange of ligands in such systems is extremely slow, so that the link between two monomers resembles a covalent bond. In order to design *reversible* coordination polymers, kinetically labile metal complexes must be used in coordinating solvents. Very few reversible coordination polymers have been studied so far.[10,11]

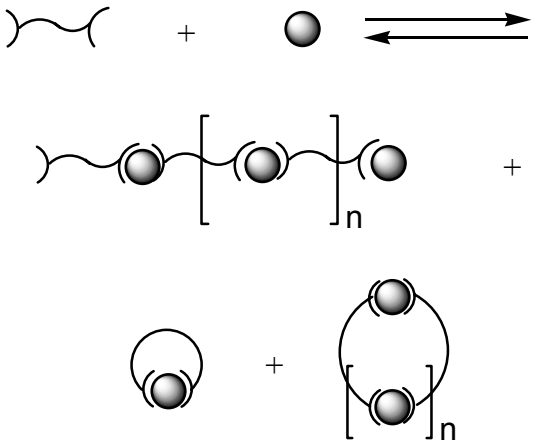

***Scheme 1**: Schematic representation of the formation of polymers and rings.*

When a solution of bifunctional ligands is mixed with metal ions, two types of complexes can be formed as depicted in scheme 1: linear chains and rings. In this chapter, a theoretical model for the coordination polymerization into rings and chains is developed in section 2.2. In section 2.3, the experimental results for water-

soluble bifunctional ligands with terdendate chelating groups are presented. The bifunctional ligands are based on pyridine-2,6-dicarboxylic acid groups connected at the 4-position of the pyridine ring by ethyleneoxide spacers (scheme 2). These chelating groups are known to form complexes with several transition metal ions such that one metal ion is coordinated by two terdendate ligand groups (6-coordination). Reversible polymers are formed when transition metal ions are added to a solution of these ligands. In this study, we use Zn^{2+} as the metal ion because the coordination chemistry with the chelating groups is known and because its complexes are kinetically labile. Viscosity measurements are used to study the polymer formation as a function of the ratio between metal ion and ligand concentration, the total monomer concentration, and the temperature. An increase in viscosity indicates an increase in the average molar mass of the polymers. ^{1}H NMR measurements are used to estimate the fractions of monomers in chains and rings. The experimental results are compared to the theoretical predictions of the model described in section 2.2.

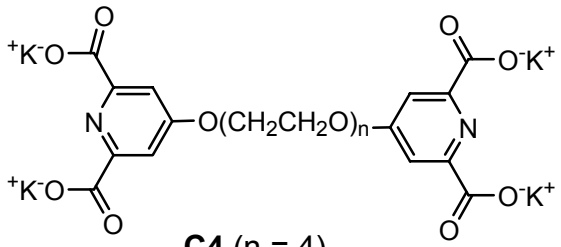

***Scheme 2**: Water-soluble bifunctional ligands, **C4**, **C5**, **C6** and **C7.4**.*

2.2 Ring-chain equilibrium: model calculations

2.2.1 Model

In this section, a method to calculate the molecular weight distributions of chains and rings based on the model of Jacobson and Stockmayer is presented.[16] These authors considered the equilibrium between chains and rings in polycondensation polymers. Here, the model of Jacobson and Stockmayer is applied to solutions of coordination polymers. Coordination polymerization is analogous to polycondensations involving two different monomers that form an alternating copolymer (case III, "adipic acid-decamethylene glycol", in the paper of Jacobson and Stockmayer). In the present case, one type of monomer is the bifunctional ligand, and the other is the metal ion.

Consider a solution of bifunctional ligands L_2 ("monomers") and metal ions M. Every monomer has two identical ligand groups L bridged by a spacer. The total molar concentration of monomers is C_{L2}, and the total concentration of metal ions is C_M. We assume that the ligand groups can form two types of complexes with the metal ions: a 1:1 complex ML in which a metal ion is coordinated by one ligand group (and one or more solvent molecules), and a 1:2 complex ML_2 in which a metal ion is coordinated by two ligand groups. The ML_2 complexes are the bonds between two monomers, while the ML complexes or the free ligand groups L constitute the chain-ends. We assume that all ligand groups react independently, i.e., the probability that a ligand group is involved in a certain type of complex does not depend on the degree of polymerization. The stability constants of the two types of complexes are defined as:

$$K_1 = \frac{[ML]}{[M][L]} \tag{1}$$

$$K_2 = \frac{[ML_2]}{[ML][L]} \tag{2}$$

where [L], [M], [ML], and [ML_2] are the molar concentrations of free ligand groups, free metal ions, and metal ions coordinated by one and two ligand groups, respectively. For most coordination complexes, K_2 is smaller than K_1 because the first ligand group causes some repulsion for the second ligand group. This is different for alternating copolymers, for which the two stability constants are usually the same.

First, we consider the linear (open) chains. Let $c(n,m)$ be the concentration in moles per liter of chains of n monomers and m metal ions. Obviously, $|n\text{-}m| \leq 1$. Like for other equilibrium polymerizations, the distribution of chain lengths is exponential, as derived first by Flory[17]

$$c(n,m) = X_C C_{L2} A_{n-m} (pq)^{n-1} \tag{3}$$

Here the factor p is the fraction of ligand groups in chains that are coordinated to a metal ion, and q is the fraction of these coordinated ligand groups that is involved in an ML_2 complex. Hence, the probability for a bond between two monomers (i.e., an ML_2 complex) is equal to pq, and the probability for n - 1 consecutive bonds is $(pq)^{n-1}$. The probabilities p and q are determined by the stability constants K_1 and K_2 and by the concentrations of monomers and metal ions. The factor X_C is a normalization constant, and A_{n-m} accounts for the probabilities of the chain ends. The probability for a ligand group in a chain to be free is (1 - p), and the probability to form an ML complex is p(1 - q). Hence:

$$A_{n-m} = \begin{cases} (1-p)^2 & (n-m=1) \\ 2(1-p)p(1-q) & (n-m=0) \\ p^2(1-q)^2 & (n-m=-1) \end{cases}$$

The factor 2 for $n - m = 0$ takes into account that there are twice as many configurations for a chain with two different ends than for a chain with two identical ends. The total molar concentration of chains consisting of n monomers is:

$$c(n) = c(n,n-1) + c(n,n) + c(n,n+1) = X_C C_{L2} (1-pq)^2 (pq)^{n-1} \tag{4}$$

and the total molar concentration of monomers incorporated in linear chains is found as $C_C = \sum_n nc(n) = X_C C_{L2}$. Hence, the proportionality constant X_C in equation 3 gives the fraction of monomers in linear chains.

The equilibrium between rings and chains is determined by the difference in free energy between a chain and a ring of given length. When a chain is closed to form a ring, two end segments are removed (i.e., an *ML* complex and a free ligand group *L* react to form an ML_2 complex). This results in a negative free energy contribution. On the other hand, the conformational entropy is reduced upon ring closure, giving a positive free energy contribution. The equilibrium between rings and chains is a result of the balance between these two contributions. Jacobson and Stockmayer calculated the entropy difference between a chain and a ring, assuming that the chains and rings may be considered as ideal Gaussian chains. They derived the following distribution $r(n)$ for the rings:[16]

$$r(n) = B\frac{(pq)^n}{n^{5/2}} \quad (n\nu \geq 1) \tag{5}$$

with $$B = \frac{10^{24}}{2N_{Av}l_k^3}\left(\frac{3}{2\pi\nu}\right)^{3/2}$$

where N_{Av} is Avogadro's number, l_k is the length of a statistical (Kuhn) segment expressed in nanometers, and ν is the number of Kuhn segments per monomer. The Kuhn length[18] l_k is a measure for the stiffness of the monomers, and it depends on the type of spacer between the two ligand groups. The prefactor *B* has the dimension of concentration (moles per liter). From equation 5 we see that rings of many monomers are very unlikely. The reason for this is that the entropy loss upon ring-closure is larger for long chains than for short ones. Moreover, rings are unimportant for very long spacers ($\nu >> 1$), or for very stiff spacers (large l_k).

The Gaussian chain approximation is an adequate description for chains and rings of many Kuhn segments ($n\nu >> 1$), but a serious oversimplification for small chains and rings. Shimada and Yamakawa used the wormlike chain model to predict

ring-closure probabilities in the tight bending limit.[19] They showed that rings shorter than the Kuhn length ($n\nu < 1$) are strongly suppressed. Therefore, we explicitly forbid rings shorter than the Kuhn length here ($r(n) = 0$ for $n\nu < 1$), and we use equation 5 for $n\nu \geq 1$.

The total molar concentration of monomers in rings is

$$C_R = \sum_n nr(n) = B \sum_{n \geq \nu^{-1}} n^{-3/2} (pq)^n \tag{6}$$

and the fraction of monomers in rings is $X_R = 1\text{-}X_C = C_R/C_{L2}$.

The number average length of the chains can be calculated as:

$$\langle n_C \rangle = \frac{\sum_n nc(n)}{\sum_n c(n)} = \frac{1}{1-pq} \tag{7}$$

For the chains the polydispersity index, defined as the weight-average length divided by the number-average length, equals $1 + pq$, which is approximately 2 if the average length is large ($pq \approx 1$). The number average length of the rings is:

$$\langle n_R \rangle = \frac{\sum_n nr(n)}{\sum_n r(n)} = \frac{\sum_{n \geq \nu^{-1}} n^{-3/2} (pq)^n}{\sum_{n \geq \nu^{-1}} n^{-5/2} (pq)^n} \tag{8}$$

and the total number-average length is:

$$\langle n \rangle = \frac{\sum_n n[c(n) + r(n)]}{\sum_n [c(n) + r(n)]} \tag{9}$$

The length distributions of chains and rings are given in terms of the probabilities p and q. We will now relate these probabilities to the stability constants K_1 and K_2 and the concentrations of monomers and metal ions. The concentrations of the various species obey the mass conservation laws for monomers and metal ions:

$$2C_{L2} = \alpha[L] + [ML] + 2[ML_2] \tag{10}$$

$$C_M = [M] + [ML] + [ML_2] \tag{11}$$

The factor 2 on the left hand side of equation 10 is added because each monomer has two ligand groups. The factor α accounts for the protonation of the ligand groups:

$$\alpha = 1 + [HL]/[L] + [H_2L]/[L] + \cdots = 1 + K_{a1}[H] + K_{a2}[H]^2 + \cdots \tag{12}$$

where H denotes a proton, and $K_{a1} = [HL]/[H][L]$ and $K_{a2} = [H_2L]/[H]^2[L]$ are the first and second protonation constant, respectively. At high enough pH the protonation of the ligands may be neglected.

The concentrations of free ligand [*L*], and of the two types of complexes [*ML*] and [ML_2], can be found from the chain and ring distributions *c(n,m)* and *r(n)* by counting the number of end-segments and bonds:

$$\alpha[L] = \sum_n \left[2c(n,n-1) + c(n,n)\right] = 2X_C C_{L2}(1-p) \tag{13}$$

$$[ML] = \sum_n \left[c(n,n) + 2c(n,n+1)\right] = 2X_C C_{L2} p(1-q) \tag{14}$$

$$[ML_2] = \sum_n \left[(n-1)c(n) + nr(n)\right] = X_C C_{L2} pq + B\sum_{n>\nu^{-1}} n^{-3/2}(pq)^n \tag{15}$$

Substitution of equations 13-15 in equations 1, 2, 10, and 11 gives four equations that can be solved numerically to find *p*, *q*, X_C, and [*M*] for given values of the stability constants and monomer and metal concentrations.

2.2.2 General trends

In this section, we present some general trends for the equilibrium between chains and rings as predicted by the model. In section 2.3, we compare the model to the experimental data using specific values of the various parameters.

The total concentration of monomers in rings is given by equation 6. From this equation, we can see that for a given type of monomers (i.e., given ν and l_k), there is an upper limit C^{cr} to the concentration of monomers in rings. The maximum value that the probabilities *p* and *q* can have is unity (for high stability constants, at high monomer concentration and at a 1:1 metal to ligand ratio), so that:

$$C^{cr} = B\sum_{n\geq\nu^{-1}} n^{-3/2} \tag{16}$$

For $\nu \geq 1$, this gives $C^{cr} \approx 2.6B$.

The concentrations of monomers in chains and rings as a function of the total concentration are shown in figure 1 for two metal/monomer ratios *y* and with l_k = 3 nm, ν = 3, $K_1 = 10^7$ M^{-1}, and $K_2 = 10^6$ M^{-1}. We examine the case that pH >> pK_{a1}, pK_{a2}, so that the protonation is negligible. The concentrations have been divided by C^{cr} (which is 5.1 mM for the parameters used). Clearly, at low concentrations most monomers are incorporated in rings, while at higher concentrations chains become more important. For $y \equiv C_M/C_{L2}$ equal to unity and low concentrations, $C_R \approx C_{L2}$, while at higher concentrations ($C_{L2} >> C^{cr}$) the concentration of rings goes asymptotically to a plateau, given by $C_R \approx C^{cr}$. Hence, $2C^{cr}$ can be regarded as the concentration below which rings dominate and above which chains dominate (for *y* = 1). For finite values of the stability constants the transition from the ring-dominated regime to the chain-dominated regime is rather smooth, but it becomes sharper when the stability constants become larger. For infinite values of K_1 and K_2 at *y* = 1 (the dashed lines in figure 1), C^{cr} may be considered as a critical

concentration at which the formation of chains starts. (This is analogous to the critical micelle concentration in surfactant systems.) This can also be seen from equations 13-15: for infinite K_1 and K_2, and $C_M = C_{L2}$, both [L] and [ML] are equal to zero, while [ML_2] = C_{L2}. According to equations 13 and 14, this means that either X_C = 0, or p and q are equal to unity. From equations 15 and 16, we see that p and q must be smaller than unity if $C_{L2} < C^{cr}$, while X_C must be larger than zero for $C_{L2} > C^{cr}$. Hence, we have $C_C = 0$ and $C_R = C_{L2}$ for concentrations below C^{cr}, whereas $C_R = C^{cr}$ and $C_C = C_{L2} - C^{cr}$ for concentrations above C^{cr}.

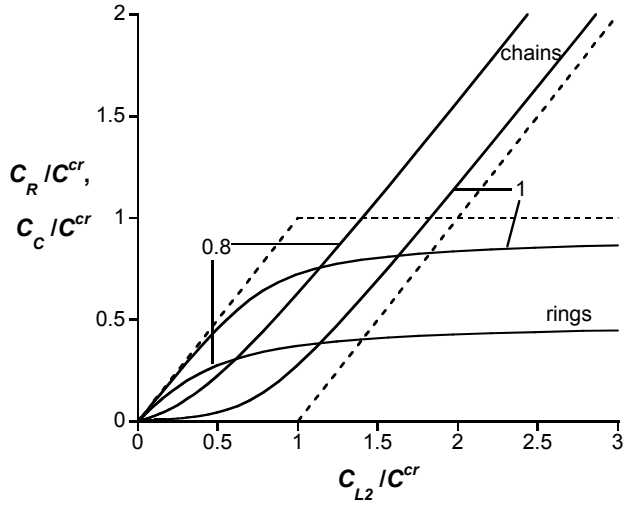

***Figure 1**: Theoretical: concentrations of monomers in rings (C_R) and chains (C_C) (normalized with respect to C^{cr}) as a function of monomer concentration for metal to monomer ratios of 1 and 0.8 (as indicated), with l_k = 3 nm, ν = 3, $K_1 = 10^7\ M^{-1}$, and $K_2 = 10^6\ M^{-1}$. Dashed lines correspond to infinite values of K_1 and K_2 at a 1:1 ratio.*

If the ratio y between monomers and metal ions is not equal to unity, rings are less prominent because the excess component can form extra chain ends. The maximum concentration of rings for this case is smaller than C^{cr}. In figure 2, we have plotted the plateau value of the ring concentration $C_R^{\max}$ as a function of y for several values of the stability constants. For an excess of monomers (y < 1), the maximum ring concentration is determined by y only. The probability p that a monomer in a chain is coordinated to a metal ion is at most $y = C_M / C_{L2}$ for this case, while q is close to unity at high concentrations. For example, for y = 0.8 (shown in figure 1), the maximum value of p is 0.8, and we find from equation 6 that the maximum concentration of monomers in rings is equal to $1.2B \approx 0.46C^{cr}$. As we can see in figure 2, for an excess of metal ions (y > 1), the maximum ring concentration depends on the ratio between the stability constants. The probability p is close to unity for this

case, while q is determined by the ratio K_1/K_2. Rings are favored if ML_2 complexes are relatively stable, which is the case if K_2 is large compared to K_1.

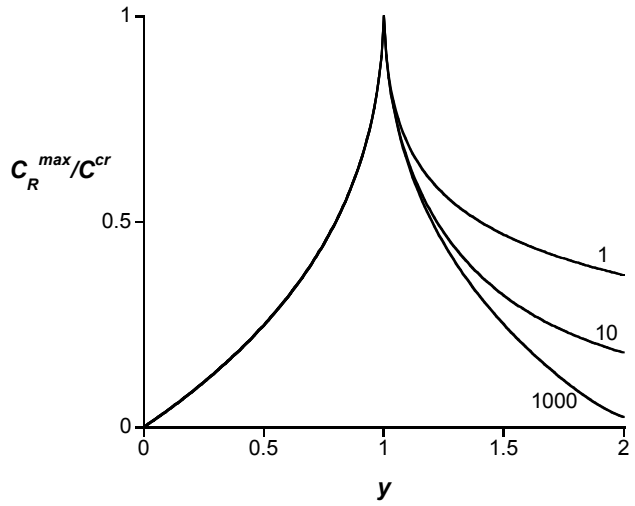

***Figure 2**: Theoretical: plateau of the concentration of monomers in rings as a function of the metal/monomer ratio y for various ratios K_1/K_2.*

The number-averaged length of the chains and the rings is plotted in figure 3 as a function of the monomer concentration for several values of y and the same parameters as in figure 1. As expected, the chains are much larger than the rings. With increasing concentration, both chains and rings become larger. The average size of the rings remains small and goes to a plateau value at high monomer concentrations. From equation 7 we can find the maximum value of the average size of the rings by setting p and q equal to unity. For monomers with $\nu \geq 1$ the maximum average ring size is 1.9 monomers (at a 1:1 ratio). For other ratios, the average size is slightly smaller. The chains on the other hand become much longer. For y = 1, the average length of the chains at high concentrations increases with C_{L2} as:

$$< n_C > \; = \sqrt{K_2 C_{L2}} \qquad (C_M = C_{L2} >> C^{cr}) \tag{17}$$

This is similar to other equilibrium polymers.[20] It can be found from equations 2, 10, and 11, by taking $C_{L2} \approx [ML_2] >> [ML] >> [M]$ and using $< n_C > = 2\, C_{L2}/([L] + [ML])$ (which is valid if rings can be neglected, i.e., for $C_{L2} >> C^{cr}$). For $y \neq 1$ the average length is smaller and goes to a plateau at high concentrations. Figure 4 shows the plateau of the average length of the chains and the rings as a function of y for several ratios K_1/K_2. Obviously, for y = 1, the average length of the chains does not reach a plateau but increases with concentration according to equation 17. For y < 1, the average chain length depends only on the value of y. Since p can reach a maximum value of y

= C_M/C_{L2} and q is close to unity, the maximum of the average length is, according to equation 7:

$$< n_C >^{\max} = \frac{C_{L2}}{C_{L2} - C_M} \qquad (C_M < C_{L2}) \tag{18}$$

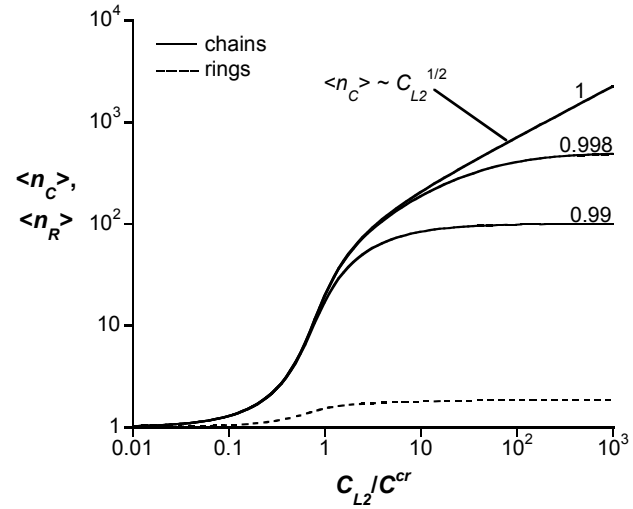

***Figure 3**: Theoretical: number average length of chains and rings as a function of the monomer concentration for several metal/monomer ratios. Same parameters as in figure 1.*

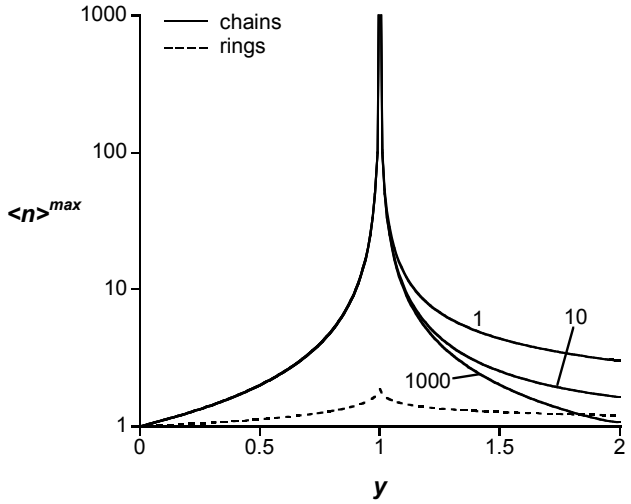

***Figure 4**: Theoretical: maximum values of the average length of chains and rings as a function of the metal/monomer ratio y for several ratios K_1/K_2.*

For $y > 1$, the average chain length depends on the ratio between the two stability constants, just like the maximum ring concentration in figure 2. The average length is larger if ML_2 complexes are favored, i.e., if K_2 is large compared to K_1. For a small

excess of metal, the curve in figure 4 is symmetric around the peak, and the average length $\langle n_C \rangle^{max}$ is given by $C_M/(C_M-C_{L2})$. It can be seen in figure 4 that the rings also have a maximum length for $y = 1$, but even at the peak it is still very small.

In this section we presented some general results for coordination polymerization into chains and rings. We investigated the effect of the metal/monomer ratio and the total monomer concentration on the equilibrium between chains and rings and their average lengths. In section 2.4, we will compare the model to experimental data for two water-soluble bifunctional terdendate ligands.

2.3 Experimental results and discussion

Water-soluble bifunctional ligands **C4**, **C5**, **C6** and **C7.4** (see scheme 2), with 4, 5, 6 and 7.4 ethylene oxide units as spacer respectively, were synthesized in three steps from commercially available chelidamic acid. The acid groups were first protected as ethyl esters[21], after which the appropriate dibromooligoethylene oxide spacer[22] was coupled to the aromatic OH-group using K_2CO_3 as a base. In the last step the ester groups were hydrolyzed, yielding the final ligands as potassium salts.

These ligands and their complexes with Zn^{2+} are water-soluble over a wide pH range. The complexation gives an almost undetectable change in the UV-spectra of the ligands upon addition of a Zn^{2+} solution, but the stoichiometry of complexation was confirmed by isothermal titration calorimetry (ITC) measurements. Besides stoichiometry, ITC measurements also give information about the complexation constants. However, when the constants are very high ($K > 10^5$ M^{-1}), it is difficult to obtain these values accurately with this method. On the basis of the ITC measurements, we conclude that the complexation constants between the ligands and Zn^{2+} ions are larger than 10^5 M^{-1}. Complexation constants reported by Anderegg[23] of structurally equivalent 2,6-pyridinedicarboxylic acid and Zn^{2+} ions confirm our results: $K_1 = 10^{6.4}$ and $K_2 = 10^{5.5}$ for the 1:1 and 1:2 complexes, respectively. Anderegg reported also acidity constants for the same ligands: $K_{a1} = 10^{4.7}$ and $K_{a2} = 10^{6.8}$. Proton titrations with our ligands suggest that K_{a1} and K_{a2} are somewhat larger than this. We tried measuring the stability constants K_1 and K_2 using proton titrations in the presence of Zn^{2+}, but unfortunately we did not succeed because the stability constants are too high to measure with this method. The measurements do suggest, however, that K_1 and K_2 for our ligands are also somewhat higher than reported by Anderegg. Model calculations indicate that the behavior is rather insensitive to the values of the stability constants. In fact, the model results are hardly affected if all K values are made larger by a factor 100.

Therefore, in our calculations we use the values reported by Anderegg for K_1, K_2, K_{a1} and K_{a2}. The value of α with these values is 1.2 at pH 5.4.

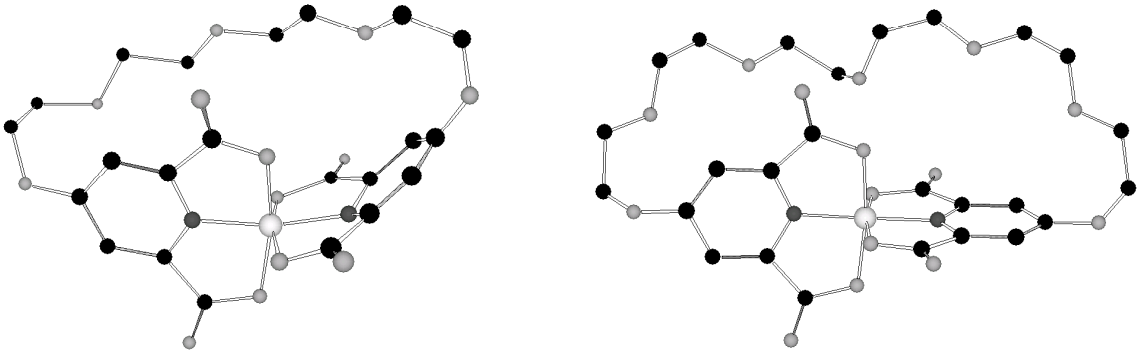

***Scheme 3**: 3D-structures of monomer rings of **C4** (left) and **C6** (right) around a Zn^{2+} ion. Strain in the pyridine rings and spacer are found in the monomer ring of **C4**, which makes it highly unlikely that this kind of ring is formed. For **C6** no strain is found in the 3D-structure.*

To compare the experimental results described in this section to model calculations, we need realistic values for l_k and ν. A molecular model shows that for the ligand with the shortest spacer, **C4**, at least two monomers are needed for a ring, while the one with a spacer of six ethylene oxide units, **C6**, is just able to form an intramolecular complex (a ring of one monomer) without strain in the ring. In scheme 3, the three-dimensional structures of the monomer rings of both **C4** and **C6** are shown. As can be seen, some strain in the pyridine rings and in the spacer are found in the monomer ring of **C4**. For that reason, this structure is not likely to be formed. For **C6** no strain is found in the 3D-structure. Hence, we take the Kuhn length equal to the length of **C6**: l_k = 3.3 nm. We furthermore assume that the Kuhn length is the same for the two monomers. This is an oversimplification, because the relative contribution of the stiff complexed chelidamic acid groups is larger for **C4** than for **C6**, but here we neglect this. The length of **C6** is about 3.3 nm (i.e., ν = 1), and that of **C4** is about 2.7 nm (i.e., ν = 0.83). With these parameters we find that the maximum concentration of monomers in rings C^{cr} is 19.8 mM for ν = 1 (**C6**) and 16.2 mM for ν = 0.83 (**C4**). We note that the estimation of the various parameters in the model is somewhat crude, but the choice of the parameters does not change the results qualitatively.

2.3.1 Molar ratio dependence

We measured the reduced viscosity as a function of the molar ratio Zn^{2+}: bifunctional ligand for **C4** and **C6** in buffer. The pH (= 5.4) was chosen high enough to favor metal complexation over protonation of the ligands and low enough to

prevent the formation of insoluble zinc hydroxide. Figure 5a displays the reduced viscosity of ligand **C4** as a function of the molar ratio Zn^{2+}:**C4** for two concentrations of **C4**. In the experiments a concentrated $Zn(ClO_4)_2$ solution (approximately 1.0 M) was titrated to the ligand solution. After mixing, the viscosity reached equilibrium immediately. It is well known that the reduced viscosity of polymer solutions increases with the average chain length of the polymers. We observe an increase in reduced viscosity for increasing molar ratio until a ratio of 1 is reached. Beyond a ratio of 1, it decreases again. Excess of either bifunctional ligands or metal ions will yield extra chain ends. Since for linear chains the average number of monomers per chain is inversely proportional to the number of chain ends, the viscosity decreases again at molar ratios larger than 1. That this decrease occurs implies that the complexes are reversible, so that the chains that are formed initially break up. For a ligand concentration approximately twice as high, a three times higher reduced viscosity was found. This indicates that longer polymers are formed at higher concentrations.

For ligand **C6**, with a longer spacer a radically different plot is observed (figure 5b). For the highest concentration of 34.5 mM a peak was found at a molar ratio of 1. The shape of the curve is the same as for **C4**. However, the peak is not as high as for a similar concentration of **C4**. Surprisingly, for the lower concentration of 17.8 mM a dip in the curve was found at a molar ratio 1, instead of a peak. At first we were rather puzzled by this, but it turns out that the model described in section 2.2 can explain these results in terms of ring formation.

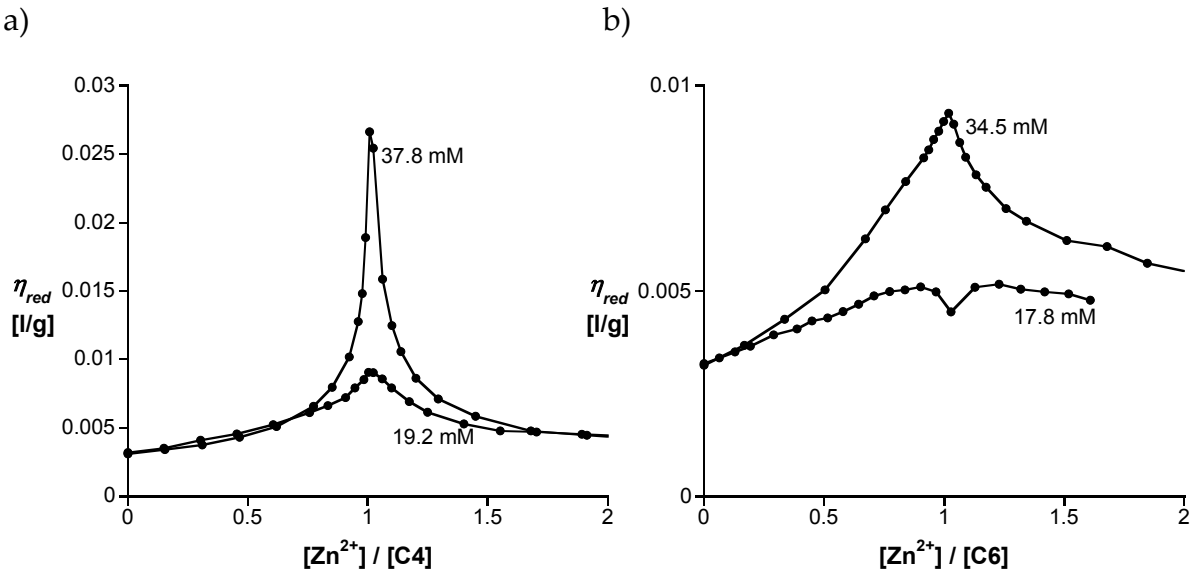

***Figure 5**: Experimental: reduced viscosity of ligands as a function of molar ratio $Zn(ClO_4)_2$/ ligand in 0.1 M PIPES buffer pH 5.4 at 298 K for (a) ligand **C4** (12.7 and 25.6 g/l) and (b) ligand **C6** (13.4 and 26.9 g/l).*

Figure 6 shows the theoretical weight fractions of monomers in rings X_R as a function of the ratio between the metal and monomer concentration y for both monomers at the concentrations used in the experiments. As already explained in section 2.2, rings are most important at low concentrations and at a 1:1 metal:ligand ratio. We see in figure 6 that the fraction of rings is slightly lower for the monomers with a shorter spacer ($\nu = 0.83$) than for the monomers with the longer spacer ($\nu = 1$). The reason for this is that the shorter monomer needs at least two monomers to form a ring. As a result, C^{cr} is somewhat smaller for $\nu = 0.83$ (**C4**) than for $\nu = 1$ (**C6**). Because rings have a smaller degree of polymerization and a more compact conformation than linear chains (see figures 3 and 4), the viscosity is lower in the region where rings are most abundant. In figure 7 we have plotted the calculated total average length <n> as a function of y for the two monomers and for the concentrations used in the experiments. It can be seen that for the monomers with $\nu = 1$ the average length <n> has a dip at the lowest concentration at $y = 1$, as has the viscosity of **C6**. At this ratio almost all monomers are in rings as can be seen in figure 6. Because the rings are very small, the viscosity has a minimum at $y = 1$. At higher concentrations ($C_{L2} >> C^{cr}$) the dip vanishes because rings are less important then. For the monomers with the shorter spacer ($\nu = 0.83$) the dip does not occur, just like in the viscosity measurements. At least two monomers are needed for a ring in this case, and as a result the amount of rings is smaller.

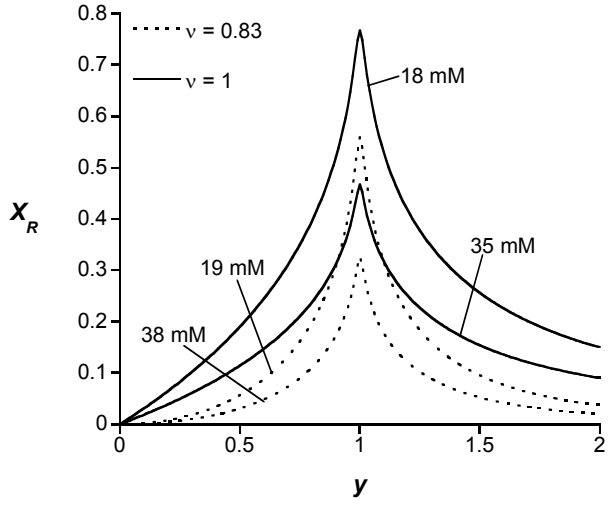

***Figure 6**: Theoretical: weight fraction of monomers in rings X_R as a function of the metal/monomer ratio y and monomer concentration for monomers with $\nu = 0.83$ and $\nu = 1$ at the concentrations used in the experiments.*

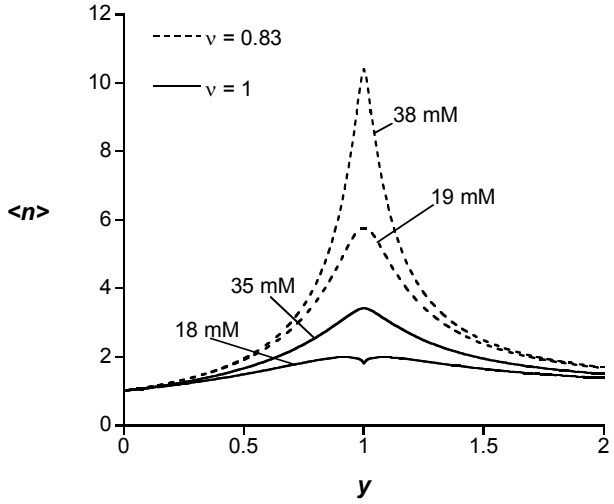

***Figure 7**: Theoretical: total average length as a function of y for ν = 0.83 and ν = 1 (corresponding to **C6** and **C4**) matching the experimentally used concentrations.*

2.3.2 Concentration dependence

In section 2.2, we have seen that the fraction of monomers in rings is a function of the total concentration of monomers. Experimentally, the concentrations of monomers in chains and rings can be measured with ^{1}H NMR spectroscopy provided rings and chains give rise to different peaks in the spectrum. Indeed, two sets of signals are obtained in the ^{1}H NMR spectra of monomers and metal ions at a 1:1 ratio. To assign the peaks correctly to the different species DOSY NMR (Diffusion Ordered Spectroscopy)[24] experiments were performed.

Figure 8 shows the DOSY-spectrum for **C4** and Zn^{2+} ions in a 1:1 ratio at 36 mM in D_2O. On the horizontal axis the proton NMR-spectrum is plotted, and on the vertical axis the logarithm of the diffusion coefficient (D) corresponding to the proton peaks is plotted. The peaks on the horizontal axis (^{1}H NMR spectrum) between 3.5 and 4.7 ppm originate from the OCH_2-groups in the spacer. The singlets around 7.8 ppm originate from the aromatic protons of the pyridine ring. The residual solvent peak is very large and therefore gives a high DOSY signal. The solvent signal has the highest intensity at log D = -8.62, which corresponds to the diffusion coefficient of water at 25 °C of $2.4 \cdot 10^{-9}$ m^2/s. Two groups of peaks can be seen in the DOSY spectrum. One group (denoted with an R) has a maximum intensity at log D = -8.9 (or $D = 1.2 \cdot 10^{-9}$ m^2/s). The other (denoted with a C) gives signals over a wide range of diffusion coefficients from about log D = -9.5 ($D = 3.1 \cdot 10^{-10}$ m^2/s) to the measurement limit of log D = -10.1 ($D = 7.9 \cdot 10^{-11}$ m^2/s). It may be expected that the rings are smaller than the chains (see figures 3 and 4), so that they have a larger diffusion coefficient.

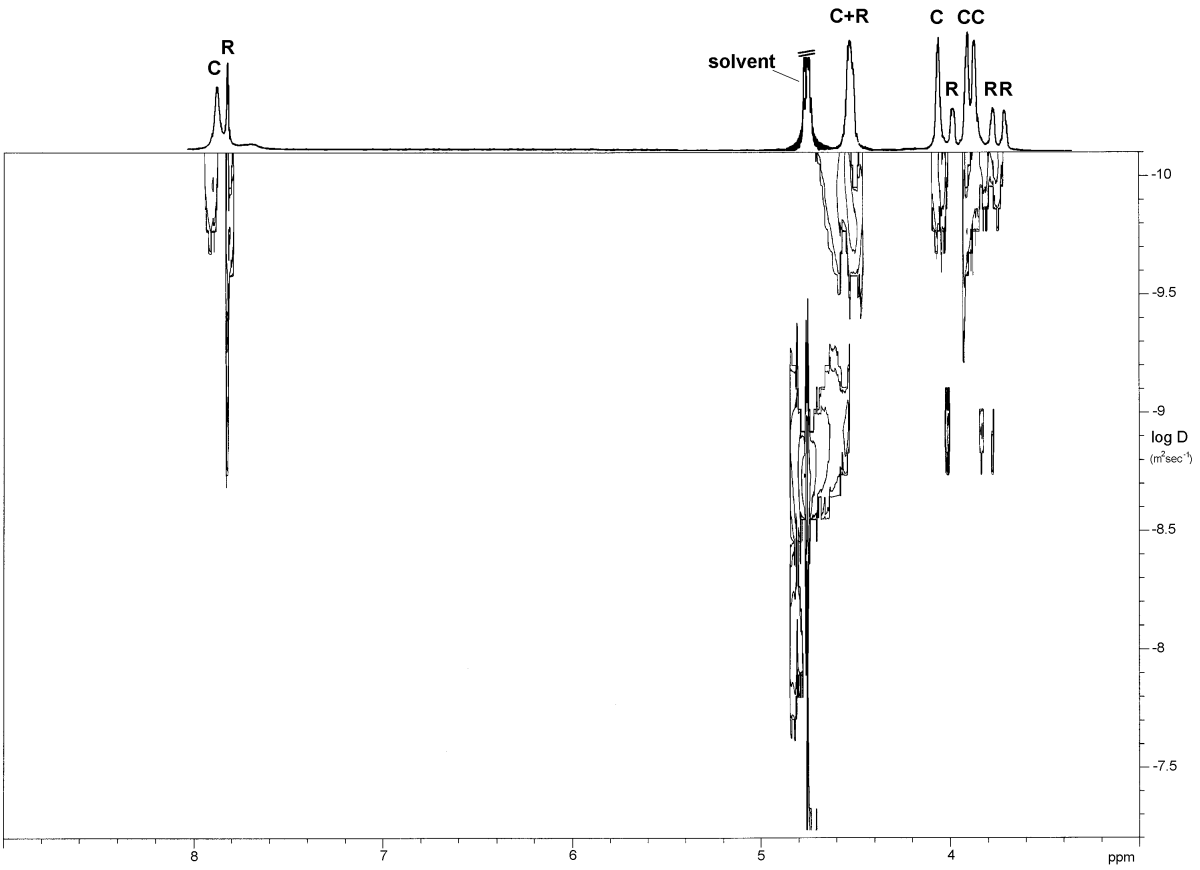

***Figure 8**: DOSY NMR spectrum of a 36 mM of **C4** and Zn^{2+} solution in D_2O at 298 K. The signal of HDO is cut off.*

Hence, we assume that the peaks with a high diffusion coefficient (denoted with an R) correspond to rings, while those with a lower diffusion coefficient (denoted with a C) correspond to chains. Larger compounds give broader peaks in ^1H NMR spectra, which is another indication that the broad peaks correspond to protons in chains and the sharp peaks to the smaller cycles. For the triplet signals of the OCH_2 groups it is hard to see the difference in sharpness of the peaks for chains and rings, but for the singlet signal at about 7.8 ppm the peak of the chains is much broader than of the rings. For one of the peaks (4.4-4.5 ppm) the ring and chain signal overlap. The large range of diffusion coefficients for the chains can be explained by their polydispersity. An exponential chain length distribution is expected (see equations 3 and 4). Most peaks denoted with an R also show some signals in the same region of diffusion coefficients as the peaks denoted with a C. The explanation for the different diffusion coefficients belonging to one peak is that molecules exchange between cyclic and open structures on the time scale of the measurement. This exchange was also proven by a ROESY NMR (Rotating Frame Nuclear Overhauser Enhancement Spectroscopy) experiment, which showed cross peaks due to through bond coupling between R and C signals. The time scale of both 2D

experiments (DOSY and ROESY) is about 200 msec, which is much larger than for the 1D-proton spectra. The exchange between rings and chains on the time scale of the 1D-proton spectra can be neglected.

Figure 9 shows the ^{1}H NMR spectra for compound **C4** and Zn^{2+} ions at a 1:1 ratio in D_2O at 298 K at different concentrations. The spectrum at the lowest concentration (figure 9c) resembles the spectrum of the ligand molecules without metal ions present. However, the chemical shifts are different, which indicates that the metal ions are bound to the ligand, as already expected from the known association constants. The most notable difference is the number of peaks originating from the spacer. Without metal ions present the spacer shows only three signals instead of four because two of them have the same chemical shift, which is not the case when metal ions are present.

The spectra at different concentrations show the two sets of signals denoted with C (chains) and R (rings) that are assigned on the basis of the DOSY NMR results and the sharpness of the peaks. At low concentrations the ring signals are very high compared to the chain signals. Upon increasing the concentration the chain signals become larger.

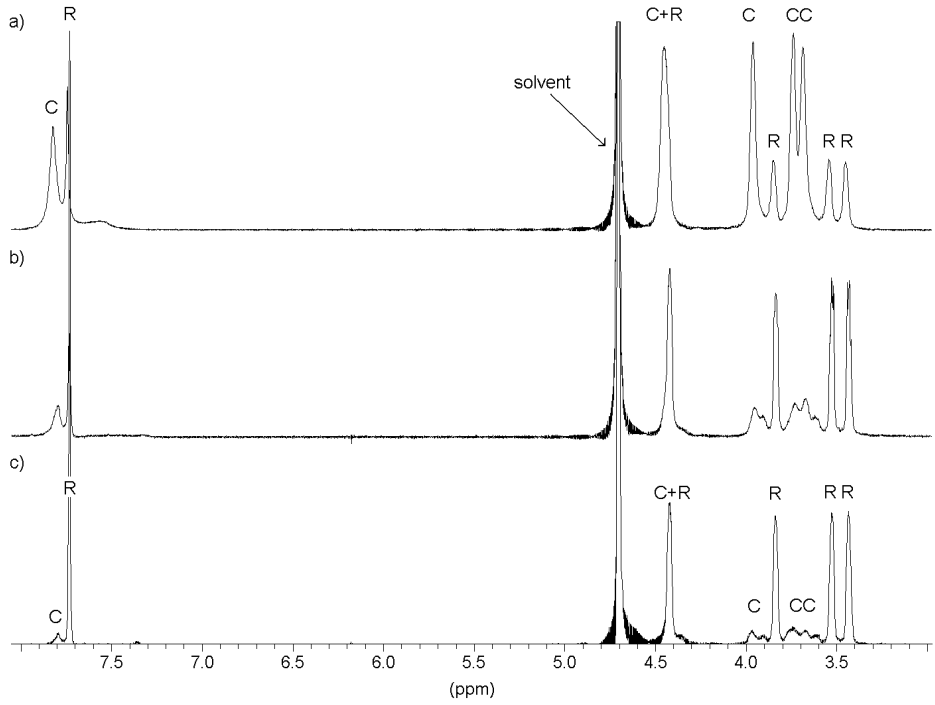

***Figure 9**: ^{1}H NMR spectra of compound **C4** with Zn^{2+} (1:1 ratio) in D_2O at 298 K at various concentrations: 36 mM (a), 13 mM (b), 6.5 mM (c). Signals assigned to chains and rings are denoted with C and R, respectively.*

^{1}H NMR spectra for compound **C6** and Zn^{2+} at a 1:1 ratio also gave two sets of signals that could be ascribed to rings and chains (not shown). As expected, the peaks ascribed to chains increase with concentration, but they are lower than for the **C4** system at the same concentrations. The relative amounts of rings and chains can be determined from the integrals of the peaks in the 1D proton spectra, since exchange between rings and chains can be neglected here. Figure 10 shows the concentrations of both monomers, **C4** and **C6**, in chains and rings as a function of the total monomer concentration. Clearly, at low concentrations most monomers are incorporated in rings, while at higher concentrations chains are more important. At higher concentrations, the concentration of monomers in rings seems to level off towards a constant value, as predicted by the model (figure 1). For **C4** the concentration of rings is lower than for **C6** at the same overall concentration. This is caused by the possibility of **C6** to form monomeric rings, while **C4** needs at least two monomers for a ring. In the same figure the results of the model calculations are shown for both monomers (the full and dashed curves). The agreement between the experimental data and the theoretical curves is very good, especially for **C6** ($\nu = 1$). For **C4** ($\nu = 0.83$) the agreement is not as good as for **C6**. The model overestimates the amount of rings. The reason for this may be that we have used the same value for the Kuhn length for both **C4** and **C6**. In reality, however, the Kuhn length is probably somewhat higher for **C4** than for **C6** because the stiff ligand groups are relatively more important for the smaller monomer. We note that, by choosing a larger value for the Kuhn length (4 nm), we can obtain a very good agreement between experiment and theory for the **C4** monomers, too.

In figure 5, we have seen that the reduced viscosity depends on the concentration of monomers. With increasing concentration the fraction of monomers in rings decreases, as seen from the NMR measurements. Also, the average length of the chains and rings increases with increasing concentration (see figure 3). Figure 11 shows the reduced viscosity of compounds **C4** and **C6** as a function of the concentration at a metal-ligand ratio close to 1 (within 0.5%), at pH 5.4 and 298 K. For low concentrations, the increase in viscosity with increasing concentration is small. At these concentrations mainly small rings are present, with only a small influence on the viscosity. For **C4** the viscosity starts to increase more steeply at a concentration of about 11-13 mM. This is caused by the formation of more (and larger) linear chains at these concentrations (see figure 10). For **C6** the effect of the concentration is somewhat different. The slope of the first part of the curve is the same as for **C4,** but the increase in viscosity above 11-13 mM is much smaller. This is probably caused by the larger amount of rings (mainly monomers) present at all concentrations in the solution of **C6** (see figure 10).

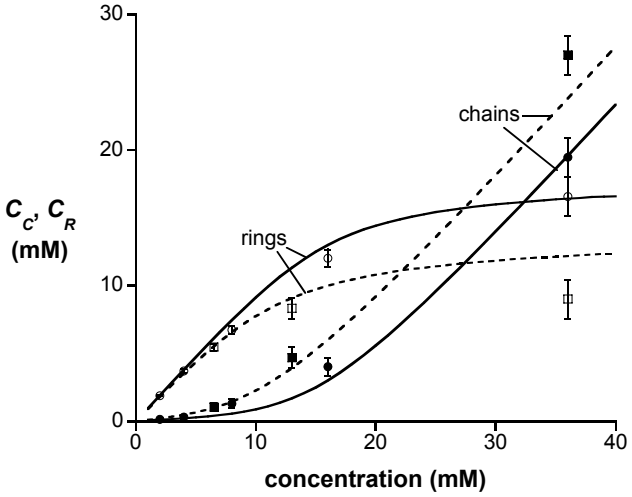

***Figure 10**: The concentrations of monomers in chains (**C4**: ▪, **C6**: ●) and rings (**C4**: □, **C6**: o) as a function of the monomer concentration with Zn^{2+} (1:1 ratio) in D_2O at 298 K, determined from the integrals of the peaks in ^1H NMR spectra. The curves refer to results of the theoretical model: full curves $\nu = 1$ and $l_k = 3.3$ nm (corresponding to **C6**), dashed curves $\nu = 0.83$ and $l_k = 3.3$ nm (corresponding to **C4**).*

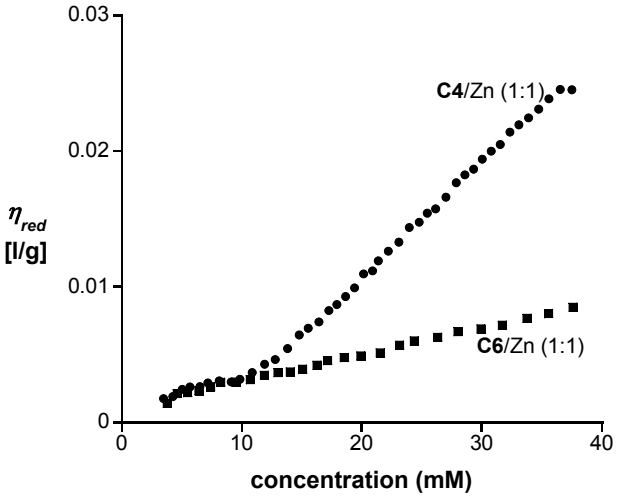

***Figure 11**: Reduced viscosity of ligands **C4** and **C6** as a function of concentration at a $Zn(ClO_4)_2$/ ligand ratio of 1 in 0.1 M PIPES buffer pH 5.4 at 298 K.*

As already explained, the viscosity of a polymer solution is determined by the average size of the molecules. In figure 12, we have plotted the concentration dependence of the total average length <*n*>, calculated using the model of section 2.2 for both ligands at a metal/monomer ratio equal to unity. The increase in chain length with concentration is obvious. At low concentrations, all monomers are in rings, and the average length is equal to the size of a minimal ring: one for **C6** and

two for **C4**. With increasing concentration, the average size increases, mainly because the rings become larger. Above a certain concentration ($\approx C^{cr}$), the increase of the average length becomes steeper because chains start to grow. For $\nu = 0.83$ the increase in average length is faster than for $\nu = 1$. The shape of the calculated curves is in qualitative agreement with the viscosity data in figure 11. For **C4** a change of slope is observed at a concentration of around 12 mM, which can also be seen in the calculated curve of figure 12. For **C6** the viscosity increases more slowly with concentration, just like the calculated average length. We note that the increase of the viscosity with concentration is caused not only by an increase of the average length but also by the difference in conformation of chains and rings. Because the structure of a ring is more compact than that of a chain, its contribution to the viscosity is probably smaller than that of a chain of the same size.

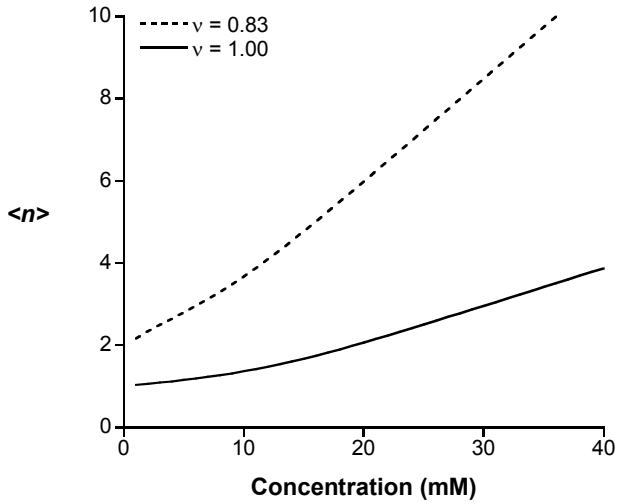

***Figure 12**: Theoretical: total average length as a function of the monomer concentration for a metal/monomer ratio equal to unity for $\nu = 0.83$ and $\nu = 1$.*

2.3.3 Temperature dependence

^{1}H NMR spectra of 6.5 mM of **C4** and Zn^{2+} (1:1) in D_2O at different temperatures reveal a strong temperature dependence of the ring-chain equilibrium (see figure 13). With increasing temperature the ring peaks become smaller and the chain peaks become larger. Upon cooling, the initial spectra were found again, which confirms the reversibility of the system. At higher temperatures there is some overlap between ring and chain peaks, and when the temperature exceeds 333 K, the different peaks are hardly discernible. Because of this overlap the values of the integrals of both types of peaks become less accurate for increasing temperature. Furthermore, the solvent peak shifts to lower ppm values (from 4.8 to 4.4) due to

increasing temperature. It overlaps with one of the sample peaks at these temperatures, which makes it difficult to interpret that part of the spectrum. Nevertheless, we estimated the fraction of monomers in chains and rings from the integrals of the peaks. The results are plotted in figure 14. Although the error bars are large due to the overlap of the peaks, the increase of the chain fraction for increasing temperature is obvious. For **C4** at 6.5 mM the chain fraction increases from about 0.15 at 298 K to about 0.55 at 343 K. For **C6** at 8 mM the fraction of monomers in chains is lower than for **C4** as found earlier in the concentration dependent experiments. The chain fraction also increases with temperature, from 0.14 at 298 K to about 0.40 at 343 K.

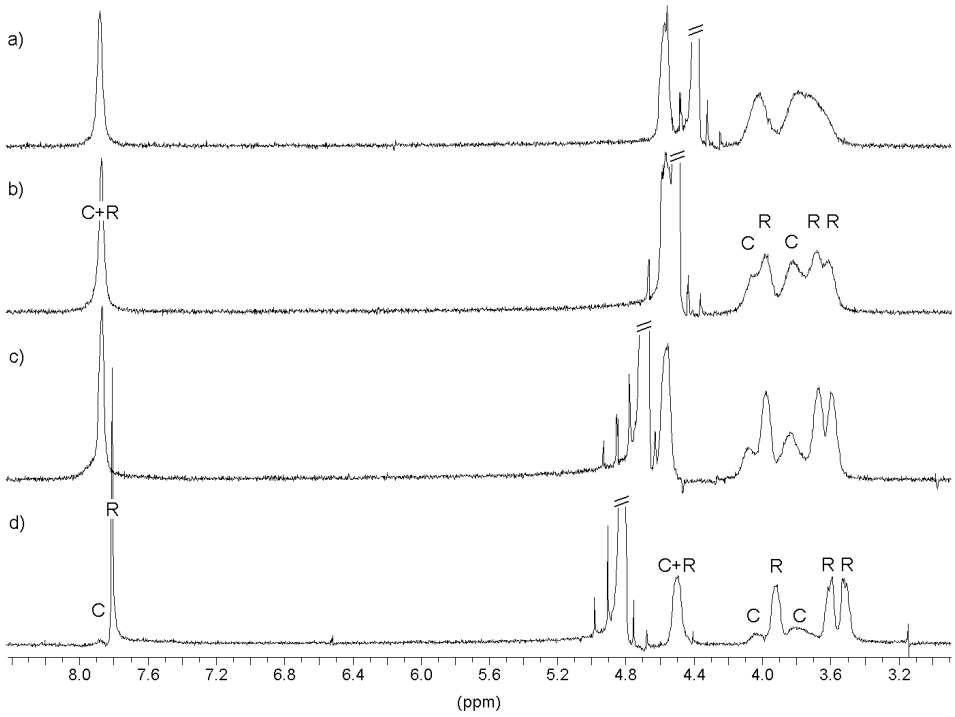

***Figure 13**: ^1H NMR spectra of a 6.5 mM solution of **C4** and Zn^{2+} (1:1 ratio) in D_2O at various temperatures: 343 K (a), 333 K (b), 318 K (c), 303 K (d). Signals from chains and rings are denoted with C and R, respectively. The signal of HDO is cut off.*

This temperature effect on the relative amounts of rings and chains yields a quite unusual temperature-viscosity dependence. Both compounds **C4** and **C6** (Zn^{2+}:ligand ratio = 1) show an increase in reduced viscosity upon heating due to ring opening (Figure 15). This effect is largest for **C4**. When the temperature is increased above 340 K, the viscosity decreases again slightly. For conventional covalent polymers, increasing the temperature results in a higher mobility of the chains and therefore in a decrease in viscosity. Also, for supramolecular polymers a decrease in viscosity is common upon heating[25], although a hydrogen bonded supramolecular polymer

described by Folmer et al. shows a similar increase in viscosity upon heating due to ring opening.[26,27] The novelty of our system is that besides concentration and temperature also the metal-ligand ratio can be used to tune the system. To show the large effect of metal-ligand ratio, also a curve is shown in figure 15 for **C4** at a ratio of 1.02. The decrease in viscosity is very large for only a small change in ratio.

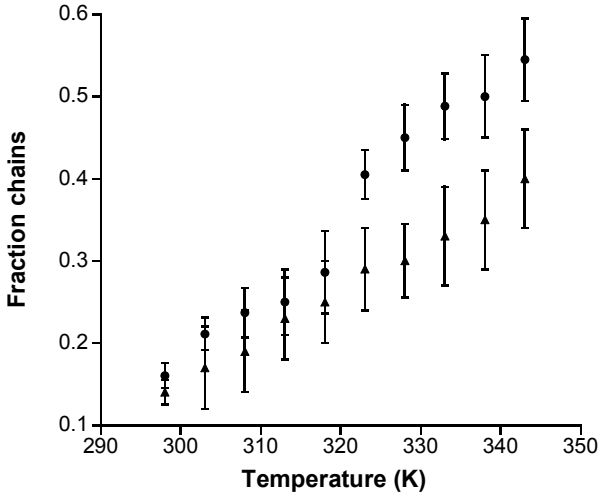

***Figure 14**: Fraction of chains of ligands **C4,** 6.5 mM (•) and **C6,** 8.0 mM (▲) as a function of temperature in D_2O at a $Zn(ClO_4)_2$/ ligand ratio of 1, determined from the integrals of the peaks in ^1H NMR spectra.*

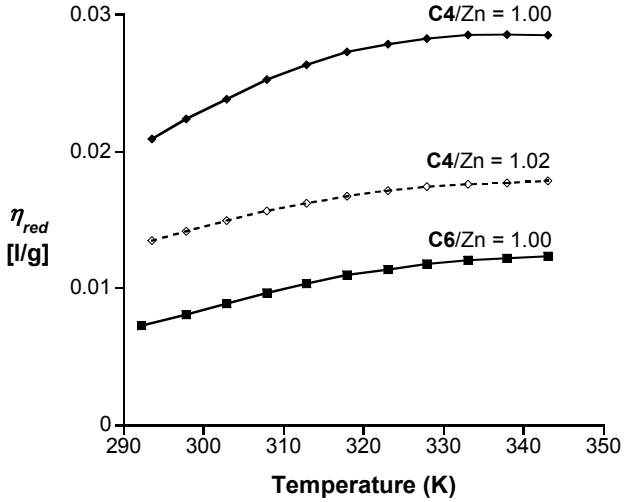

***Figure 15**: Reduced viscosity of ligands **C4** (37.8 mM) and **C6** (37.6 mM) as a function of temperature at a $Zn(ClO_4)_2$/ ligand ratio close to 1 in 0.1 M PIPES buffer pH 5.4.*

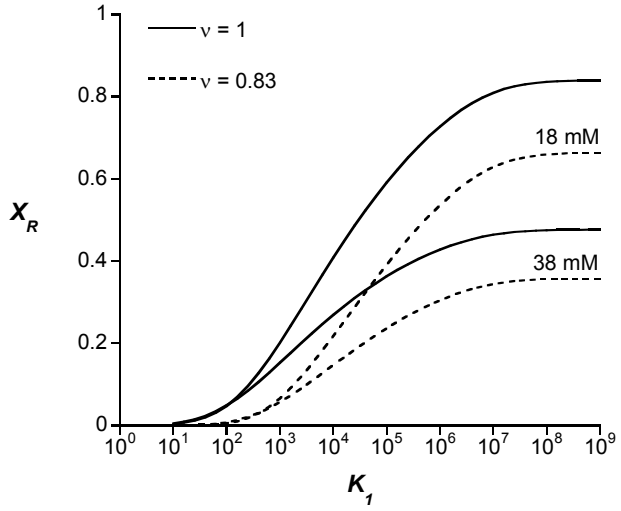

***Figure 16**: Calculated fraction of monomers in rings as a function of K_1 for $\nu = 0.83$ and $\nu = 1$ at two concentrations and $y = 1$. $K_2 = K_1/8$, $K_{a1} = K_1/50$, and $K_{a2} = K_1/2.5$.*

The effect of the temperature on the equilibrium between chains and rings, observed in the experiments, is a result of the variation of the stability constants K_1 and K_2 and the protonation constants K_{a1} and K_{a2} with temperature. With increasing temperature the stability constants become smaller. This results in a decrease of the fraction of monomers in rings, as shown in figure 16 for both monomers, at two concentrations and for $y = 1$. The ratio between the different stability constants K_1, K_2, K_{a1}, and K_{a2} was fixed in these calculations. (Note that, in reality, the various stability constants may have a different temperature dependence, so that the ratio between them may vary with temperature.) The fraction of rings X_R increases with K and reaches a plateau at high K values. In this region the values of the stability constants are not very important for the ring-chain equilibrium. The effect of the stability constants on the average length is shown in figure 17. It can be seen in this figure that for high values of the stability constants (low temperatures) the average length reaches a plateau. In this region, the calculations are not very sensitive to the K values. For small values of K_1, the average length decreases as K_1 decreases. At low monomer concentrations, the average length of the chains may increase slightly and pass a maximum with decreasing K_1 (or increasing temperature). The reason for this is that some of the rings open up and form chains that are somewhat larger. At higher concentrations this effect cannot be observed. The slight increase in the average length may be the reason for the observed increase in viscosity with increasing temperature. For the concentrations used in figure 15, however, such an increase could not be observed in the calculations. Nevertheless, the viscosity may still increase, even though the average length does not, because the contribution to

the viscosity of a ring of certain length is probably smaller than that of a chain of the same length, because the structure of a ring is more compact.

For a better interpretation of figure 15, it is necessary to know how the temperature affects the stability constants. We have assumed in the calculations that the ratio between the different stability constants remains constant, which is not necessarily true. We note furthermore that a decrease of the pH may have a similar effect as the temperature: the competition with protons also results in a decrease of the amount of rings, and may therefore also result in an increase in viscosity.

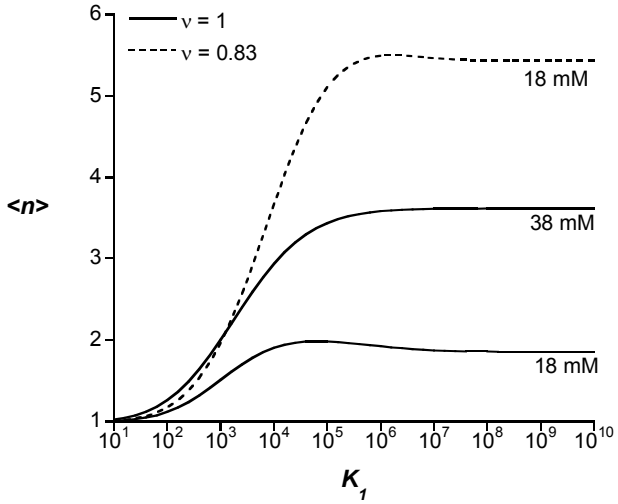

***Figure 17**: Calculated average length as a function of K_1 for $\nu = 0.83$ and $\nu = 1$ at two concentrations and $y = 1$. $K_2 = K_1/8$, $K_{a1} = K_1/50$, and $K_{a2} = K_1/2.5$.*

2.4.4 Spacer length dependence

In the previous three paragraphs the behavior of only two molecules differing in spacer length were described. Their behavior is very different and therefore we also synthesized **C5** and **C7.4**. **C5** has five ethylene oxide units and **C7.4** is a mixture of bifunctional ligands with an average of 7.4 ethylene oxide units. Figure 18 displays the viscosity as a function of the molar ratio for all four compounds at approximately 36 mM. **C5** and **C6** yield basically the same curves. This means that **C5** is able to form monomer rings as well. **C7.4** gives a viscosity between **C4** and **C5**/**C6**. Obviously, **C7.4** is long enough to form monomer rings. However, for entropic reasons the formation of rings is not as favorable as for **C5** and **C6**. The longer the spacer becomes, the smaller the probability that two ends of one molecule meet one another. For that reason, **C7.4** forms relative more chains than **C5** and **C6**. This was also shown with ^{1}H NMR measurements. Figure 19 shows the fraction of chains as a function of concentration for all compounds determined by ^{1}H NMR. **C5** and **C6** give

again similar results. **C4** forms much less rings, and **C7.4** is in between. Hence, the NMR results are completely in line with the viscosity experiments.

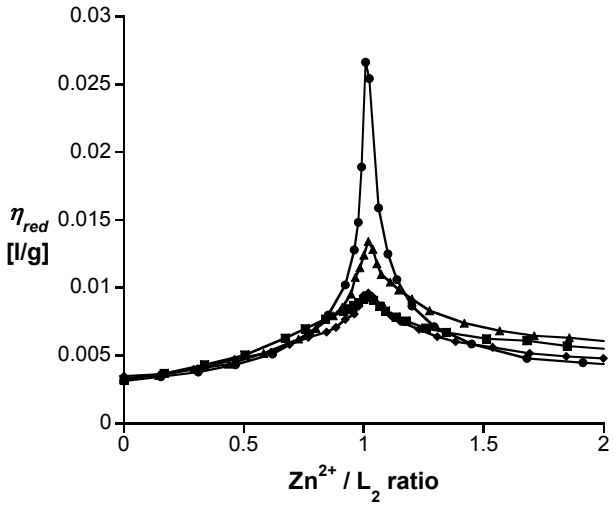

***Figure 18**: Reduced viscosity of ligands as a function of molar ratio $Zn(ClO_4)_2$/ ligand in 0.1 M PIPES buffer pH 5.4 at 298 K for ligand **C4** (37.8 mM, •), **C5** (35.0 mM,♦), **C6** (34.5 mM, ▪), **C7.4** (35.6 mM, ▲).*

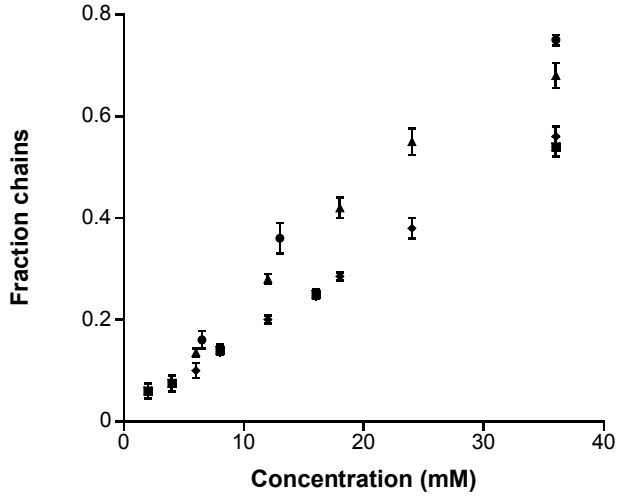

***Figure 19**: Fraction of chains of ligands **C4** (•), **C5** (♦), **C6** (▪) and **C7.4** (▲) as a function of concentration in D_2O at a $Zn(ClO_4)_2$/ ligand ratio of 1 at 298 K, determined from the integrals of the peaks in ^1H NMR spectra.*

A final remark should be made. These experiments show that **C5** is able to form monomer rings. The length of this molecule is smaller than the length of **C6**. In the theoretical model the length of **C6** was used as the Kuhn length, because these molecules are just able to form monomer rings. Looking at the results of **C5**, the

Kuhn length in the model should be a little bit smaller. Nevertheless, we did not change the model, since the model fits nicely with the results of **C4** and **C6** and the model was developed mainly to show the effect of ring formation. In the derivation of the length distribution of rings, we have assumed that the polymers can be described as Gaussian chains, which is a reasonable assumption for long chains. However, since the average length reaches only a few Kuhn segments (see figure 7), this assumption is certainly not valid. Therefore, we expect that the calculated data are not quantitatively correct for these small monomers, and we do not try to calculate viscosities from the theoretical data to make a more direct comparison. The qualitative agreement between the experiments and the calculations is very encouraging however. In principle, a more thorough comparison between the model and experiments should be possible for monomers with a longer spacer ($\nu >> 1$), for which the Gaussian approximation is better.

2.4 Concluding remarks

In this chapter, we presented coordination polymers that are water-soluble at every metal:ligand ratio. The reversibility of the coordinative bonds is evident from the dependence of the viscosity and ^{1}H NMR measurements on the concentration and molar ratio. For monomers with a spacer that is just long enough to form an intramolecular complex without strain, rings are dominant at low concentrations. This causes a minimum in the viscosity at a 1:1 metal:ligand ratio. The ring fraction at a 1:1 ratio of metal ions and ligands decreases with both increasing concentration and increasing temperature and it is lower for monomers with a shorter spacer. Reversible ring opening at higher temperatures causes an increase in viscosity, which is a rare phenomenon.

A model developed by Jacobson and Stockmayer was used to calculate the molecular weight distributions of chains and rings. The model is in qualitative agreement with the experimental results. In principle, a more direct comparison between theory and experiments would be possible for monomers with a longer spacer, for which the Gaussian chain assumption, adopted in the model, is better.

2.5 Experimental section

All commercial chemicals were obtained from Acros or Aldrich and were used as received. Chelidamic acid was purchased from Acros. Diethyl 4-hydroxypyridine-2,6-dicarboxylate[21] and dibromooligoethylene oxide[22] (tetra, penta, hexa and oligo) were prepared according to literature. ^{1}H NMR (200 MHz) and ^{13}C NMR spectra

were recorded on a Bruker AC-E 200 spectrometer. DOSY NMR (400 MHz) spectra were recorded and calculated using standard Bruker software on a Bruker DPX 400 spectrometer at room temperature. Isothermal titration calorimetry measurements are performed on a Microcal MCS ITC. Viscosity measurements were performed in a 100 mM 1,4-piperazinebis(ethanesulfonic acid) buffer (PIPES) pH 5.4, on a LAUDA Processor Viscosity System PVS1. The reduced viscosity is defined as the specific viscosity divided by the ligand concentration *C* in grams per liter, $\eta_{red} = \eta_{sp}/C = (\eta_s - \eta_0)/(\eta_0.C)$ with η_s the viscosity of the sample and η_0 the viscosity of the solvent.

Synthesis of 1,11-bis(2,6-dicarboxypyridin-4yloxy)-3,6,9-trioxaundecane, C4.

Diethyl 4-hydroxypyridine-2,6-dicarboxylate (2.99 g, 12.5 mmol), 6.25 mmol of dibromo-tetra-ethylene oxide and 4.2 g K_2CO_3 were refluxed in 2-butanone for 3 days under N_2 atmosphere. The reaction can be followed by TLC analysis using 5% MeOH in CH_2Cl_2 as eluents. The solvent was removed, and a 1:1 mixture of ethanol-water was added. This mixture was stirred overnight at 70 ºC. The resulting water-soluble product was purified by C_{18} reversed-phase chromatography (40 μm prep. LC) using water as eluent. This purification step was repeated several times. Compound **C4** was purified further using size exclusion chromatography (Sephadex G10, water as eluent). The product was freeze-dried.

For compounds **C5**, **C6** and **C7.4** the same procedure was followed. These products were pure after chromatography over a C_{18} reversed-phase column and purification based on size exclusion was not required.

For the spacer of **C7.4** an oligoethylene oxide (average M_n ca. 400) was used. The OH-groups were replaced by bromines using PBr_3.[22] To purify the brominated ethyleneoxides, they were extracted into diethyl ether. The longest ethyleneoxides are more polar and are less easily extracted into the organic phase than the shorter ones. When we stopped extracting, we obtained a brominated ethylene oxide with an average of 7.4 ethylene oxide units and used this for the preparation of the final ligands according to the method described above. Upon further extraction of the aqueous layer longer brominated ethylene oxides can be obtained in the organic layer.

The number of the ethylene oxide units in the spacer of compound **C7.4** ranges from six to nine ethyleneoxides. This was determined based on elution volume on a C_{18} reversed phase column and compared with similar monodisperse compounds (4, 5, 6, 12 ethylene oxide units).

C4: yield 20% (mp > 300 ºC). ^{1}H NMR (D_2O): δ 3.50 (8H, m, CH_2O), 3.71 (4H, t, CH_2O), 4.14 (4H, t, CH_2O), 7.33 (4H, s, aromatic H), ^{13}C-NMR (D_2O): δ 69.68, 70.73, 71.65, 71.84, 113.64, 156.18, 169.28, 173.83.

C5: yield 24% (mp > 300 ºC). ^{1}H NMR (D_2O): δ 3.43 (12H, m, CH_2O), 3.74 (4H, t, CH_2O), 4.17 (4H, t, CH_2O), 7.36 (4H, s, aromatic H). ^{13}C NMR (D_2O) : δ 70.10, 71.07, 71.99, 72.05, 72.21, 114.08, 156.43, 169.77, 173.95.
C6: yield 18% (mp > 300 ºC). ^{1}H NMR (D_2O): δ 3.46 (16H, m, CH_2O), 3.71 (4H, t, CH_2O), 4.14 (4H, t, CH_2O), 7.34 (4H, s, aromatic H). ^{13}C NMR (D_2O) : δ 69.88, 71.05, 71.97, 72.09, 72.10, 72.12, 113.88, 156.90, 169.26, 173.81.
C7.4: Yield 21% (mp > 300 ºC). ^{1}H NMR (D_2O): δ 3.44 (21.6 H, m, CH_2O), 3.74 (4H, t, CH_2O), 4.18 (4H, t, CH_2O), 7.39 (4H, s, aromatic H). ^{13}C NMR (D_2O): δ 70.75, 71.04, 71.08, 72.10, 72.12, 72.33, 72.39, 115.41, 157.18, 169.31, 173.92.

2.6 References

1. Lehn, J.-M. *Supramolecular Chemistry, Concepts and Perspectives*; VCH: Weinheim, **1995**.
2. Ciferri, A. *Supramolecular polymers*; Marcel Dekker: New York, **2000**.
3. Brunsveld, L.; Folmer, B. J. B.; Meijer, E. W.; Sijbesma, R. P. *Chem. Rev*. **2001**, *101*, 4071–4097.
4. Zimmerman, N.; Moore, J. S.; Zimmerman, S. C. *Chem. Ind*. **1998**, 604–610.
5. Whitesides, G. M.; Mathias, J. P.; Seto, C. T. *Science* **1991**, *254*, 1312–1319.
6. Fogleman, E.A.; Yount, W.C.; Xu, J.; Craig, S.L. *Angew. Chem. Int. Ed.* **2002**, *41*, 4026-4028.
7. Chen, H. C.; Cronin, J. A.; Archer, R. D. *Macromolecules* **1994**, *27*, 2174–2180.
8. Kelch, S.; Rehahn, M. *Macromolecules* **1997**, *30*, 6185–6193.
9. Bernhard, S.; Takada, K.; Déaz, D. J.; Abrũna, H.D.; Mürner, H. *J. Am. Chem. Soc.* **2001**, *123*, 10265–10271.
10. Velten, U.; Rehahn, M. *Chem. Commun.* **1996**, 2639–2640.
11. Velten, U.; Lahn, B.; Rehahn, M. *Macromol. Chem. Phys.* **1997**, *198*, 2789–2816.
12. Lahn, B.; Rehahn, M. *e-Polymers*, **2002**, *1*, 1-33.
13. Schütte, M., Kurth, D.G., Linford, M.R., Cölfen, H., Möhwald, H. *Angew. Chem. Int. Ed.* **1998**, *37*, 2891-2893.
14. Schubert, U.S.; Eschbaumer, C. *Angew. Chem. Int. Ed.* **2002**, *41*, 2892-2926.
15. Schubert, U.S.; Eschbaumer, C. *Polymer Preprints* **2000**, *41*, 676-677.
16. Jacobson, H.; Stockmayer, W.H. *J. Chem. Phys.* **1950**, *18*, 1600-1606.
17. Flory, P.J. *Chem. Rev.* **1946**, *39*, 137.
18. Kuhn, W. *Kolloid Z.* **1934**, *68*, 2
19. Shimada, J.; Yamakawa, H. *Macromolecules* **1984**, *17*, 689-698.
20. Cates, M. E.; Candau, S. J. *J. Phys. Condens. Matter* **1990**, *2*, 6869.
21. Chessa, G.; Scrivanti, A. *J. Chem, Soc., Perkin Trans 1* **1996**, 307-311.
22. Liu, S.-G.; Liu, H.; Bandyopadhyay, K.; Gao, Z.; Echegoyen, L. *J. Org. Chem.* **2000**, *65*, 3292-3298.
23. Anderegg, G. *Helv. Chim. Acta* **1960**, *43*, 414-424.
24. Johnson Jr., C.S. *Prog. Nucl. Magn. Spectrosc.* **1999**, *34*, 203-256.
25. St. Poucain, C.B.; Griffin, A.C. *Macromolecules* **1995**, *28*, 4116-4121.

26. Folmer, B.J.B.; Sijbesma, R.P.; Meijer, E.W. *J. Am. Chem. Soc.* **2001**, *123*, 2093-2094.
27. Söntjens, S.H.M.; Sijbesma, R.P.; Van Genderen, M.H.P.; Meijer, E.W. *Macromolecules* **2001**, *34*, 3815-3818.

Three-dimensional water-soluble reversible neodymium(III) and lanthanum(III) coordination polymers

Chapter 3

*The formation of soluble supramolecular three-dimensional coordination polymers with Nd^{3+} and La^{3+} in aqueous solution is studied for two bifunctional ligands, consisting of two pyridine-2,6-dicarboxylate groups connected at the 4-position by a tetra- or hexa-ethylene oxide spacer (**C4** and **C6** respectively). Viscosity measurements were used to monitor the network formation as a function of the ligand concentration and the ratio between metal ions and ligands. For corresponding conditions **C4** solutions with Nd^{3+} always gave much higher viscosities than **C6** solutions with Nd^{3+}. **C6** is long and flexible enough to bind with both chelating groups to only one metal ion (ring-formation). This causes the polymers to stop growing, resulting in smaller average sizes of the three-dimensional polymers. The ring-structures could be demonstrated by ^1H NMR spectroscopy using **C6** and La^{3+} at low concentrations.*

This chapter was published in slightly modified form: Vermonden, T.; De Vos, W. M.; Marcelis A. T. M.; Sudhölter E. J. R. *Eur. J. Inorg. Chem.* **2004**, 2847-2852.

3.1 Introduction

In the past few decades the field of supramolecular chemistry has grown into an important part of chemistry related science. Supramolecular structures can be built using several non-covalent intermolecular interactions such as hydrogen bonding, π–π-stacking interactions, Van der Waals interactions and coordinative bonding (metal-ligand bonding).[1]

Metal-ligand bond strengths span a wide range with the strength depending on both the metal ion and the ligand. In some cases the bond strengths are comparable to covalent bonds.[1] The reversibility of the binding can be tuned by the choice of solvent. When a coordinating solvent such as water or acetonitrile is used the reversibility of the binding increases.[2,3]

In chapter 2, we described the reversible formation of linear polymers in aqueous solutions of Zn^{2+} ions with bifunctional ligands, consisting of two terdendate pyridine-2,6-dicarboxylate groups connected through a tetra- or hexa-oligoethylene oxide spacer, **C4** and **C6**, respectively.[4] The bifunctional ligands can form not only linear polymers through metal ion coordination, but also rings. The rings can be formed by one ligand molecule and one metal ion (monomer rings), if a long and flexible spacer links the ligand groups. If the spacer is shorter or less flexible, at least two ligand molecules and two metal ions are necessary to form rings (dimer and larger rings). We showed that the amount of rings depends on spacer length, concentration, temperature and the molar ratio of metal ions/ligand molecules (M/L).[4] The total amount of rings is much higher when the ligand is long enough to form monomer rings than when only dimer and larger rings can be formed. The larger the rings become, the smaller the probability of them being formed. Consequently, the amount of small rings will always be higher than the amount of larger rings. When the molecules are able to form monomer rings, there will still be dimer and larger rings present in solution, but their relative amounts will be much smaller. This also means that when two ligand molecules differing in spacer length are compared, the solution with molecules able to form monomer rings will show a greater overall formation of rings than the solution with molecules able to form only dimer and larger rings.[5]

The rings are dominant at low concentration, where the probability of meeting a ligand group of another molecule is smaller than at high concentrations. On going from a low to a high concentration, mainly rings are formed in the first instance and after reaching a critical concentration, linear polymers are formed besides the rings.[6] The total amount of rings stays approximately the same, but the amount and average length of linear polymers increases. By considering the relative amounts we can say

that rings play an important role at low concentrations, but can be ignored at high concentrations. The relation between the formation of rings and linear chains for coordination polymers is not studied much,[7] but more so for reversible hydrogen bonded supramolecular polymers.[8-10]

Another very important role in the equilibrium between rings and linear polymers is the molar ratio between metal ions and ligand molecules (M/L). The ideal ratio to form linear polymers is one, but this is also the ideal ratio for ring formation. Overall it can be said that the influence of rings is largest at a molar ratio of unity and at low concentrations.[4]

In the field of coordination chemistry, the interest in the lanthanide metal ions has grown considerably in the last two decades. Because of their larger size, lanthanide ions can generally support higher coordination numbers than transition metal ions. Not many self-assembled structures of lanthanide ions in solutions have been reported,[11,12] although some lanthanide-containing helicates have been reported in water.[13-15] A few lanthanide coordination polymers having a three-dimensional network have also been reported, but mainly solid state properties have been studied.[16-20]

In this chapter, we describe the reversible formation of three-dimensional polymers of the bifunctional ligands, **C4** and **C6**, with Nd^{3+} and La^{3+} ions. Neodymium(III) and lanthanum(III) both belong to the lanthanide ions and are large enough to form complexes with three terdendate ligands (9-coordination).[21] Compared with first-row transition metal ions like Zn^{2+} or Ni^{2+}, which give 6-coordination with terdendate ligands, Nd^{3+} and La^{3+} can bind an additional ligand group by self-assembly, which makes the formation of a three-dimensional network possible. Additionally, we show that the possibility to form rings plays an important role in this system.

3.2 Results and discussion

The ligands we used are **C4** and **C6**, displayed in figure 1. The complexing groups are based on 2,6-pyridine-dicarboxylic acid. The complexation behavior of this group has been well studied with numerous metal ions. The complexation constants (*pK*) of the subsequent binding of three 2,6-pyridine-dicarboxylic acid molecules to one Nd^{3+} ion are 8.78, 6.72 and 5.06 as reported by Grenthe.[22]

In our study we did not verify these stability constants but only the stoichiometry of binding. This was done using a monofunctional ligand with only an ethoxy group at the 4-position of the pyridine moiety in an isothermal titration calorimetric experiment (ITC). As can be seen in figure 2, an inflection point was found at a molar

ratio Nd^{3+}/monoligand of 0.33. This experiment confirms that the Nd^{3+} center is surrounded by three terdendate monofunctional ligands.

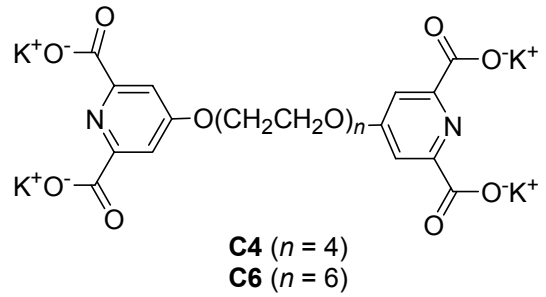

Figure 1: *Bifunctional ligands **C4** and **C6**.*

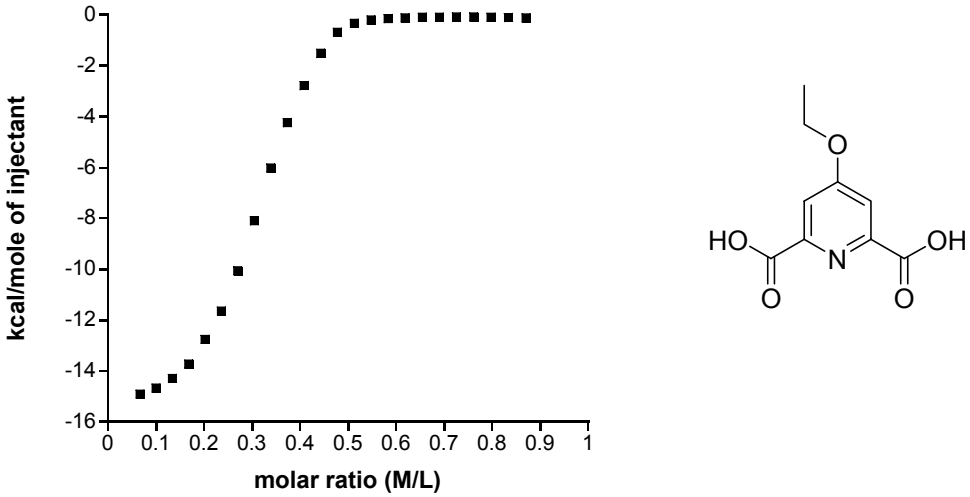

Figure 2: *ITC-curve of monofunctional ligand, 4-ethoxy-2,6-pyridine-dicarboxylic acid, (1.07 mM in cell) and $Nd(NO_3)_3$ (9.65 mM in burette) in a 0.1 M PIPES buffer pH 5.4 at 298 K.*

In chapter 2, we showed that ligands **C4** and **C6** display different behavior towards Zn^{2+} although they only differ in spacer length (tetra ethylene oxide vs. hexa ethylene oxide).[4] One **C6** molecule is long enough to form a ring around one zinc ion (monomer ring). On the other hand, **C4** cannot form a monomer-ring and needs at least two ligand molecules and two zinc ions to form a ring. This implies that the total amount of rings formed is much higher when **C6** is used than **C4** at all concentrations as explained in section 3.1.

The situation is different when Nd^{3+} is used instead of Zn^{2+}. The ligands will still form rings with the metal ion and **C6** more so than **C4**, but the metal ion has still one binding site left. This makes the system more complicated. Although monomer rings alone will not be present anymore, they can act as chain stoppers as shown in figure 3a. **C4** is shorter and therefore similar chain-stopping rings cannot be formed; the

smallest possible rings do not prevent the polymer from growing longer as shown in figure 3b.

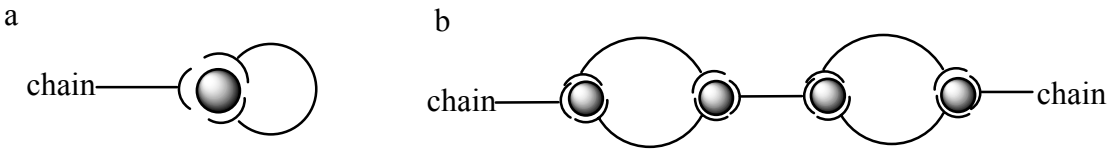

Figure 3: *Schematic representation of the smallest possible rings for* ***C6*** *(a) and* ***C4*** *(b) and their influence on polymer formation.*

Viscosity measurements were used to study the solution properties as a function of the molar ratio. We titrated a ligand solution in a 0.1 M PIPES buffer pH 5.4 with an $Nd(NO_3)_3$ solution in the same buffer. A precipitate was always initially formed upon the addition of neodymium ions, but this completely dissolved after mixing. After each addition the viscosity was measured. Above a molar ratio M/L of 1 the precipitate did not dissolve anymore and no viscosities could be measured above that ratio. At much larger ratios (M/L > 2) precipitates easily dissolved again upon shaking. In figure 4 the reduced viscosity of **C4** and Nd^{3+} is plotted as a function of the molar ratio at three different concentrations of ligand (20.0 mM; 36.7 mM and 53.6 mM). We found a peak in the viscosity at a molar ratio of about 2:3 (metal:ligand), which can be expected when mixing a bifunctional ligand with a metal ion capable of binding three ligand groups. However, the most noticeable fact is the enormous effect of concentration. At the lowest concentration (20 mM) the highest reduced viscosity is 0.017 l/g. When the concentration is increased further to 37.6 mM, the highest reduced viscosity is already 0.071 l/g, and when the concentration is increased to 53.6 mM, the reduced viscosity goes up to at least 2.5 l/g. This shows that the size of the aggregates increases enormously with concentration through the formation of three-dimensional networks. The presence of a peak shows that the process is reversible; an excess of metal ions (> 0.67) causes the network to break down.

Upon close inspection of the graphs it can be seen that the peak is a little shifted compared to the 2:3 ratio. With increasing concentration the peak shifted to a slightly higher molar ratio. We will explain this after discussing the viscosity plots of **C6**.

Figure 5 shows the viscosity of **C6** and Nd^{3+} as a function of molar ratio at four different concentrations. Most noticeable here is that although the viscosity increases with increasing concentration, this effect is much smaller than observed for **C4**. The curves are also much more asymmetric than the ones of **C4**. Another effect is the clear shift of the peak to higher molar ratios with increasing concentration. This shift

is larger than for **C4**. The shifts of the peaks are plotted in figure 6 for both ligands as a function of concentration.

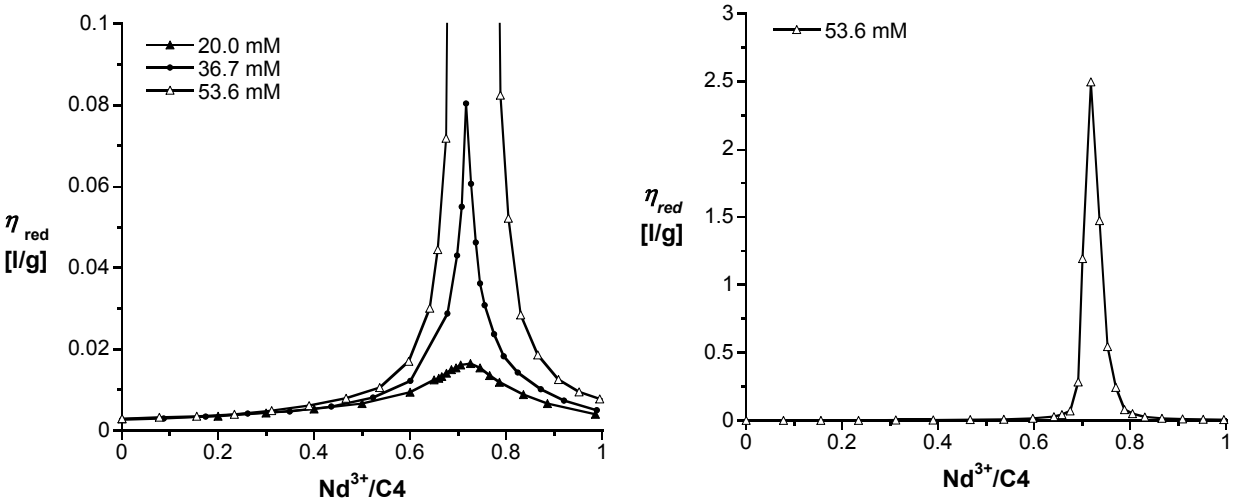

***Figure 4**: Reduced viscosity of **C4** as a function of molar ratio $Nd(NO_3)_3$/**C4** in 0.1 M PIPES buffer pH 5.4 at 298 K at different concentrations.*

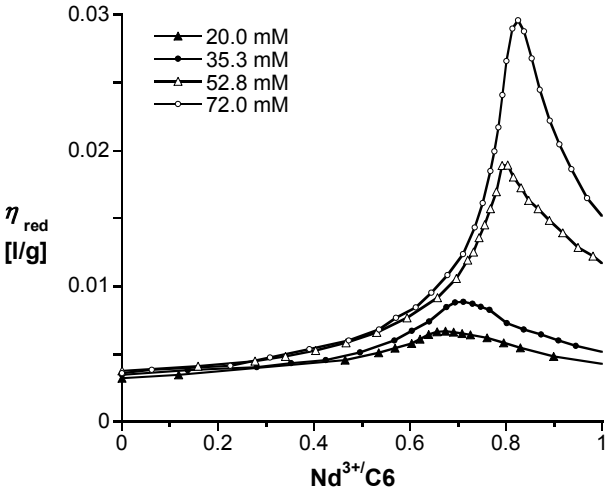

***Figure 5**: Reduced viscosity of **C6** as a function of molar ratio $Nd(NO_3)_3$/**C6** in 0.1 M PIPES buffer pH 5.4 at 298 K at different concentrations.*

The explanation for the low viscosity, asymmetric curves and the large shift of the peak of **C6** compared to **C4** can only be found in the much stronger tendency of **C6** to form small rings. Since **C6** is able to form monomer rings, which can act as chain stoppers (see figure 3a), the structures cannot grow as large as for **C4**. This causes the much lower viscosity of **C6** and Nd^{3+} at all concentrations. The ideal molar ratio for formation of those rings is 0.67. At larger molar ratios (M/L) the amount of

the rings decreases, allowing the formation of longer chains and therefore the highest reduced viscosity is reached at higher molar ratios. This also explains the asymmetric curves. At higher molar ratios (above 0.67) the rings open and become part of the polymers. This effect contributes to higher viscosities. However, at these higher molar ratios, the metal ions will not all be coordinated to three chelating groups, which causes the viscosity to drop. Both effects counteract each other, leading to a slower decrease in viscosity than expected based on only the explanation of the excess of metal ions.

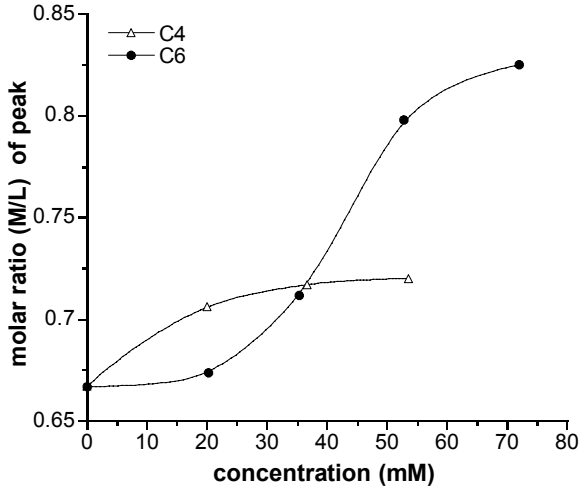

Figure 6: *Molar ratio at the highest viscosity of solutions of **C4** and **C6** with Nd^{3+} as a function of concentration.*

C4 also shows a shift in the viscosity peak, but it is much smaller. The origin of the shift here can, however, not be found in end capping by ring formation, since the rings can be part of a polymer chain (see figure 3b). Therefore, the shift found for **C4** has an explanation different from that for **C6**. The shift for **C4** may be explained by the fact that more expanded structures can be formed when not every metal ion is complexed with three ligand groups in a three-dimensional network. This expansion causes a higher viscosity even though the molar mass of the structures is not larger. Expanded polymers take a larger volume and therefore their solutions give higher viscosities than solutions of polymers with the same length but that are more compact.

For **C4** a concentration dependent viscosity plot was also measured at a constant molar ratio of M/L = 0.71, corresponding to the average molar ratio of the top of the peak at concentrations above 20 mM. Although the top of the peak for concentrations below 20 mM is lower than at M/L = 0.71, the influence of this is negligible due to the broadness of the peak at lower concentrations. This plot is

shown in figure 7 to illustrate the enormous effect of concentration on the viscosity and thus on the size of the self-assembled structures. With increasing concentration the influence of the rings becomes smaller and the three-dimensional polymers become larger, resulting in the steep increase in viscosity (see figure 8).

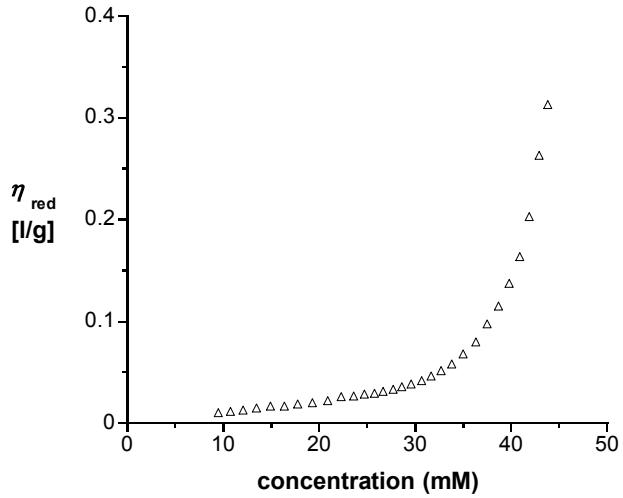

Figure 7: *Reduced viscosity of **C4** as a function of concentration at an $Nd(NO_3)_3$/ligand ratio of 0.71 in 0.1 M PIPES buffer pH 5.4 at 298 K.*

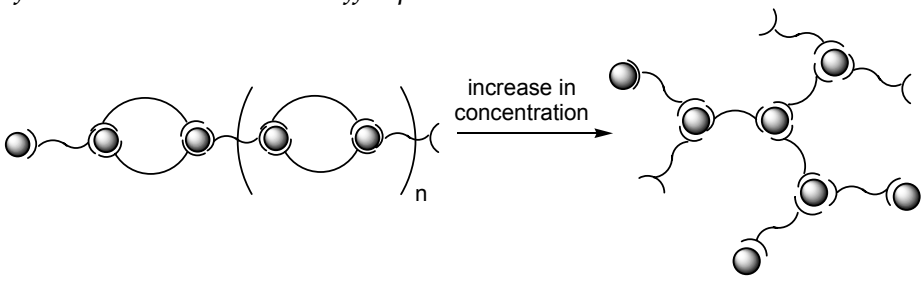

Figure 8: *Changes in the structures of **C4**/Nd^{3+} coordination aggregates as a function of concentration.*

Some NMR experiments were performed in order to examine more closely the shift of the peaks in the viscosity plots with respect to the molar ratio. The different causes for the shifts for **C6** and **C4** can be illustrated by ^{1}H NMR experiments. These experiments were performed using lanthanum(III) as metal ion instead of neodymium(III), because neodymium broadens the signals in the spectrum. La^{3+} has properties similar to those of Nd^{3+}. They both belong to the lanthanides and are known to exhibit 9-coordination.[21,22] The stoichiometry was checked by isothermal titration calorimetry and showed indeed that three ligand groups are bound to one lanthanum ion. The curve was less steep than shown in figure 2 for neodymium due to lower complexation constants, which is in agreement with reported values in literature. The reported complexation constants (*pK*) of La^{3+} with three dipicolinic

acid molecules (structure of complexing group similar to the ones we use) are: 7.98, 5.81 and 4.27.[22]

The reduced viscosity plots of both metal ions give comparable results for both ligand molecules. At the measured concentrations a similar shift of the peak with respect to the molar ratio is found for both Nd^{3+} and La^{3+} and for both ligands. However, the viscosity of the ligands with lanthanum was found to be lower than with neodymium (figure 9). This can be explained by the lower complexation constants of the ligand groups with La^{3+} than with Nd^{3+}.

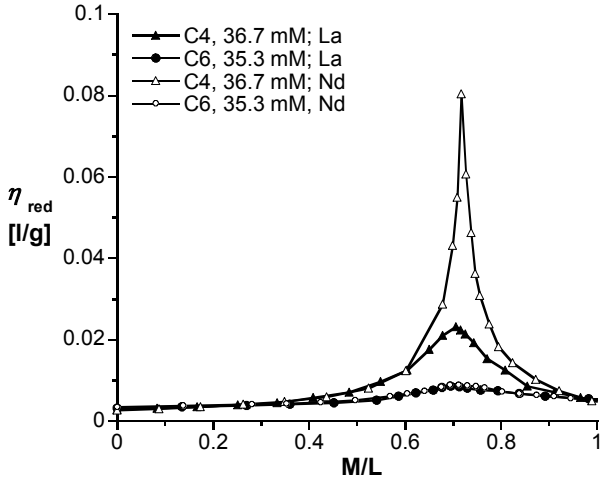

Figure 9: *Reduced viscosity of **C4** (triangles) and **C6** (circles) as a function of molar ratio $Nd(NO_3)_3$/ligand (open) and $La(NO_3)_3$/ligand (full) in 0.1 M PIPES buffer pH 5.4 at 298 K.*

The NMR-spectra in D_2O were recorded for both ligands as a function of concentration at a M/L ratio of 0.71 and as a function of M/L ratio at a ligand concentration of 40 mM. A precipitate was also formed upon addition of La^{3+} ions to a ligand solution, but this subsequently dissolved after mixing. For ligand **C4** few changes occur in the spectra when metal ions are added to a 40 mM solution of **C4** in D_2O at pH 5.8 (figure 10). The signals between δ = 3.0 and 4.5 ppm originate from the OCH_2 protons in the spacer, the signal at approximately δ = 7.4 ppm originates from the aromatic protons in the pyridine ring. The signals became a little broader upon addition of La^{3+} ions, but no new signals appear. The aromatic signal at δ = 7.35 ppm also shifted to 7.45 upon complexation up to a molar ratio of 0.72. Above that ratio, this signal shifts back to δ = 7.40 ppm. The proton signals of the spacer shift a little to high field. The broadening of signals instead of the formation of separated signals for free and coordinated ligand upon addition of metal ions points to an exchange process between the ligand molecules at a moderate rate on the NMR time scale.[23]

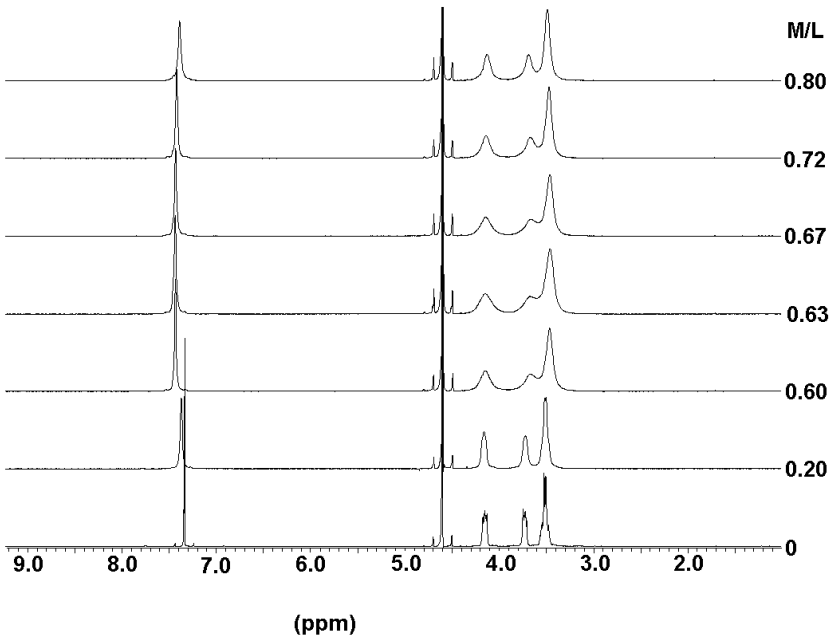

Figure 10: *^{1}H NMR spectra of compound **C4** with La^{3+} at 40 mM in D_2O at 298 K, pH 5.8 at various molar ratios.*

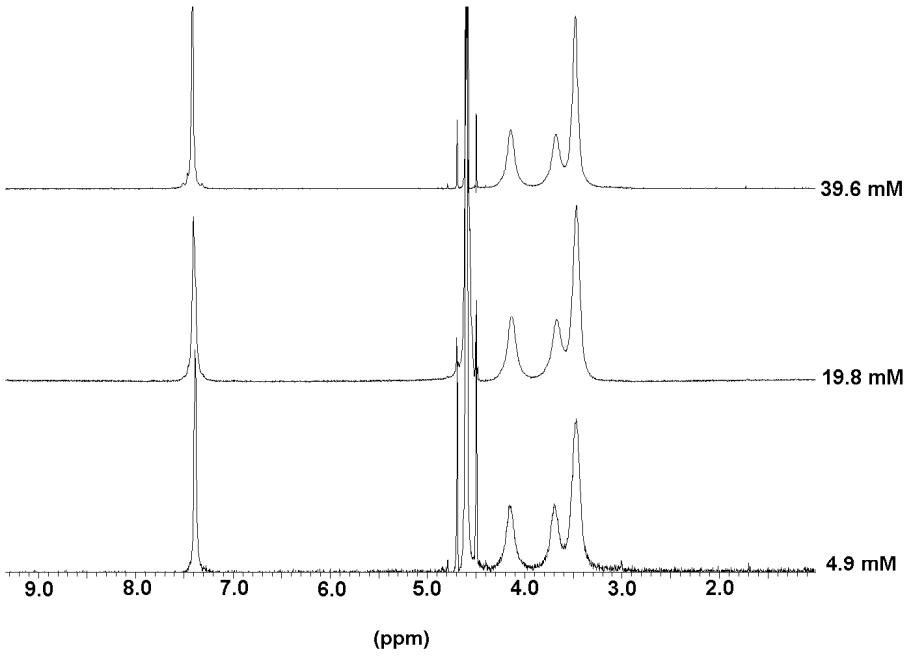

Figure 11: *^{1}H NMR spectra of compound **C4** with La^{3+} at molar ratio of 0.71 in D_2O at 298 K, pH 5.8 at various concentrations.*

No significant changes occur in the ^{1}H NMR-spectra upon dilution of a solution with a constant metal/ligand ratio of 0.71 in D_2O (figure 11). This implies that at all concentrations either the exchange between different species is fast, or that only one kind of species (three dimensional polymers) is present.

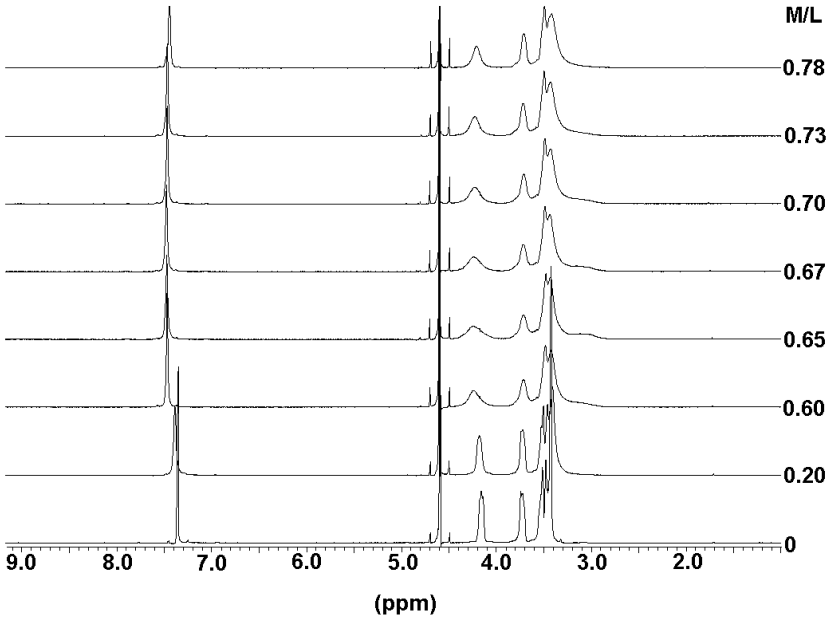

***Figure 12**: ^1H NMR spectra of compound **C6** with La^{3+} at 40 mM in D_2O at 298 K, pH 5.8 at various molar ratios.*

For **C6** a new signal appears both in the molar ratio dependent spectra (figure 12) and in the dilution spectra (figure 13). We observed the new signal as a broad bump in the molar ratio dependent series at δ = 3.1 ppm with the highest intensity at a molar ratio of 0.67. The highest amount of small ring-like species would be expected at a molar ratio of 0.67, which is the ideal ratio to form rings around metal ions with 9-coordination. These small structures containing many rings could for example look like the representation in figure 14.

We indeed observed that upon increasing the molar ratio the bump became bigger until a molar ratio of 0.67. This signal in the NMR spectrum is therefore most likely caused by the structure of the rings. At higher ratios the height of the bump decreases rapidly, because here larger open structures are more dominantly present. The larger structures do not seem to give unique signals; they cause only broadening and slight shifting of the signals, which are also present without metal ions. The broadening of the signals is itself an indication of the formation of large structures. The disappearance of the "ring-signal" at δ = 3.1 ppm above M/L = 0.67 is in agreement with the viscosity plots. Here the viscosity increases above a molar ratio of 0.67 due to the opening of ring structures, which contribute to larger structures with higher viscosity. Since we did not see this "ring-signal" in the NMR-spectra of **C4**, the presence of these kinds of structures can be ruled out here. This is logical, because **C4** is not long and flexible enough to act as a chain stopper.

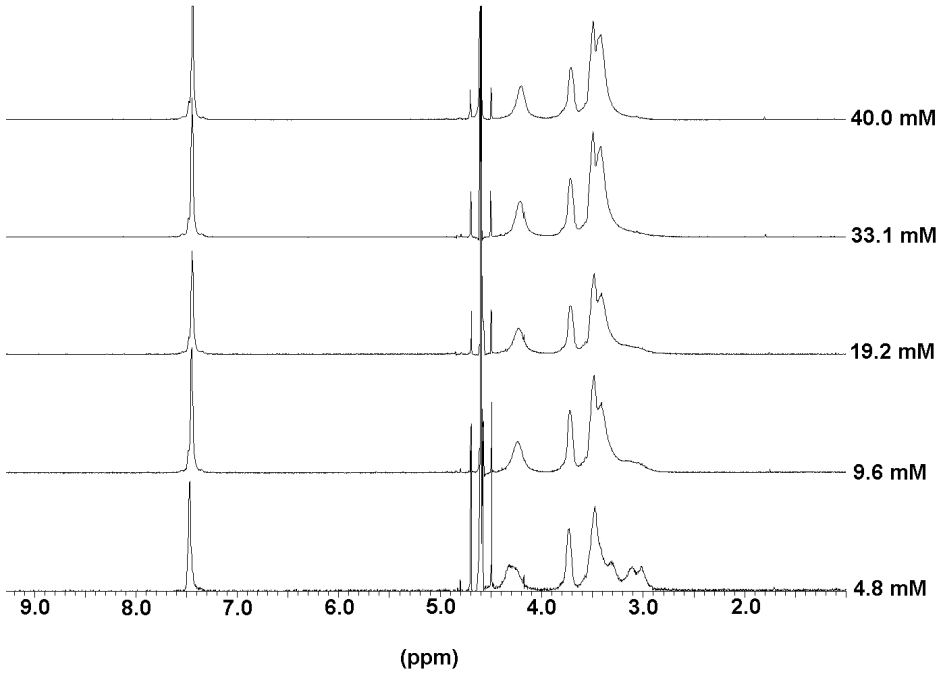

***Figure 13**: ^1H NMR spectra of compound **C6** with La^{3+} at molar ratio of 0.71 in D_2O at 298 K, pH 5.8 at various concentrations.*

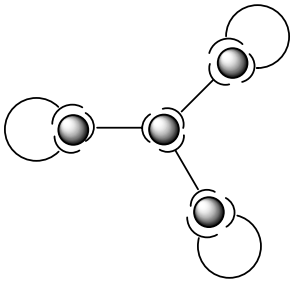

***Figure 14**: Schematic representation of an example of a small structure containing multiple rings that can be formed by **C6** and La^{3+} ions at low concentrations and a molar ratio (M/L) close to 0.67.*

In the dilution series (figure 13) no clear signal is found at 3.1 ppm at 40 mM, but a broad bump is coming up starting from about 20 mM, which becomes resolved into two peaks at about 5 mM. Upon dilution the only species that can become dominant in this system are chain-stopping rings. At low concentration the probability of a ligand meeting another metal ion is small and therefore more rings are formed using only one metal ion to bind both chelating groups of a ligand molecule.

3.3 Conclusions

In this chapter, we described water-soluble lanthanide containing reversible coordination polymers and the viscosities of their aqueous solutions as a function of

both the concentration and the molar ratio of metal ions/ligands. The investigated bifunctional ligands self-assemble in aqueous solution in the presence of neodymium and lanthanum ions to give reversible polymers or networks. The use of these ligands in combination with lanthanide ions gives rise to much higher viscosities than when transition metal ions like zinc are used, that yield linear coordination polymers and rings.[4] A comparison of the viscosity and ^{1}H NMR spectra of **C4** and **C6** shows that under the same conditions **C6** always gives smaller structures with lanthanide ions than **C4**. Ligand **C6** has a long enough spacer to bend around one metal ion. In this way it can act as a chain-stopper, which causes the structures to stop "growing" and remain small. The ideal metal to ligand ratio for formation of these rings is at 0.67. The opening of the rings at higher M/L ratios causes a rather asymmetrical curve and a shift of the peak in the molar ratio dependent viscosity plots. The ring structures can also be seen in the ^{1}H NMR spectra of **C6** at low concentrations and at a molar ratio close to 0.67, giving separate signals at approximately δ = 3.1 ppm. The ^{1}H NMR spectra of **C4** do not show this signal at any concentration or molar ratio. Also in the viscosity plots the shifts of the peaks with respect to the molar ratio are much smaller and the curves are more symmetrical, showing that rings acting as chain-stoppers are not present here. Coordination structures formed by **C4** and neodymium are therefore able to become much larger. The small shifts of the viscosity peaks here originate from expansion of the structures when metal ions are only slightly in excess.

3.4 Experimental section

The syntheses of compounds **C4** and **C6** are reported in chapter 2.[4] All commercial chemicals were obtained from Acros or Aldrich and were used as received. ^{1}H NMR (200 MHz) spectra were recorded on a Bruker AC-E 200 spectrometer. Isothermal titration calorimetry measurements are performed on a Microcal MCS ITC with a cell volume of 1.353 ml. The experiments were performed using injections of 5 μl and 250 seconds between injections and a reference offset of 60%. Viscosity measurements were performed in a 100 mM 1,4-piperazinebis(ethanesulfonic acid) buffer (PIPES) pH 5.4 on a Schott AVS 360 capillary viscosimeter. The reduced viscosity is defined as the specific viscosity divided by the ligand concentration C in grams per liter, i.e., $\eta_{red} = \eta_{sp}/C = (\eta_s - \eta_0)/(\eta_0.C)$ with η_s being the viscosity of the sample and η_0 the viscosity of the solvent.

3.5 References

1. Lehn, J.-M. *Supramolecular Chemistry*; VCH: Weinheim, **1995**.
2. Velten, U.; Rehahn, M. *Chem. Commun.* **1996**, 2639-2640.
3. Lahn, B.; Rehahn, M. *e-Polymers* **2002**, *1*, 1-33.
4. Vermonden, T.; van der Gucht, J.; de Waard, P.; Marcelis, A. T. M.; Besseling, N. A. M.; Sudhölter, E. J. R.; Fleer, G. J.; Cohen Stuart, M. A. *Macromolecules* **2003,** *36*, 7035-7044.
5. Abed, S.; Boileau, S.; Bouteiller, L. *Macromolecules* **2000**, *33*, 8479-8487.
6. Ercolani, G.; Mandolini, L.; Mencarelli, P.; Roelens, S. *J. Am. Chem. Soc.* **1993**, *115*, 3901-3908.
7. Van der Gucht, J.; Besseling, N. A. M.; Van Leeuwen, H. P. *J. Phys. Chem. B* **2004**, *108*, 2531-2539.
8. Söntjens, S. H. M.; Sijbesma, R. P.; van Genderen, M. H. P.; Meijer, E. W. *Macromolecules* **2001**, *34*, 3815-3815.
9. Ten Cate, A. T.; Sijbesma, R. P. *Macromol. Rapid. Commun.* **2002**, *23*, 1094-1112.
10. Ten Cate, A. T.; Kooijman, H.; Spek, A. L.; Sijbesma, R. P.; Meijer, E. W. *J. Am. Chem. Soc.* **2004**, *126*, 3801-3808.
11. Beck, J. B.; Rowan, S. J. *J. Am. Chem. Soc.* **2003**, *125*, 13922-13923.
12. Zhao, Y.; Beck, J. B.; Rowan, S. J.; Jamieson, A. M. *Macromolecules* **2004**, *37*,3529-3531.
13. Elhabiri, M.; Scopelliti, R.; Bünzli, J.-C. G.; Piguet, C. *J. Chem. Soc., Chem. Commun.* **1998**, 2347-2348.
14. Lessmann, J. J.; Horrocks Jr., W. DeW. *Inorg. Chem.* **2000**, *39*, 3114-3124.
15. Elhabiri, M.; Hamacek, J.; Bünzli, J.-C. G.; Albrecht-Gary, A.-M. *Eur. J. Inorg. Chem.* **2004**, 51-62.
16. Niu, S. Y.; Yang, G. D.; Zhang, Y. L.; Jin, J.; Ye, L.; Yang, Z. Z. *J. Mol. Struct.* **2002**, *608*, 95-99.
17. Pan, L.; Huang, X.; Li, J.; Wu, Y.; Zheng, N. *Angew. Chem. Int. Ed.* **2000**, *39*, 527-530.
18. Wei, P.-R.; Wu, D.-D.; Zhou, Z.-Y.; Mak, T. C. W. *Polyhedron* **1998**, *17*, 497-505.
19. Seward, C.; Hu, N.-X.; Wang, S. *J. Chem. Soc., Dalton Trans.* **2001**, 134-137.
20. Luo, J.; Hong, M.; Wang, R.; Yuan, D.; Cao, R.; Han, L.; Xu, Y.; Lin, Z. *Eur. J. Inorg. Chem.* **2003**, 3623-3632.
21. Bünzli, J.-C. G.; Piguet, C. *Chem. Rev.* **2002**, *102*, 1897-1928.
22. Grenthe, I. *J. Am. Chem. Soc.* **1961**, *83*, 360-364.
23. Ouali, N.; Bocquet, B.; Rigault, S.; Morgantini, P.-Y.; Weber, J.; Piguet, C. *Inorg. Chem.* **2002**, *41*, 1436-1445.

Linear rheology of water-soluble reversible neodymium(III) coordination polymers

Chapter 4

The rheology of reversible coordination polymer networks in aqueous solution is studied. The polymers are formed by neodymium(III) ions and bifunctional ligands, consisting of two pyridine-2,6-dicarboxylate groups connected at the 4-positions by an ethylene oxide spacer. Neodymium(III) ions can bind three of these terdendate ligand groups. At high concentrations, the polymer networks yield viscoelastic materials, which can be described with the Maxwell model. The scaling of the elastic modulus, relaxation time and zero-shear viscosity with concentration are in good agreement with the predictions of Cates' model that describes the dynamics of linear equilibrium polymers. This indicates that the networks have only few cross-links and can be described as linear equilibrium polymers. The gels are also thermo-reversible. At high temperatures, fast relaxation was found, resulting in liquid like behavior. Upon cooling, the viscoelastic properties returned immediately. From the temperature dependence of the relaxation time, an activation energy of 49 kJ/mol was determined for the breaking and reptation of the polymers.

This chapter was published as: Vermonden, T.; Van Steenbergen, M. J.; Besseling, N. A. M.; Marcelis, A. T. M.; Hennink, W. E.; Sudhölter, E. J. R.; Cohen Stuart, M. A. *J. Am. Chem. Soc.* **2004** , *126*, 15802-15808.

4.1 Introduction

4.1.1 Reversible coordination polymers

Reversible or equilibrium polymers are polymers that can reversibly break and re-form by non-covalent interactions.[1-4] These interactions can be, for example, hydrogen bonding, π-π-stacking interactions, Van der Waals interactions, and coordinative bonding (metal-ligand bonding). Although reversible polymers reproduce many properties of covalent polymers, they exhibit new features due to breaking and recombination on experimental time scales. Until now hydrogen bonded polymers are the most studied.[4-7]

Another promising group of reversible polymers are the coordination polymers.[8-12,14] Linear polymers are formed by bifunctional ligands and metal ions if ligand groups and metal ions form 2:1 complexes. This is usually the case when bifunctional terdendate ligands are used in combination with transition metal ions, such as Zn^{2+} or Cd^{2+}.[13,14] For these coordination polymers, the average chain length varies not only with concentration and temperature, but also with the molar ratio of metal ions to bifunctional ligands. When the molar ratio equals unity, the average chain length is larger than when either metal ions or ligands are in excess. However, when lanthanide ions such as La^{3+} or Nd^{3+} are used with the same ligands, polymeric networks may be obtained. This is because lanthanide ions are large and can accommodate 9-coordination, which implies that each ion can bind three terdendate ligand groups. By using lanthanide ions, the formation of reversible networks instead of linear polymers is expected.[15] Recently, the formation of coordination polymers was described with bifunctional terdendate ligands, a few percent lanthanide ions (La^{3+} or Eu^{3+}) and over 95% transition metal ions (Zn^{2+} or Co^{2+}) in an organic solvent.[16] The lanthanide ions indeed act as cross-linkers and give the solutions interesting rheological properties.[17]

For linear reversible polymers some rheological properties have been reported.[5,14,18-22,27] The dynamics of equilibrium polymers are supposed to have much in common with so-called wormlike micelles. Such micelles also have the possibility to break and recombine reversibly. The rheological properties of these micelles have been studied extensively, both experimentally and theoretically, in the last two decades.[21,22] At very high salt concentrations, wormlike micelles from cetylpyridinium chlorate not only form linear chains but also cross-links.[23] However, published data about the dynamics of reversible cross-linked systems or networks are scarce.[24-28]

In this chapter, we investigate the rheological properties of a water-based reversible coordination network. Neodymium(III) is a suitable metal ion, because it

is known to form complexes with three terdendate ligand groups (9-coordination).[15,29] The ligand used is a bifunctional ligand, consisting of two pyridine-2,6-dicarboxylate groups connected at the 4-positions by an ethylene oxide spacer; its synthesis has been described in chapter 2.[14] The measurements were performed for two ligands that differ only in spacer length. The results were fitted to the model of Cates to obtain insight into the molecular dynamics of the studied reversible networks. First, the existing model is explained and then compared with the experimental results as a function of concentration and temperature with this model.

4.1.2 Linear rheology of equilibrium polymers

As mentioned in section 4.1.1, the rheological behavior of equilibrium polymers has a lot in common with the rheological behavior of wormlike micelles. Maxwellian behavior was predicted in theoretical studies for wormlike micelles[21] and also has been found experimentally for entangled reversible hydrogen-bonded polymers and wormlike micelles.[5,18,22] According to the Maxwell model, the storage modulus (G') and loss modulus (G'') are given by the following equations:

$$G'(\omega) = \frac{G_0(\omega\tau)^2}{1+(\omega\tau)^2} \tag{1}$$

$$G''(\omega) = \frac{G_0\omega\tau}{1+(\omega\tau)^2} \tag{2}$$

where ω is the angular frequency and τ is the relaxation time. The inverse relaxation time ($1/\tau$) can be found as the frequency (ω) at which G' equals G'' because $G'/G'' = \omega\tau$. G_0 is the plateau modulus and corresponds to the high-frequency plateau of G'. At concentrations above the overlap value, the polymer chains are becoming entangled and looped around each other. For a polymer chain, one can envisage a number of entanglement sites occurring, which can be related to an average molar weight between effective cross-links, M_e, at short times. These effective cross-links may be "true" (reversible) cross-links or entanglements. The following equation gives the relation between the plateau modulus and the molar weight between effective cross-links, M_e:[30]

$$G_0 = \frac{\rho RT}{M_e} \tag{3}$$

where ρ is the concentration of the polymer solution (g/m^3), R is the molar gas constant, and T is the absolute temperature. ρ/M_e equals the molar concentration of

the chain fragments between entanglements, C_e (mol/m^3). The concentration C_e is related to the correlation length, ξ, of the polymer solution by $C_e \sim 1/\xi^3$. In a good solvent, $\xi \sim C^{-3/4}$, with the concentration C in g/l.[31] Consequently, the plateau modulus is also concentration dependent. For flexible chains (both equilibrium polymers and covalently bonded polymers), this dependency is approximately: [21,32,33]

$$G_0 \cong \frac{k_B T}{\xi^3} \approx C^{9/4} \tag{4}$$

where k_B is the Boltzmann constant.

For wormlike micelles, Cates et al. developed a model for the dynamical properties that also takes into account the breaking and reassembly of chains.[21,22] In this model, the relaxation of reversible polymers can be described by two time scales: the reptation time, τ_{rep}, and the lifetime of a chain, τ_{break}. The reptation time is the time needed for an entangled polymer to diffuse out of its imaginary tube.[33] This tube is made up of the network made by all of the other entangled polymer chains, which makes diffusion only possible in the direction of the tube. τ_{break} is the lifetime of a chain of mean length before it breaks into two pieces.[22] When breaking is fast as compared to reptation ($\tau_{break} << \tau_{rep}$), the relaxation time is given by

$$\tau \cong (\tau_{rep}\tau_{break})^{1/2} \approx C^{5/4} \tag{5}$$

According to the model of Cates,[34,35] the relaxation time τ scales with the concentration with an exponent of $5/4$. The zero-shear viscosity η_0 is related to the relaxation time τ and the plateau modulus G_0 by

$$\eta_0 = G_0\tau \approx C^{3.5} \tag{6}$$

and η_0 scales with the concentration with an exponent of 3.5 in the fast breaking regime.

The relaxation time τ is also related to a reaction rate constant k. The reaction involved in relaxation is a combination of reptation and dissociation of the coordination bonds, yielding a single relaxation time (equation 5). In the fast breaking regime, the reaction is therefore a first order reaction. Even when water molecules assist in the breaking of the coordination bonds, the reaction rate is a pseudo first-order reaction, because the water concentration is constant ($k_{observed} = k.[H_2O]$). Nevertheless, if we assume that the process is a first or pseudo-first-order process, k_{obs} can be described by

$$k_{obs} = 1/\tau \tag{7}$$

The Arrhenius equation gives the relation of k_{obs} and the activation energy E_a as a function of the temperature:

$$k_{obs} = Ae^{-E_a/RT} \text{ or } \tau = A^{-1}e^{E_a/RT} \tag{8}$$

with A as the preexponential factor.[36] Both the activation energy and the preexponential factor can be divided into the contributions of reptation and breaking of the chains using equation 5: $A = (A_{rep}.A_{break})^{1/2} \approx C^{-5/4}$ and $E_a = (E_{a,rep}+E_{a,break})/2$. So, E_a is the arithmetic mean of the activation energies of reptation and breaking of the chains and should not depend on the concentration.

For cross-linked systems, no theoretical scaling exponents as a function of concentration have been published yet. However, some experimental data are reported of the scaling exponents of wormlike micelles (CTAB) in which intermicellar branching occurs at high salt concentration by Khatory et al.[27] The branching of these wormlike micelles leads to a reduction of the zero-shear viscosity and scaling exponents different from those predicted by Cates for linear reversible chains. The scaling exponents found at a salt concentration of 1.5 M are: $\eta_0 \approx C^{2.42}$, $\tau \approx C^{0.57}$ and $G_0 \approx C^{1.85}$. Relaxation can occur by sliding of the linear chains along the cross-links through viscous flow of the surfactant molecules. Due to this flow, the reptation process can still take place but the reptation time decreases, because of the large number of possible paths for reptation accelerates the curvilinear motion of the cylinders between two free ends.[37]

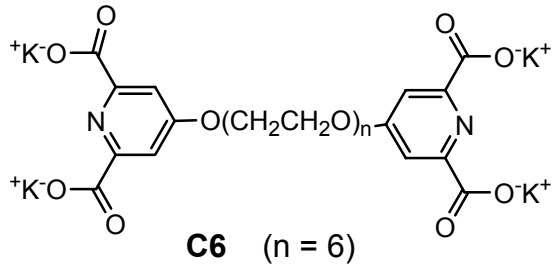

C6 (n = 6)
C7.4 (n ~7.4)

Figure 1: *Bifunctional ligands* ***C6*** *and* ***C7.4.***

4.2 Results and discussion

Bifunctional ligands **C6** and **C7.4** (figure 1) were used to form complexes with neodymium(III) ions in aqueous solution. **C6** has a spacer length of exactly 6

ethylene oxide units. **C7.4** consists of a mixture of molecules with an average spacer length of 7.4 ethylene oxide units as determined by ^{1}H NMR. Neodymium ions can bind to three of these ligand groups. The complexation constants of the subsequent binding of three 2,6-pyridine-dicarboxylic acid molecules to one Nd^{3+} ion are: $K_1 = 10^{8.78}$, $K_2 = 10^{6.72}$, and $K_3 = 10^{5.06}$ as reported by Grenthe.[29]

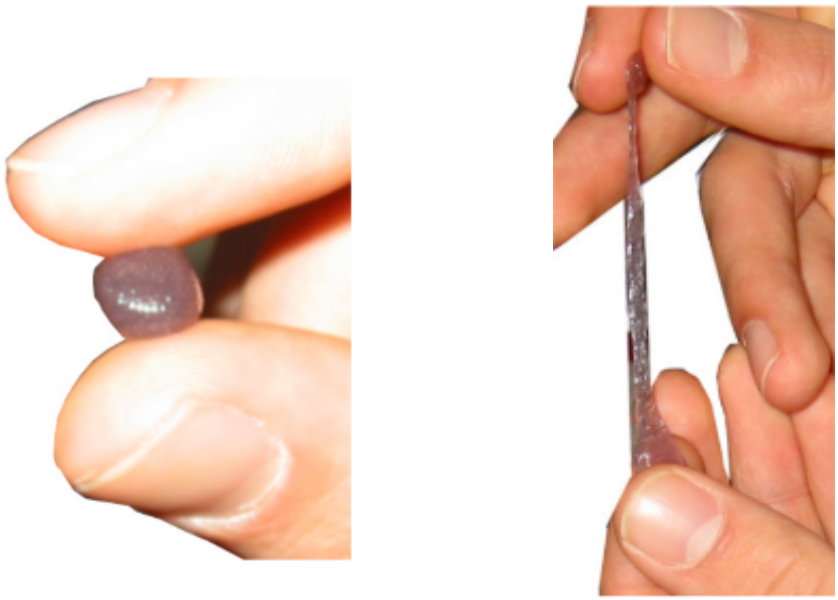

Figure 2: *Pictures of sample of 500 g/l of* ***C6*** *and 0.7 equivalent $Nd(NO_3)_3$ in 100 mM Pipes buffer pH 5.4.*

When ligands **C6** and **C7.4** were dissolved in an aqueous 1,4-piperazinebis(ethanesulfonic acid) (PIPES) buffer (pH 5.4, 100 mM) and mixed with a solution of 0.7 equivalents of $Nd(NO_3)_3$ in the same buffer, a precipitate was formed initially, which gradually dissolved upon mixing in an ultrasonic water bath. We reported earlier that samples with 0.7 equivalents of Nd^{3+} ions gave somewhat higher viscosities than those having a ratio of exactly $^2/_3$ at low concentrations (8-35 g/l) and therefore the ratio of 0.7 was also used here.[15] The gels of both **C6** and **C7.4** showed only very little recovery in creep experiments, which means that the gels are still liquidlike. The gels formed with **C7.4** were completely transparent after about 24 hours of mixing. The gels formed with **C6** were slightly turbid (figure 2). This difference is probably caused by a small difference in the polarity of the compounds. **C6** is a little less polar than **C7.4**, and this may lead to incomplete dissolution of the coordination complexes in water at the concentrations used in this study. We also tried to form gels with **C4** and **C5** (same compounds, but with a spacer length of only 4 and 5 ethylene oxide units, respectively), but in these systems, despite initial gelation, always a precipitate was formed after approximately half an hour at concentrations above 100 g/l. Solutions at lower concentrations of all compounds (**C4**

to **C7.4**) with a Nd^{3+}/bifunctional ligand ratio of 0.7 were transparent. The viscosity of these solutions at low concentration increased with increasing concentration and had a maximum when the Nd^{3+}/bifunctional ligand ratio was between 0.67 and 0.71.[15]

4.2.1 Concentration dependence

The rheological characteristics of solutions of both ligands with Nd^{3+} were measured as a function of frequency at different concentrations. Figure 3 shows the storage modulus (G') and the loss modulus (G'') as a function of the angular frequency (ω) for a **C7.4** gel with 0.7 equivalents of $Nd(NO_3)_3$ at 20 ºC at a concentration of 500 g/l (concentration of ligand and $Nd(NO_3)_3$ together). The curves show that the gel has typical viscoelastic properties. At low frequency the loss modulus dominates, while at higher frequencies the storage modulus dominates and levels off toward a plateau value. Figure 4 shows G'' as a function of G' in a so-called Cole-Cole plot for different concentrations of **C7.4** at 20 ºC. The solid lines in figures 2 and 3 correspond to the fits of the Maxwell model. The shapes of the curves measured for **C6** are comparable to those of **C7.4**.

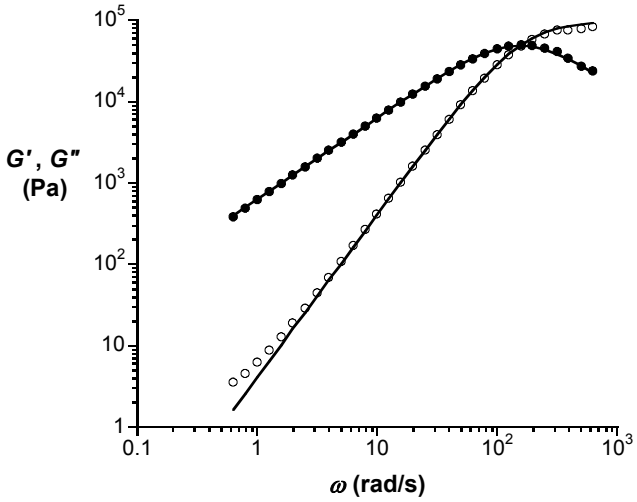

***Figure 3**: Storage modulus (○) and loss modulus (●) as a function of the angular frequency ω for a solution of 500 g/l of **C7.4** and 0.7 equivalents of $Nd(NO_3)_3$ in 100 mM PIPES buffer pH 5.4 at 20 ºC. Curves are fits to the Maxwell model, equations 1 and 2.*

As can be seen, the rheological behavior of the system can be described very well by the Maxwell model over a frequency range, which extends beyond $\omega = 1/\tau$. In figure 4, G_0 corresponds to the diameter of the semicircle and depends on the concentration. At high frequency, a small deviation from the Maxwell model is

found, which is common for reversible polymers and wormlike micelles.[20,27,32,34,35] This deviation is usually interpreted as a crossover to a different dynamical regime, where other relaxation modes are important. Whether the same explanation for the deviation can be given for this system is not clear, because *G″* decreases faster as compared to *G′* than in other reported systems.

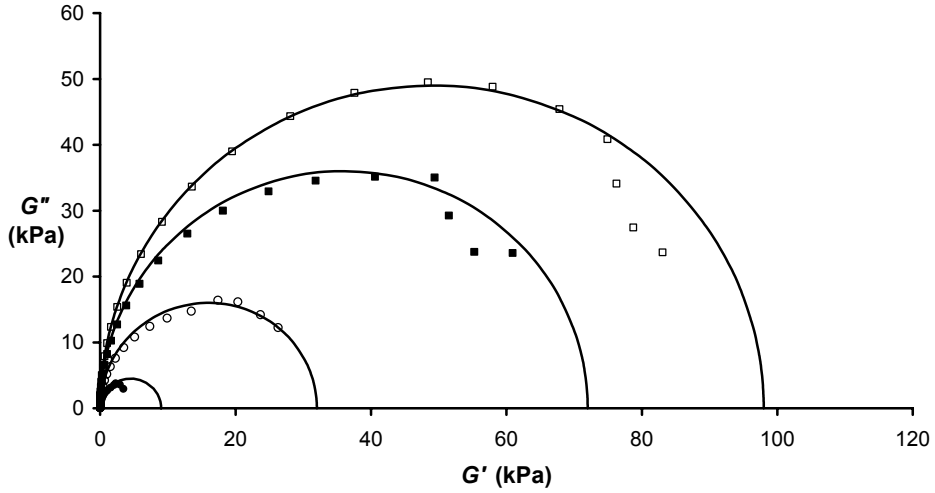

***Figure 4**: Cole-Cole plots of G′ and G″ data for **C7.4** and 0.7 equivalents of $Nd(NO_3)_3$ at 20 °C of 181 g/l (●), 308 g/l (○), 400 g/l (■), 500 g/l (□) in 100 mM PIPES buffer pH 5.4 solutions. The semicircular curves correspond to the Maxwell model, equations 1 and 2.*

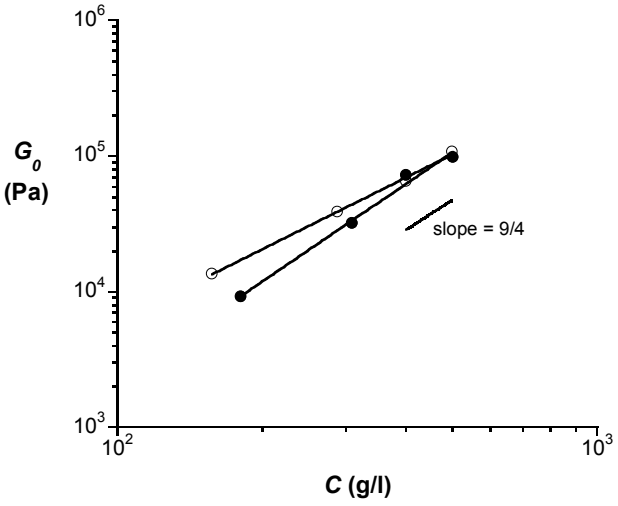

***Figure 5**: Plateau modulus (G_0) as a function of concentration for **C6** (○) and **C7.4** (●) with 0.7 equivalents of $Nd(NO_3)_3$ in 100 mM PIPES buffer pH 5.4 at 20 °C.*

Figure 5 shows the concentration dependence of G_0 for both **C6** and **C7.4** with Nd^{3+}. The data for compound **C7.4** can be fitted by $G_0 \approx 0.03C^{2.4}$ (Pa) and for compound **C6** by $G_0 \approx 1.75C^{1.8}$ (Pa). The scaling exponent of 2.4 for **C7.4** agrees well with the

theoretical scaling exponent 9/4 for linear polymers. This is an indication that the effective cross-links observed in the high frequency rheological experiments are predominantly entanglements. The slope of 1.8 for **C6** deviates from 9/4. The slope of **C6** corresponds, however, well to the scaling exponent found experimentally for cross-linked wormlike micelles mentioned in the introduction.[27] Yet because the solutions of **C6** are a little turbid, the system may be partially precipitated so that part of the material does not contribute to the polymer network. Hence, comparing the data for this system to theory or other experiments might be questionable. However, the different behavior of **C6** could not be caused only by partial dissolution of the coordination complexes. In that case, the curves in figure 5 (and also in figures 6 and 7) would be horizontal, because at concentrations above the solubility product no additional molecules dissolve. Most likely, the difference in behavior between **C6** and **C7.4** is due to the difference in the spacer length. However, it cannot be excluded that the difference in polydispersity is relevant as well.

From the plateau modulus, the molecular weight between effective cross-links was calculated using equation 3. The M_e values are summarized for various concentrations of both the **C6** and the **C7.4** systems in table 1. The large values for M_e indicate that we do not have many effective cross-links (the molecular weight of a bifunctional ligand plus one metal ion including counterions is about of 1.1 kg/mol).

The Maxwell model applies well for a large frequency range (considerably beyond $\omega = \tau^{-1}$, see figures 3 and 4), which is an indication that the system is fast breaking ($\tau_{break} << \tau_{rep}$). The relaxation times τ are concentration dependent (figure 6), and our experiments are in very good agreement with the model of Cates for compound **C7.4** ($\tau \approx 4 \cdot 10^{-6} C^{1.2}$). The scaling of **C6** with an exponent of 0.7 corresponds again well with the one found experimentally for the cross-linked wormlike micelles ($\tau \approx 8 \cdot 10^{-5} C^{0.7}$). However, the different scaling could also be attributed to its incomplete dissolution.

***Table 1**: Average molecular weights between effective cross-links (M_e) for various concentrations of **C7.4**/Nd^{3+} and **C6**/Nd^{3+} solutions.*

C (g/l) **C7.4**/Nd^{3+}	M_e (kg/mol)	C (g/l) **C6**/Nd^{3+}	M_e (kg/mol)
181	49	157	35
308	23	287	18
400	14	400	15
500	12	498	11

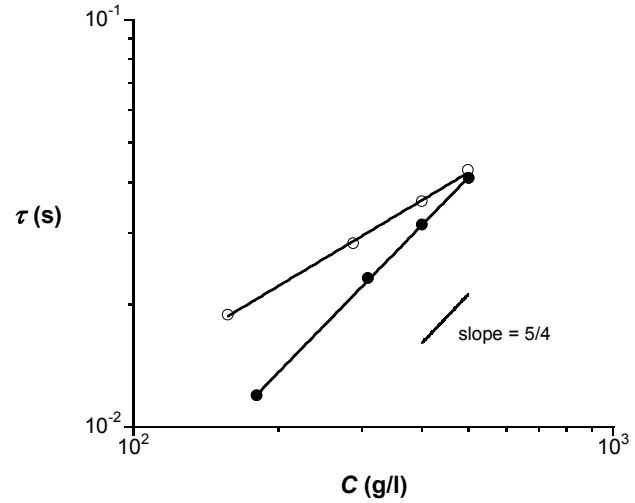

***Figure 6**: Relaxation time (τ) as a function of concentration for **C6** (○) and **C7.4** (●) with 0.7 equivalents of $Nd(NO_3)_3$ in 100 mM PIPES buffer pH 5.4 at 20 ºC.*

Although the exponents for τ are comparable to those found experimentally for linear hydrogen-bonded reversible polymers, the absolute relaxation times are much smaller.[5,13] The relaxation time is build up by two contributions: τ_{rep} and τ_{break} (equation 5). In our system, τ_{break} may be much smaller due to the role of the solvent. The rheological properties of the hydrogen-bonded polymers reported were studied in organic solvents. These solvents do not play an active role in the breaking and recombination. Water, on the other hand, coordinates metal ions and stabilizes the free or partially bound metal ions, resulting in shorter relaxation times as compared to the hydrogen-bonded polymers in organic solvents. Whether τ_{rep} contributes also to smaller overall relaxation times in our system than in hydrogen-bonded polymers is harder to foresee, because τ_{rep} is related to the curvilinear diffusion coefficient, which depends among other things on the average chain length and the viscosity of the solvent.

Figure 7 shows the zero-shear viscosity η_0 as a function of concentration. The data can be fitted with a line of slope 3.6 for compound **C7.4** and 2.5 for compound **C6**. The scaling exponent predicted by Cates for linear reversible polymers is 3.5. Compound **C7.4** with Nd^{3+} corresponds again very well with this model. For compound **C6** and Nd^{3+}, all scaling exponents correspond nicely to the exponents found in cross-linked wormlike micelles. On the basis of these results, one might conclude that the **C6** system forms indeed a cross-linked network and the **C7.4** system forms linear chains.

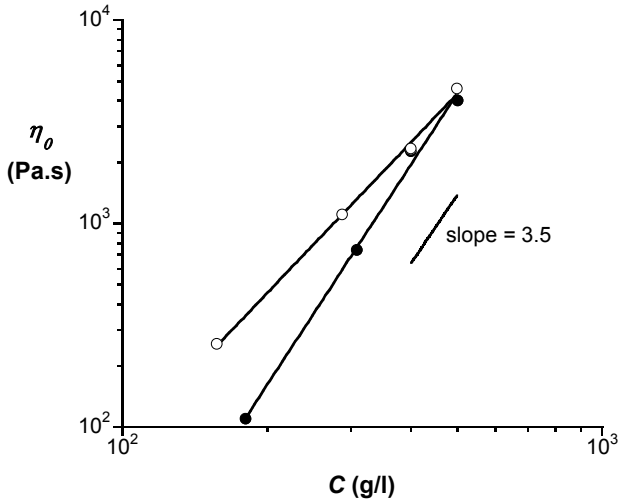

***Figure 7**: Zero-shear viscosity (η_0) as a function of concentration for **C6** (○) and **C7.4** (●) with 0.7 equivalents of $Nd(NO_3)_3$ in 100 mM PIPES buffer pH 5.4 at 20 °C.*

Because neodymium ions bind to three ligand groups, one would expect the formation of cross-linked networks. A possible explanation, which reconciles the fact of three-fold coordinated Nd^{3+} ions and the occurrence of linear chains of **C7.4**/Nd^{3+} as suggested by the rheological results, may be the structure depicted in figure 8. However, based on this structure no good reason can be given why **C7.4** would give these linear chains and **C6** would not. The results indicate that **C6** rather forms cross-links than rings such as in figure 8. However, in systems with transition metal ions, the formation of rings consisting of two **C6** molecules and two metal ions seemed well possible.[14] So, we still cannot exclude the explanation that **C6** gives different scaling exponents than **C7.4** due to partial precipitation in the **C6**/Nd^{3+} system.

***Figure 8**: Schematic representation of linear chains formed by bifunctional ligands and lanthanide ions.*

The results of the **C7.4**/Nd^{3+} system can, however, be explained very well using the representation of linear chains in figure 8. The ligands are known to form ringlike structures at low concentrations around transition metal ions.[14] When at the concentrations used for the measurements a reasonable amount of rings, such as in figure 8, is still present, the solution may well behave as a solution of linear chains instead of a network. Unfortunately, it is very difficult to assess whether linear

polymers, networks, or a combination of the two are present in our reversible system. With increasing concentration, the relative amount of rings is expected to decrease and the relative amount of cross-links is expected to increase. However, cross-linking is unfavorable because every cross-link yields an extra chain end (figure 9). A chain end always has either an uncomplexed ligand group, a metal ion with free coordination sites, or a bifunctional ligand that forms a loop around one metal ion (monomer ring). These are all unfavorable, the first two possibilities for enthalpic reasons, the last for entropic reasons. Therefore, the branching of the chains is unfavorable and the formation of linear chains is more likely also at high concentrations. At very high concentrations, the branch points may connect two chains and not yield extra chain ends. However, to connect all possible branch points such as this, extremely high concentrations are needed, and this is not feasible in this system.

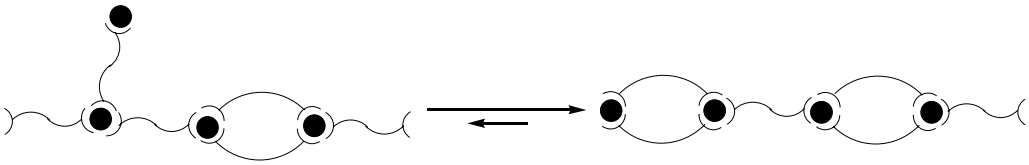

***Figure 9**: Branching leads to more chain ends. This favors the equilibrium towards linear chains.*

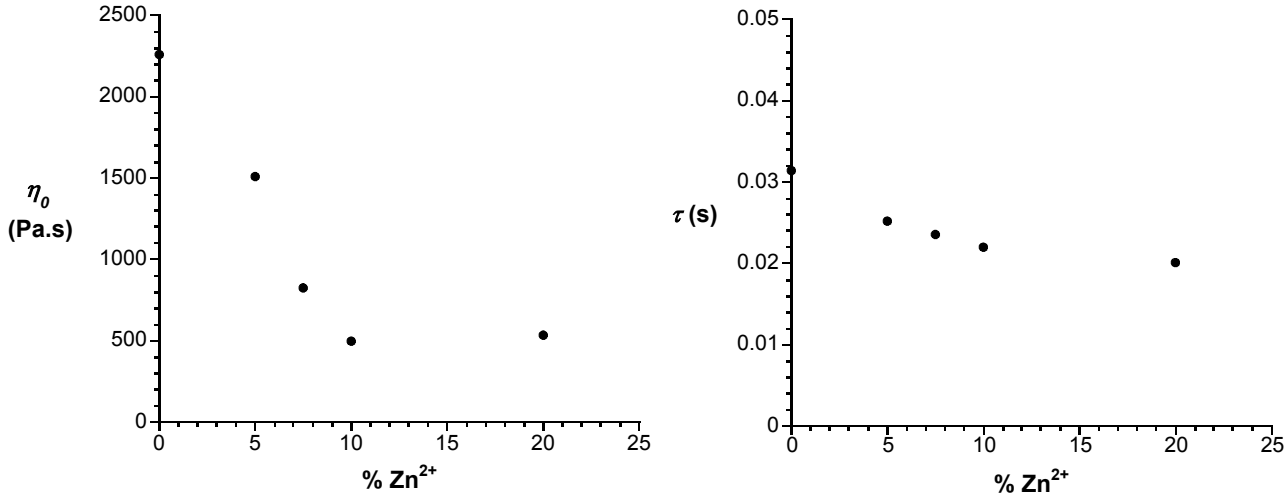

***Figure 10**: Dependence of η_0 and τ upon the % Zn^{2+} in a sample of 400 g/l **C7.4** and Nd^{3+} in 100 mM PIPES buffer pH 5.4 at 20 °C.*

For comparison, we also prepared samples with Zn^{2+} ions instead of Nd^{3+}, which binds two ligand groups per metal ion and leads to the formation of linear chains and rings.[14] At a concentration of 500 g/l a sample of **C7.4** with Zn^{2+} was completely

liquidlike, whereas the Nd^{3+} samples gave viscoelastic materials. We also prepared samples with a concentration of 400 g/l of **C7.4** with Nd^{3+} and varying amounts of Zn^{2+}. The samples were prepared such that the amount of binding places on the metal ions was equal to the amount of binding groups. This is necessary because Zn^{2+} ions bind only two ligand groups, while Nd^{3+} binds three ligand groups. Both G_0 and η_0 (figure 10a) decreased substantially with increasing percentages of Zn^{2+}. The relaxation time decreases only slightly with increasing percentages of Zn^{2+} (figure 10b). Samples containing over 25% Zn^{2+} were completely liquidlike. So, we conclude that at a concentration of 400 g/l both the viscosity and the relaxation time decrease with decreasing amounts of trifunctional metal ions. A reason may be that the complexation constants for the binding of Zn^{2+} to the chelating group ($10^{6.4}$ and $10^{5.5}$) are smaller than the first two complexation constants of Nd^{3+}.[29] This will lower the average chain length and the solution viscosity. Yet the most important reason for lowering the viscosity is probably that the ligands are able to form rings around Zn^{2+} as well. Here, ring formation leads to chain ends as depicted in figure 11. Such rings yield additional chain ends and hence reduce the average chain length. Transition metal ions added to a system consisting of terdendate bifunctional ligands and lanthanide ions might act as "chain stoppers" similarly to how monofunctional molecules do in solutions of bifunctional hydrogen-bonded polymers.[28,38]

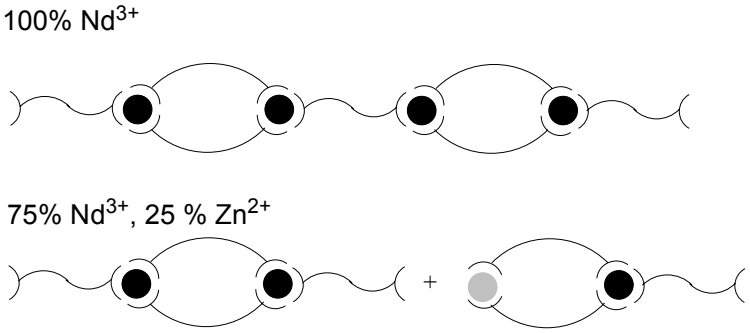

***Figure 11**: Schematic representation of the influence of replacement of Nd^{3+} ions (black circles) by Zn^{2+} ions (gray circle).*

4.2.2 Temperature dependence

Besides the concentration dependence of the rheological properties, also a clear temperature dependence was observed. Figure 12 shows the storage and loss modulus as a function of temperature of **C7.4** and Nd^{3+} at a concentration of 400 g/l for a frequency of 100 Hz. The storage modulus decreases with increasing temperature. At about 37 ºC, the loss modulus becomes larger than the storage modulus. At high temperatures, the mobility of the molecules increases but also the complexation constants between metal ions and ligands decrease, leading to smaller

chains and eventually single molecules. Upon cooling, the storage and loss modulus return immediately to the same level as before the sample was heated, demonstrating the reversibility of the system.

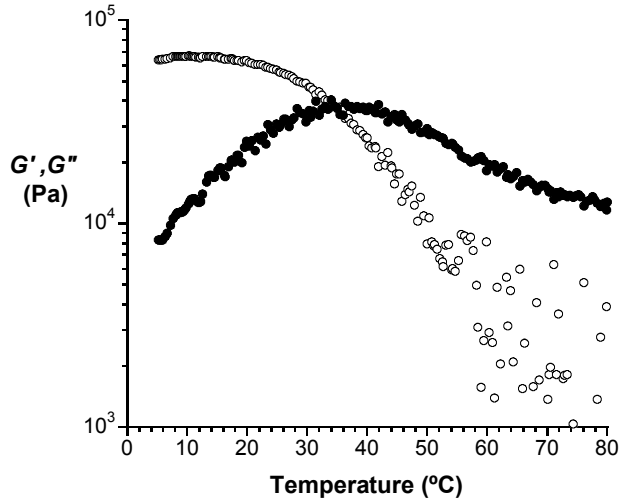

***Figure 12**: Storage modulus (○) and loss modulus (●) as a function of temperature for a 400 g/l solution of **C7.4** and $Nd(NO_3)_3$ in 100 mM PIPES buffer pH 5.4 at a frequency of 627.7 rad/s and 1% strain.*

Increasing the temperature leads to a decrease in the relaxation time τ. Because ω is constant (100 Hz) during the temperature dependent measurements, at each temperature τ can be calculated from G' and G'' using equations 1 and 2. For all concentrations, the relaxation time drops until nearly zero at approximately 60 ºC (not shown). This means that with increasing temperature the sample loses its (visco)elastic properties and becomes a liquid.

From the relaxation times, the reaction rate k_{obs} was calculated (equation 7) as a function of temperature. In figure 13, the Arrhenius plot is displayed for **C7.4** at three different concentrations. The curves are normalized for concentration to the power $^5/_4$, which corresponds to the concentration dependence of τ and therefore also for $1/k_{obs}$. Due to normalization the Arrhenius plots for different concentrations collapse onto one single curve. The intercept at $1/T = 0$ equals to $\ln(A \bullet C^{5/4})$. Normalization for concentration has no effect on the slopes that correspond to the activation energy, E_a. Although a lot of scatter is present at high temperatures, the slope can easily be determined at lower temperatures. The slope yields an activation energy E_a of 49 kJ/mol, which is not very high. For the **C6**/Nd^{3+} system, the exact same slope and thus the same activation energy were found. As discussed in section 4.1.2, this activation energy E_a is the arithmetic mean of the activation energies of reptation and breaking of the chains. Because we cannot determine the values for the

activation energy for reptation and breaking separately, we can only say that the activation energy for breaking is lower than 49 kJ/mol. A low value for the activation energy is realistic for a reversible process.

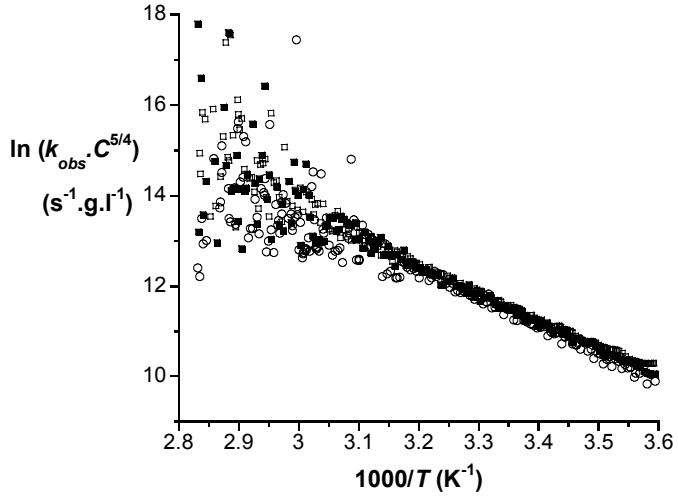

Figure 13: *Arrhenius plot of ln k_{obs} against 1/T for* ***C7.4*** *and 0.7 equivalents of $Nd(NO_3)_3$ normalized for a concentration of 308 g/l (○), 400 g/l (■), 500 g/l (□) in 100 mM PIPES buffer pH 5.4 solutions.*

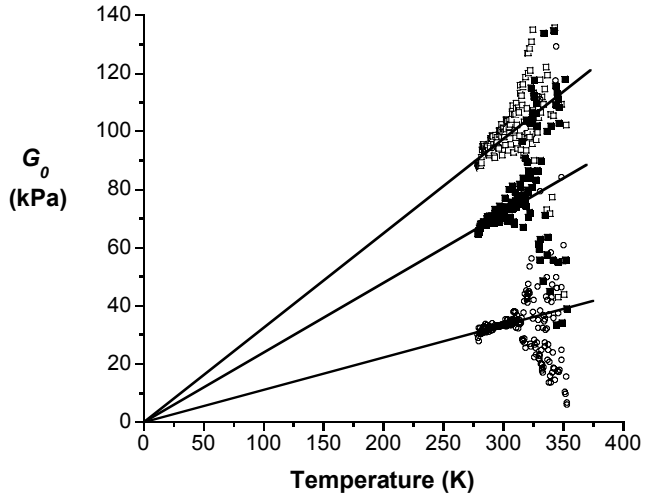

Figure 14*: Plateau modulus as a function of temperature for* ***C7.4*** *and 0.7 equivalents of $Nd(NO_3)_3$ of 308 g/l (○), 400 g/l (■), 500 g/l (□) in 100 mM PIPES buffer pH 5.4 solutions.*

Besides the relaxation time also the plateau modulus as a function of temperature can be determined assuming that the Maxwell model is valid over the whole temperature range. The plateau modulus G_0 can be calculated using equation 1 or 2, because ω is constant (100 Hz), τ was calculated, and G' and G'' were measured. The

results are shown in figure 14. The plateau modulus increases with temperature. This is in line with equation 3 if the amount of entanglements does not change with increasing temperature. From the slopes of the lines in figure 13, the average molecular weight between the entanglements M_e can be calculated again. The M_e values found here from the slopes are the same as the values in table 1.

4.3 Concluding Remarks

In conclusion, we presented here the rheological properties of reversible coordination polymers swollen in water. For **C7.4**, the rheological properties fit nicely with the model of Cates for linear reversible polymers. Therefore, it is concluded that we have mainly linear chains in our system by the formation of alternatively rings and connecting ligands (figure 7). The addition of Zn^{2+} ions, which can bind only two ligand groups, yields solutions with a substantially decreased viscosity.

Temperature-dependent measurements of G' and G'' gave information about the changes in relaxation time and plateau modulus with temperature. Using the information of the relaxation time (or the rate constant), an activation energy of 49 kJ/mol was obtained at all concentrations for both the **C7.4**/Nd^{3+} and the **C6**/Nd^{3+} systems. The low value for the activation energy matches a reversible system. The temperature dependent plateau modulus showed that the average molecular weight between effective cross-links or entanglements decreases with increasing concentration.

4.4 Experimental section

All commercial chemicals were obtained from Acros or Aldrich and were used as received. The synthesis of **C6** and **C7.4** was reported in chapter 2.[14] All measurements were performed in a 100 mM 1,4-piperazinebis(ethanesulfonic acid) buffer (PIPES), pH 5.4, and concentrations are given in weight per volume. The rheology experiments were performed on a TA Instruments AR1000-N rheometer using a cone-plate geometry (steel, 20 mm diameter with an angle of 1º). A solvent trap was used to prevent evaporation of the solvent. All experiments were performed at 1% strain. The temperature dependent experiments were performed with a temperature ramp of 1º C/min.

4.5 References

1. Lehn, J.-M. *Supramolecular Chemistry*; VCH: Weinheim, **1995**.

2. Ciferri, A. *Supramolecular Polymers*; Marcel Dekker: New York, **2000**.
3. Brunsveld, L.; Folmer, B. J. B.; Meijer, E. W.; Sijbesma, R. P. *Chem. Rev.* **2001**, *101*, 4071-4097.
4. Sijbesma, R. P.; Beijer, F. H.; Brunsveld, L.; Folmer, B. J. B.; Hirschberg, J. H. K. K.; Lange, R. F. M.; Lowe, J. K. L.; Meijer, E. W. *Science* **1997**, *278*, 1601-1604.
5. Lortie, F.; Boileau, S. ; Bouteiller, L.; Chassenieux, C.; Demé, B.; Ducouret, G.; Jalabert, M.; Lauprêtre, F.; Terech, P. *Langmuir* **2002**, *18*, 7218-7222.
6. Xu, J.; Fogleman, E. A., Craig, S. L. *Macromolecules* **2004**, *37*, 1863-1870.
7. Folmer, B. J. B.; Sijbesma, R. P.; Meijer, E. W. *J. Am. Chem. Soc.* **2001**, *123*, 2093-2094.
8. Velten, U.; Rehahn, M. *Chem. Commun.* **1996**, 2639-2640.
9. Velten, U.; Lahn, B.; Rehahn M. *Macromol. Chem. Phys.* **1997**, *198*, 2789-2816.
10. Schubert, U. S.; Eschbaumer, C. *Angew. Chem. Int. Ed.* **2002**, *41*, 2892-2926.
11. Paulusse, J. M. J.; Sijbesma, R. P. *Chem. Commun.* **2003**, 1494-1495.
12. Paulusse, J. M. J.; Sijbesma, R. P. *Angew. Chem. Int. Ed.* **2004**, *43*, 4460-4462.
13. Van der Gucht, J.; Besseling, N. A. M.; Van Leeuwen, H. P. *J. Phys. Chem. B,* **2004**, *108*, 2531-2539.
14. Vermonden, T.;Van der Gucht, J.; De Waard, P.; Marcelis, A. T. M.; Besseling, N. A. M.; Sudhölter, E. J. R.; Fleer, G. J., Cohen Stuart, M. A. *Macromolecules*, **2003**, *36*, 7035-7044.
15. Vermonden, T.; De Vos, W. M.; Marcelis, A. T. M.; Sudhölter, E. J. R. *Eur. J. Inorg. Chem.* **2004**, 2847-2852.
16. Beck, J. B.; Rowan, S. J. *J. Am. Chem. Soc.* **2003**, *125*, 13922-13923.
17. Zhao, Y.; Beck, J. B.; Rowan, S. J.; Jamieson, A. M. *Macromolecules* **2004**, *37*, 3529-3531.
18. Van der Gucht, J.; Besseling, N. A. M.; Knoben, W.; Bouteiller, L.; Cohen Stuart, M. A. *Phys. Rev. E* **2003**, *67*, 051106.
19. Terech, P.; Schaffhauser, V.; Maldivi, P.; Guenet, J. M. *Langmuir* **1992**, *8*, 2104-2106.
20. Shikata, T.; Ogata, D.; Hanabusa, K. *J. Phys. Chem. B* **2004**, *108*, 508-514.
21. Cates, M. E. *Macromolecules* **1987**, *20*, 2289-2296.
22. Cates, M. E.; Candau, S. J. *J. Phys.: Condens. Matter* **1990**, *2*, 6869-6892.
23. Khatory A.; Kern, F., Lequeux, F.; Appell, J.; Porte, G.; Morie, N.; Ott, A.; Urbach, W. *Langmuir* **1993**, 933-939.
24. Leibler, L.; Rubinstein, M.; Colby, R. H. *Macromolecules* **1991**, *24*, 4701-4707.
25. Regalado, E. J.; Selb J.; Candau F. *Macromolecules* **1999**, *32*, 8580-8588.
26. St. Pourcain C. B.; Griffin A. C. *Macromolecules* **1995**, *28*, 4116-4121.
27. Khatory, A.; Lequeux, F.; Kern, F.; Candau, S. J. *Langmuir* **1993**, *9*, 1456-1464.
28. Lange, R. F. M.; Van Gurp, M.; Meijer, E. W. *J. Polym. Sci.: Part A: Polym. Chem.* **1999**, *37*, 3657-3670.
29. Grenthe, I. *J. Am. Chem. Soc.* **1961**, *83*, 360-364.
30. Goodwin, J. W.; Hughes, R. W. *Rheology for Chemists, an Introduction*; The Royal Society of Chemistry: Cambridge, **2000**.
31. De Gennes, P. G. *Scaling Concepts in Polymer Physics*; Cornell University Press: Ithaca: London, **1979**.
32. Kern, F.; Lequeux, F.; Zana, R.; Candau, S. J. *Langmuir* **1994**, *10*, 1714-1723.

33. Doi, M.; Edwards, S. F. *The Theory of Polymer Dynamics*; Clarendon: Oxford, **1986**.
34. Turner, M. S.; Cates, M. E. *J. Phys. II France* **1992**, *2*, 503-519
35. Turner, M. S.; Marques, C.; Cates, M.E. *Langmuir* **1993**, *9*, 695-701.
36. Atkins, P. W., *Physical Chemistry*; Oxford University Press: Oxford, fifth edition, **1994**.
37. Lequeux, F. *Europhys. Lett.* **1992**, *19*, 675-681.
38. Ten Cate, A. T.; Sijbesma R. P. *Macromol. Rapid Commun.* **2002**, *23*, 1094-1112.

Synthesis of 4-functionalized terdendate pyridine-based ligands

Chapter 5

Four different 4-functionalised pyridine-based ligands were synthesized with aminomethyl, oxazolinyl, pyrazolyl and methylimidazolyl groups at the 2- and 6-position. The nitrogens of these groups together with the pyridine nitrogen can act as terdendate ligands for metal ions. Synthetic handles on the 4-position of the pyridine group were introduced via ether or ester bonds leading to monofunctional, bifunctional and amphiphilic ligands.

This chapter was published as: Vermonden, T.; Branowska, D.; Marcelis, A. T. M.; Sudhölter, E. J. R. *Tetrahedron* **2003**, *59*, 5039-5045.

5.1 Introduction

Terdendate N-heterocyclic ligands have been used over the last century as effective and stable complexing agents for transition metal ions. These ligand-metal ion complexes have been used to build supramolecular coordination polymers [1-4], dendrimers[5] or ordered architectures on surfaces[6] leading to new materials with interesting catalytic, photochemical and redox properties.[7] In the last decade the most used terdendate ligands for supramolecular systems were based on terpyridine groups.[2,4,8-10]

In this chapter, the syntheses of four pyridine-based ligands with different nitrogen containing groups at the 2- and 6-positions and a functional group at the 4-position are described; these ligands can be seen as analogues of terpyridines. The aminomethyl, oxazolinyl, pyrazolyl and methylimidazolyl groups were introduced to yield planar terdendate ligands. These groups have been reported in literature to form stable complexes with metal ions. Bisaminomethylpyridine forms stable complexes with for example Cd^{2+}, Ni^{2+}, and Zn^{2+}.[11] Chiral derivatives of bisoxazolinylpyridines complexed with Rh^{3+} can act as catalysts for the reduction of ketones.[12] Ruthenium complexed bis(*N*-pyrazolyl)pyridine ligands described by Jameson et al. are both structural and redox analogues of terpyridine complexes.[13] Metal complexed methylimidazolyl groups have not often been reported, but structurally related benzimidazolyl ligands have been reported to form complexes with Ru^{2+} and Eu^{3+} with interesting redox and luminescent properties.[14-16] Furthermore, metallo-supramolecular polymers with benzimidazolylpyridine ligands have been reported with La^{3+}, Eu^{3+}, Co^{2+} and Zn^{2+}.[17]

The various chelating groups have a different preference for metal ions that they are able to coordinate. This is, amongst others, due to the fact that the chelating groups have different distances between the nitrogens of the groups at the 2- and 6-position: 4.12, 4.95, 4.81 and 4.59 Å for the aminomethyl, oxazolinyl, pyrazolinyl and methylimidazolyl pyridines respectively as seen from molecular modeling. For terpyridines this distance is 4.66 Å. The groups have different *pKa*-values, which also influences the binding properties of metal ions.

The syntheses of 4-substituted pyridine ligands have been much less explored than ones that are not substituted at the 4-position. However, some 4-substituted terpyridines have been reported.[18] To use these kinds of ligands in supramolecular chemistry a synthetic handle opposite to the complexing site of the molecule is necessary to build in additional properties. The present work was aimed at the synthesis of bifunctional ligands suitable for building linear reversible coordination polymers. To obtain long coordination polymers, high complexation constants

between metal ions and ligands are required. For that reason, terdendate ligands were chosen that are the most appropriate for complexing hexa-coordinating metal ions.

The chelating moieties were prepared with synthetic handles at the 4-position of the pyridine via ether or ester bonds, which make these compounds useful as building blocks for supramolecular structures. The synthetic methods described here were used to obtain bifunctional, monofunctional and amphiphilic monofunctional ligands. Scheme 1 shows the general structure of the synthesized bifunctional ligands. The amphiphilic ligands can be used to provide micelles or bilayer structures with metal-ion coordinating groups, which can find application in catalysis, separation[19] or supramolecular chemistry.

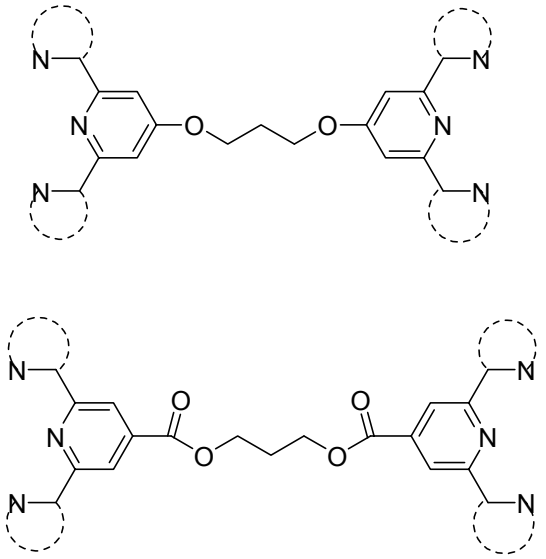

***Scheme 1**: General structures of the bifunctional terdendate ligands.*

5.2 Results and Discussion

As starting compounds for all metal ion complexing agents described here either 4-hydroxypyridine-2,6-dicarboxylic acid (chelidamic acid) or 2,6-dihydroxyisonicotinic acid were used. Scheme 2 shows the synthesis of the aminomethyl- and oxazolinylpyridines both starting from chelidamic acid. The aminomethyl ligands **5a** and **5b** were prepared by a five-step procedure. Chelidamic acid **1** was esterified in ethanol containing $SOCl_2$ to give diethylester **2** in 87% yield.[20] Diester **2** was treated with the appropriate bromoalkane in 2-butanone using K_2CO_3 as a base to give bifunctional compound **3a** (86%) and monofunctional compound **3b** (70%). Subsequently, the ester groups were reduced to hydroxymethyl groups with $NaBH_4$ in ethanol. It was possible to isolate the 2,6-bis(hydroxymethyl)-pyridines by

crystallization in cold water, but that method gave very low yields. Horváth et al. already described very low yields of similar compounds upon isolation and noticed a smaller loss of material when the crude product was used for the next reaction.[21] For that reason, we also used the crude alcohol for the next step. To transform the alcohol functionality into a better leaving group several methods were attempted. Tosylation gave a poor yield (24%) for the bifunctional compound. Mesylation gave a product that seemed not stable upon isolation. Bromination was first tried using 48% HBr, but the compounds were not stable in this very acidic environment. Bromination by PBr_3 according to a method described by Takalo et al. gave a stable product with moderate yields (45-72% for two steps).[22]

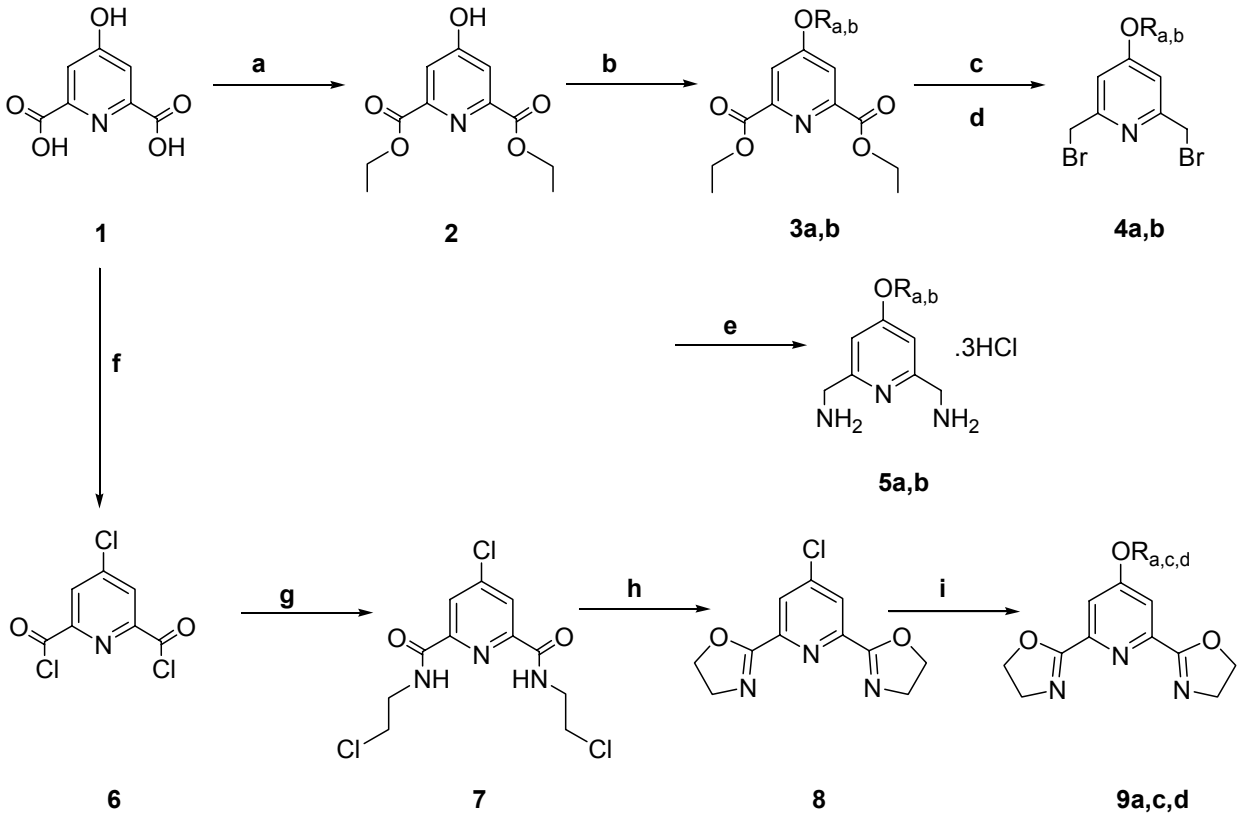

R_a = -$(CH_2)_3$-; R_b = CH_2CH_3; R_c= -CH_3; R_d = -$(CH_2)_{17}CH_3$

***Scheme 2**: (a) $SOCl_2$, EtOH (87%); (b) **3a**: $Br(CH_2)_3Br$, K_2CO_3, MEK (86%) **3b**: CH_3CH_2Br, K_2CO_3, MEK (70%); (c) $NaBH_4$, EtOH, not purified; (d) PBr_3, $CHCl_3$ (step c and d together **4a**: 72%, **4b**: 45%); (e) 1. Hexamethylenetetramine, CH_2Cl_2, 2. HCl, EtOH, H_2O (**5a**: 22%, **5b**: 27%); (f) $SOCl_2$, DMF, not purified; (g) 1. 2-aminoethanol, triethylamine, CH_2Cl_2, 2. $SOCl_2$ (step f and g together 54%); (h) NaH, THF (96%); (i) **9a**: NaH, DMF, 1,3-propanediol (73%) **9c**: NaOMe, MeOH (71%) **9d**: NaH, DMF, benzene, 1-octadecanol (38%).*

In the last step the bromines were replaced using hexamethylenetetramine in dichloromethane. The complex that was formed was subsequently hydrolyzed with acid yielding the protonated ligands **5a** and **5b**. To desalt these water-soluble compounds C18-reversed phase column chromatography was used with water as eluent. The HCl contents and purity of these compounds were determined with a potentiometric titration.

The synthesis of oxazolinylpyridine ligands **9a,c,d** started with preparing acid chloride **6** in $SOCl_2$.[23] This acid chloride was converted into the corresponding 4-chloro-bis(2-chloroethyl)-2,6-pyridinedicarboxamide **7**, by treatment with aminoethanol and subsequently $SOCl_2$ (54%) similar to the method used by Nishiyama et al.[12] Compound **7** was ring closed using NaH in THF to give 4-chloro-2,6-di-oxazolinylpyridine **8**. This compound is an ideal building block; the chloro group can easily be derivatized with all kinds of groups. We used methanol and octadecanol to obtain the monofunctional ligands, **9c** and **9d**, and propanediol was used to obtain the bifunctional ligand, **9a** (37-73%).

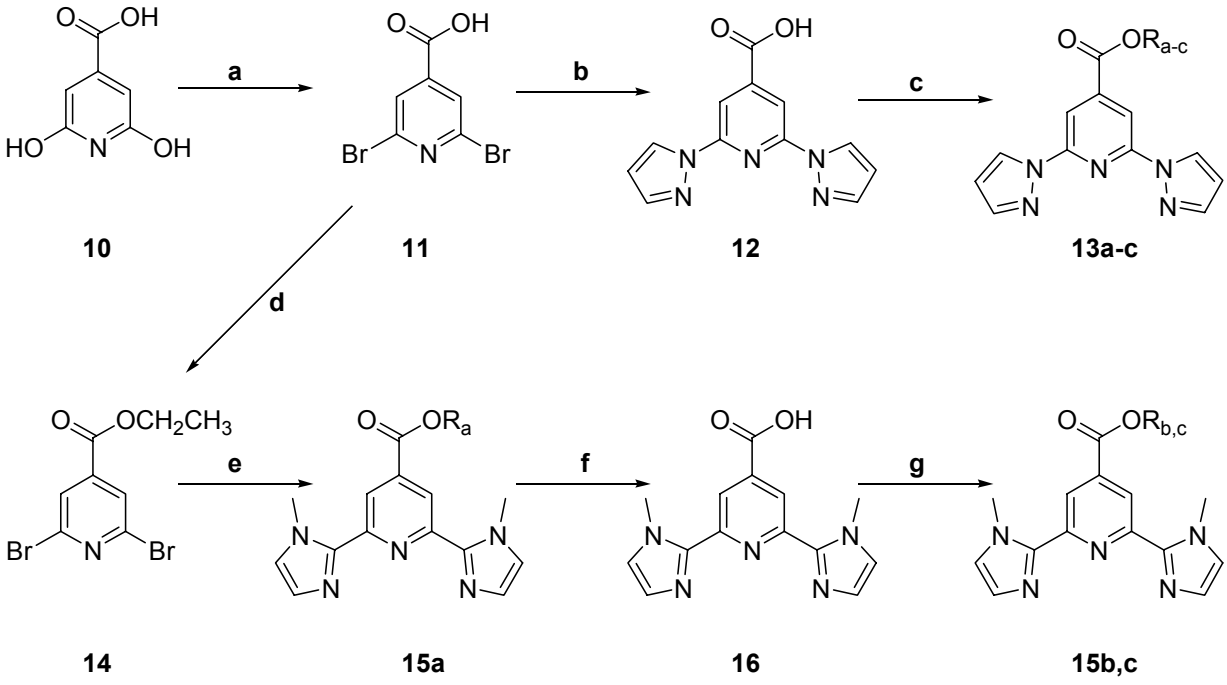

R_a = -CH_2CH_3; R_b = -$(CH_2)_3$-; R_c = -$(CH_2)_{17}CH_3$

***Scheme 3**: (a) $POBr_3$, autoclave (41%); (b) KH, pyrazole, diglyme (67%); (c) **13a**: H_2SO_4, EtOH (74%) **13b**: DCC, DMAP, CH_2Cl_2, 1,3-propanediol (36%) **13c**: DCC, DMAP, CH_2Cl_2, 1-octadecanol (83%); (d) H_2SO_4, EtOH (93%); (e) 1-methyl-2-tributylstannylimidazole, $(Ph_3P)_4Pd$, toluene (79%); (f) KOH, EtOH, H_2O (79%); (g) **15b**: DCC, CH_2Cl_2, DMAP, 1,3-propanediol (53%) **15c**: DCC, CH_2Cl_2, DMAP, 1-octadecanol (89%).*

In scheme 3, the synthesis of pyrazolyl- and methylimidazolylpyridines is depicted both starting from isonicotinic acid **10**. The hydroxyl groups were replaced by bromines using $POBr_3$ according to a procedure from literature yielding compound **11**[24], which is used for the synthesis of both types of ligands. In the case of the pyrazolylpyridine ligands the pyrazolyl groups were introduced using KH as a base. This yielded compound **12** with a carboxylic acid group at the 4-position of the pyridine that can be used as a synthetic handle to introduce other functional groups via for example ester bonds.[25] This was done with propanediol, which gave bifunctional ligand **13b**, and with ethanol and octadecanol, which gave monofunctional ligands **13a** and **13c** respectively. In the case of the methylimidazolyl ligands the carboxylic acid group at the 4-position was first protected as an ethyl ester to give **14**. Then the bromine groups were replaced by 1-methylimidazolyl groups by reaction with 1-methyl-2-tributylstannylimidazole[26] in toluene with $(Ph_3P)_4Pd$ as a catalyst yielding compound **15a** in 79%. This compound is already a monofunctional ligand with a short ethyl tail. To introduce other functionalities the ester was hydrolyzed in a basic solution to compound **16** and esterified again using propanediol and octadecanol to give a bifunctional and an amphiphilic ligand (**15b** and **15c**) respectively.

In conclusion, we have presented in this chapter the synthesis of four different kinds of 4-functionalized terdendate pyridine-based ligands. For each case, the synthesis of both bifunctional and monofunctional ligands is described. Using the methods described here, it will be possible to synthesize dervatives with other spacers and tails. The ligands can find application in supramolecular chemistry, (reversible) coordination polymers, catalysis and separation.

5.3 Experimental Section

All solvents were of p.a. quality and reactions were carried out under dry N_2 when dry atmosphere was required. Chemicals were purchased and used without further purification. 4-Hydroxypyridine-2,6-dicarboxylic acid (chelidamic acid) was obtained from 4-oxo-*4H*-pyrane-2,6-dicarboxylic acid (chelidonic acid)[27]. Diethyl 4-hydroxypyridine-2,6-dicarboxylate, **2**[20], 4-chloro-2,6-pyridinedicarbonyl dichloride, **6**[23], 2,6-dibromoisonicotinic acid **11**[24], ethyl 2,6-dibromoisonicotinate **14**[24,28] and 1-methyl-2-tributylstannylimidazole[26] were prepared according to literature. ^{1}H NMR (200 MHz) and ^{13}C NMR spectra were recorded on a Bruker AC200 spectrometer at room temperature. MS and HRMS data were obtained with a Finnigan MAT 95 spectrometer. Elemental analysis was performed with an Elemental Analyser EMASyst1106. Some of the compounds were too hygroscopic to obtain correct

elemental analyses. UV spectra of the final products were measured on a Perkin Elmer Lambda 18 UV/VIS spectrophotometer.

Tetraethyl 4,4'-(1,3-propoxy)-bis-2,6-pyridinedicarboxylate 3a.
A mixture of compound **2** (8.3 g, 34.7 mmol), 1,3-dibromopropane (3.5 g, 17.3 mmol) and 10.4 g K_2CO_3 were refluxed in 2-butanone for 3 days under a N_2 atmosphere. The solvent was evaporated and CH_2Cl_2 was added to the residue. Salts were removed by filtration and the filtrate was concentrated and purified using column chromatography (1% MeOH in CH_2Cl_2). Yield: 86% oil (7.2 g, 14.9 mmol). ^{1}H NMR ($CDCl_3$): δ 1.41 (t, *J*=7.1 Hz, 12 H, CH_3), 2.38 (m, *J*=5.8 Hz, 2H, CH_2), 4.35 (q, *J*=5.8 Hz, 4H, OCH_2), 4.46 (q, *J*=7.2 Hz, 8H, CH_2OC=O), 7.77 (s, 4H, aromatic H). $C_{25}H_{30}N_2O_{10}$: calcd. C 57.9, H 5.8, N 5.4; found C 58.1, H 5.8, N 5.5.

Diethyl 4-ethoxy-2,6-pyridinedicarboxylate 3b.
Yield: 70% oil. ^{1}H NMR ($CDCl_3$): δ 1.44 (t, *J*=6.8 Hz, 6H, CH_3), 1.47 (t, *J*=5.9 Hz, 3H, CH_3), 4.21 (q, *J*=7.0 Hz, 2H, OCH_2), 4.46 (q, *J*=7.1 Hz, 8H, CH_2OC=O), 7.76 (s, 2H, aromatic H). $C_{13}H_{17}NO_5$: calcd. C 58.4, H 6.4, N 5.2; found C 58.3, H 6.5, N 5.1.

1,3-Bis(2,6-bis[bromomethyl]pyridin-4-yloxy)propane 4a.
Compound **3a** (1.1 g, 2.3 mmol) was dissolved in 30 ml absolute ethanol at 0 ºC. In small amounts $NaBH_4$ (1.4 g, 37 mmol) was added. The reaction mixture was stirred for another 0.5 h at 0 ºC and then refluxed overnight. The solvent was removed, 25 ml of a saturated $NaHCO_3$ solution was added and the mixture was subsequently refluxed for 1 h. The solvent was evaporated and the crude 1,3-bis(2,6-bis[hydroxymethyl]pyridin-4-yloxy)propane was used without purification for the next reaction step. ^{1}H NMR (D_2O/MeOD): δ 2.32 (quint, *J*=6.0 Hz, 2H, CH_2), 4.31 (t, *J*=6.1 Hz, 4H, CH_2O), 4.61 (s, 8H, CH_2OH), 6.98 (s, 4H, aromatic H).
PBr_3 (4.11 g, 15.2 mmol) in 35 ml $CHCl_3$ was added dropwise to a suspension of 1,3-bis(2,6-bis[hydroxymethyl]pyridin-4-yloxy)propane (0.71 g, 2.0 mmol) in 60 ml $CHCl_3$ at room temperature. This reaction mixture was refluxed overnight. To the cooled reaction mixture was added 25 ml of a 5% $NaHCO_3$ solution and the mixture was stirred for another hour until the system became clear. The organic layer was washed with water and dried over Na_2SO_4. The crude product was purified using column chromatography (0.5% MeOH in CH_2Cl_2). Yield: 72% (0.87g, 1.4 mmol) for two steps, mp 129 ºC. ^{1}H NMR ($CDCl_3$): δ 2.32 (quint, *J*=5.9 Hz, 2H, CH_2), 4.21 (q, *J*=5.9 Hz, 4H, CH_2O), 4.47 (s, 8H, CH_2OH), 6.90 (s, 4H, aromatic H). $C_{17}H_{18}N_2O_2Br_4$: calcd. C 33.9, H 3.0, N 4.6; found C 33.9, H 2.9, N 4.4.

2,6-Bis(bromomethyl)-4-ethoxypyridine 4b.
2,6-Bis(hydroxymethyl)-4-ethoxypyridine: ^{1}H NMR (D_2O/MeOD): δ 1.41 (t, *J*=7.0 Hz, 3H, CH_3), 4.20 (q, *J*=7.0 Hz, 2H, CH_2O), 4.62 (s, 4H, CH_2OH), 6.95 (s, 2H, aromatic H). Yield: 45% (for two steps), mp 71 ºC. ^{1}H NMR ($CDCl_3$): δ 1.44 (t, *J*=7.0 Hz, 3H, CH_3), 4.12 (q, *J*=7.0 Hz, 2H, CH_2O), 4.47 (s, 4H, CH_2Br), 6.87 (s, 2H, aromatic H). $C_9H_7NOBr_2$: calcd. C 35.5, H 2.3, N 4.6; found C 35.3, H 2.6, N 4.4.

1,3-Bis(2,6-bis[aminomethyl]pyridin-4-yloxy)propane hexahydrochloride 5a.
To a refluxing solution of hexamethylenetetramine (0.9 g, 6.4 mmol) in 20 ml CH_2Cl_2 a solution of **4a** (0.87 g, 1.45 mmol) in CH_2Cl_2 was added dropwise. This reaction mixture was refluxed overnight. The obtained precipitate was filtered, dissolved in a mixture of 10 ml ethanol and 10 ml water and acidified to pH 3 with concentrated HCl. This mixture was stirred for 3 h and kept at pH < 4 at 40 ºC. The solvent was removed and the crude product was purified and desalted using C18-reversed phase column chromatography with water as eluent. The product was recrystallized with water/acetone. Yield: 22% (0.18 g, 0.32 mmol), mp > 300 ºC. ^{1}H NMR (D_2O): δ 2.15 (quint, *J*=6.0 Hz, 2H, CH_2), 4.07 (s, 8H, CH_2N), 4.10 (m, *J*=6.0 Hz, 4H, CH_2O), 6.78 (s, 4H, aromatic H); ^{13}C NMR (D_2O): δ 30.20 (CH_2) 45.53 (4xCH_2NH_2), 68.08 (2xOCH_2), 111.27 (4xCH), 156.24 (4xCN), 169.35 (2xCO). $C_{17}H_{32}N_6O_2Cl_6$: calcd. C 36.1, H 5.7, N 14.9; found C 36.5, H 5.4, N 15.1. UV (H_2O): λ_{max} (log ε) = 219 nm (4.71).

2,6-Bis(aminomethyl)-4-ethoxypyridine trihydrochloride 5b.
Yield: 27%, mp > 300 ºC. ^{1}H NMR (D_2O): δ 1.33 (t, *J*=7.0 Hz, 3H, CH_3), 4.16 (q, *J*=7.0 Hz, 2H, OCH_2), 4.24 (s, 4H, CH_2N), 6.95 (s, 2H, aromatic H); ^{13}C NMR (D_2O): δ 16.44 (CH_3), 45.54 (2xCH_2NH_2), 67.78 (OCH_2), 111.38 (2xCH), 156.16 (2xCN), 169.41 (CO). $C_9H_{18}N_3OCl_3$: calcd. C 37.2, H 6.2, N 14.5; found C 37.4, H 6.0, N 14.8. UV (H_2O): λ_{max} (log ε) = 211 nm (4.23).

4-Chloro-N^2,N^6-bis(2-chloroethyl)-2,6-pyridinedicarboxamide 7.
To a solution of 2-aminoethanol (1.62 g, 20.6 mmol) and triethylamine (7.92 g, 78.3 mmol) in CH_2Cl_2 (50 ml) was slowly added a solution of 2.03 g (10.0 mmol) acid chloride **6** in CH_2Cl_2 (50 ml) at 0 ºC. The mixture was stirred for 24 h at room temperature. Then $SOCl_2$ (33 ml) was added at 0-10 ºC, and the mixture was refluxed for 9 h and poured slowly into ice water. The organic layer was collected, washed with brine and dried over Na_2SO_4. The product was purified by column chromatography (5% ether in CH_2Cl_2). Yield: 54% (1.76 g, 5.4 mmol), mp 173-174 ºC. ^{1}H NMR ($CDCl_3$): δ 3.74 (t, *J*=5.1 Hz, 4H, CH_2Cl), 3.83 (q, *J*=5.4 Hz, 4H, CH_2N), 8.10

(s, 2H, NH), 8.34 (s, 2H, aromatic H). HRMS calcd for $C_{11}H_{12}N_3O_2Cl_3$ 322.9995, found 322.9991.

4-Chloro-2,6-di(4,5-dihydro-1,3-oxazol-2-yl)pyridine 8.

To a suspension of NaH (0.68 g, 60% oil, 17.0 mmol) in THF (12 ml) was added a solution of **7** (1.76 g, 5.4 mmol) in THF (25 ml). The mixture was stirred overnight. After filtration and concentration, the residue was extracted with ether. The extract gave a solid upon evaporation of the solvent, which was recrystallized from hexane/ethyl acetate to give **8** as white needles. Yield: 96% (1.3 g, 5.17 mmol), mp 179–180 ºC. IR (KBr disk) 1636, 1562, 1385, 1275, 1124, 945, 783 cm^{-1}, ^1H NMR ($CDCl_3$): δ 4.09 (t, *J*=9.5 Hz, 4H, CH_2), 4.56 (t, *J*=9.4 Hz, 4H, CH_2), 8.16 (s, 2H, aromatic H); ^{13}C NMR ($CDCl_3$): δ 55.09 (2xCH_2N), 68.57 (2xCH_2O), 125.72 (2xCH), 145.44 (2xCN), 147.94 (CCl), 162.62 (2xOC=N). HRMS calcd for $C_{11}H_{10}N_3O_2Cl$ 251.0462, found 251.0462.

1,3-Bis(2,6-di[4,5-dihydro-1,3-oxazol-2-yl]pyridin-4-yloxy)propane 9a.

To a suspension of NaH (0.08 g, 60 % oil, 2 mmol) in dry DMF was added 0.08 g (1.0 mmol) of 1,3-propanediol. After stirring at room temperature for 1 h compound **8** was added (0.50 g, 2.0 mmol) and the mixture was heated at 40 ºC for 2 days. The solvent was evaporated and the residue was extracted using hot ethyl acetate to give **9a** as a white solid. Yield: 73% (0.37 g, 0.7 mmol), mp 207-209 ºC. ^1H NMR (CD_3OD): δ 2.11 (m, *J*=6.0 Hz, 2H, CH_2), 3.81 (t, *J*=9.6 Hz, 8H, CH_2), 4.12 (t, *J*=6.0 Hz, 4H, CH_2O), 4.29 (t, *J*=9.8 Hz, 8H, CH_2), 7.41 (s, 4H, aromatic H); ^{13}C NMR (CD_3OD): δ 30.48 (CH_2), 56.49 (4xCH_2N), 67.47 (4xCH_2O), 70.86 (2xCH_2O) 116.01 (4xCH), 150.40 (2xCN), 166.47 (4xOC=N), 168.67 (CO). $C_{25}H_{26}N_6O_6 \cdot 0.8H_2O$: calcd. C 57.6, H 5.3, N 16.1; found C 57.8, H 5.2, N 15.9. UV (CH_3OH): λ_{max} (log ε) = 210 nm (4.64), 229 nm (4.55).

2,6-Di(4,5-dihydro-1,3-oxazol-2-yl)-4-methoxypyridine 9c.

Sodium (0.137 g, 0.596 mmol) was added to 10 ml methanol. After 15 minutes compound **8** (1.0 g, 4.0 mmol) was added. The mixture was heated at 40 ºC for 24 h. The solvent was evaporated and the residue was extracted using hot ethyl acetate to give **9c** as a white solid. Yield: 71% (0.70 g, 2.8 mmol), mp 218-220 ºC. ^1H NMR (CD_3OD): δ 3.91 (s, 3H, OCH_3), 4.18 (t, *J*=9.4 Hz, 4H, CH_2), 4.50 (t, *J*=9.7 Hz, 4H, CH_2), 7.62 (s, 2H, aromatic H); ^{13}C NMR (CD_3OD): δ 55.43 (CH_3O), 56.68 (2xCH_2N), 69.85 (2xCH_2O), 112.98 (2xCH), 149.22 (2xCN), 165.39 (2xOC=N), 168.60 (CO). $C_{12}H_{13}N_3O_3$: calcd. C 58.3, H 5.3, N 17.0; found C 58.0, H 5.3, N 17.0. HRMS calcd for $C_{12}H_{13}N_3O_3$ 247.0957, found 247.0963. UV (CH_3OH): λ_{max} (log ε) = 210 nm (4.38), 231 nm (4.32).

2,6-Di(4,5-dihydro-1,3-oxazol-2-yl)-4-octadecyloxy-pyridine 9d.

To a suspension of NaH (0.08 g, 60 % in oil, 2 mmol) in dry DMF was added 1-octadecanol (0.54 g, 2.0 mmol) and this mixture was stirred for 1 h at room temperature. Compound **8** was added (0.50 g, 2.0 mmol) and the reaction mixture was heated at 40 ºC for 2 days. The solvent was evaporated and the residue was extracted with hot ethyl acetate. After evaporation the residue was washed with hot hexane and recrystallized from ethanol to give **9d** as a white solid. Yield: 38% (0.37 g, 0.8 mmol), mp 116-117 ºC. ^{1}H NMR ($CDCl_3$): δ 0.86 (t, *J*=6.5 Hz, 3H, CH_3), 1.24 (m, 30H, CH_2), 1.79 (m, 2H, CH_2), 4.11 (t, *J*=6.6 Hz, 4H, CH_2), 4.09 (m, *J*=9.3 Hz, 2H, OCH_2), 4.51 (t, *J*=8.8 Hz, 4H, CH_2), 7.64 (s, 2H, aromatic H); ^{13}C NMR ($CDCl_3$): δ 14.15 (CH_3), 22.70-31.94 (16xCH_2), 54.99 (2xCH_2N), 68.34 (2xCH_2O), 68.82 (OCH_2), 112.04 (2xCH), 148.13 (2xCN), 163.65 (2xOC=N), 166.01 (CO). $C_{29}H_{47}N_3O_3 \cdot 1.4H_2O$: calcd. C 68.2, H 9.8, N 8.2; found C 68.2, H 9.4, N 8.1. HRMS calcd for $C_{29}H_{47}N_3O_3$ 485.3617, found 485.3615. UV (CH_3OH): λ_{max} (log ε) = 210 nm (4.35), 232 nm (4.30).

2,6-Di(1-*H*-pyrazol-1-yl)isonicotinic acid 12.

To a solution of pyrazole (2.43 g, 35 mmol) in anhydrous diglyme (50 ml) was added KH (33 mmol, oil-free) and the mixture was stirred at room temperature for 2 h. 2,6-Dibromoisonicotinic acid **11** (2.81 g, 10 mmol) was added in one portion. The resulting mixture was stirred at 130 ºC for 3 days. The solvent was removed under reduced pressure. Water was added and the mixture was acidified. The obtained precipitate was filtered and purified by dissolving in methylene chloride, adding methanol, and slowly removing the methylene chloride on a rotatory evaporator. The solid material was isolated by filtration. Yield: 67% (1.7 g, 6.7 mmol), mp 263-265 ºC. ^{1}H NMR ($CDCl_3$/CD_3OD): δ 6.52 (dd, *J*=1.4 and 2.6 Hz, 2H, CH=C), 7.76 (d, *J*=1.4 Hz, 2H, CH=N), 8.31 (s, 2H, aromatic H), 8.60 (d, *J*=2.6 Hz, 2H, CH=N); ^{13}C NMR ($CDCl_3$/CD_3OD): δ 108.15 (2xCH), 108.99 (2xCH), 127.38 (2xNCH), 142.57 (2xN=CH), 144.16 (C), 150.41 (2xNCN), 165.36 (CO_2H). HRMS calcd for $C_{12}H_9N_5O_2$ 255.0756, found 255.0760.

Ethyl 2,6-di(1-*H*-pyrazol-1-yl)isonicotinate 13a.

A mixture of compound **12** (0.26 g, 1.0 mmol) and concentrated H_2SO_4 (0.5 ml) in 10 ml of ethanol was heated for 3 h. The solvent was removed by evaporation and water was added to the residue. The precipitate was filtered and purified by recrystallization from ethanol/water to give a white solid. Yield: 74% (0.21g, 0.7 mmol), mp 143-144 ºC. ^{1}H NMR ($CDCl_3$): δ 1.43 (t, *J*=7.16 Hz, 3H, CH_3), 4.45 (q, *J*=7.1 Hz, 2H, OCH_2), 6.50 (dd, *J*=1.4 and 2.6 Hz, 2H, CH=C), 7.79 (d, *J*=1.3 Hz, 2H, CH=N), 8.37 (s, 2H, aromatic H), 8.56 (d, *J*=2.6 Hz, 2H, CH=N); ^{13}C NMR ($CDCl_3$): δ 14.23

(CH_3), 62.15 (OCH_2), 108.35 (2xCH), 109.09 (2xCH), 127.16 (2xNCH), 142.76 (2xN=CH), 143.55 (C), 150.68 (2xNCN), 163.93 (CO_2). $C_{14}H_{13}N_5O_2$: calcd. C 59.3, H 4.6, N 24.7; found C 58.9, H 4.4, N 24.3. UV (CH_3OH): λ_{max} (log ε) = 208 nm (4.22), 248 nm (4.45), 268 nm (4.08), 331 nm (4.02).

1,3-Propyl bis-[2,6-di(1-*H*-pyrazol-1-yl)isonicotinate] 13b.

A mixture of 0.26 g (1.0 mmol) of compound **12** in 10 ml CH_2Cl_2, DCC (0.46 g, 2.2 mmol), 0.04 g (0.5 mmol) of 1,3-propanediol and a catalytic amount of DMAP was stirred for 2 days. The precipitate was removed by filtration, the filtrate was concentrated and the residue was purified by column chromatography (0.3% MeOH in CH_2Cl_2). Yield: 36% (0.10 g, 0.2 mmol), mp 223-225 ºC. ^{1}H NMR ($CDCl_3$): δ 2.36 (quint, *J*=5.8 Hz, 2H, CH_2), 4.61 (t, *J*=5.8 Hz, 4H, OCH_2), 6.46 (dd, *J*=1.3 and 2.3 Hz, 2H, CH=C), 7.69 (d, *J*=1.2 Hz, 2H, CH=N), 8.29 (s, 2H, aromatic H), 8.45 (d, *J*=2.4 Hz, 2H, CH=N); ^{13}C NMR ($CDCl_3$/CD_3OD): δ 30.62 (CH_2), 63.65 (2xCH_2O), 108.25 (4xCH), 108.81 (4xCH), 127.21 (4xNCH), 142.67 (2xN=CH), 142.85 (2xC), 150.35 (4xNCN), 163.92 (2xCO_2). $C_{27}H_{22}N_{10}O_4$: calcd. C 58.9, H 4.0, N 25.4; found C 58.8, H 3.9, N 25.6. UV (CH_2Cl_2): λ_{max} (log ε) = 249 nm (4.64), 270 nm (4.56), 334 nm (4.52).

Octadecyl 2,6-di(1-*H*-pyrazol-1-yl)isonicotinate 13c.

Yield 83%, mp 91-93 ºC. ^{1}H NMR ($CDCl_3$): δ 0.86 (t, *J*=6.8 Hz, 3H, CH_3), 1.30 (m, 30H, CH_2), 1.79 (m, *J*=7.1 Hz, 2H, CH_2), 4.38 (t, *J*=6.8 Hz, 2H, OCH_2), 6.55 (dd, *J*=1.2 and 2.4 Hz, 2H, CH=C), 7.80 (d, *J*=1.2 Hz, 2H, CH=N), 8.38 (s, 2H, aromatic H), 8.57 (d, *J*=2.4 Hz, 2H, CH=N); ^{13}C NMR ($CDCl_3$): δ 14.10 (CH_3), 22.66-31.89 (16xCH_2), 66.34 (OCH_2), 108.34 (2xCH), 109.11 (2xCH), 127.14 (2xNCH), 142.74 (2xN=CH), 143.59 (C), 150.69 (2xNCN), 164.03 (CO_2). $C_{30}H_{45}N_5O_2$: calcd. C 71.0, H 8.9, N 13.8; found C 70.9, H 9.1, N 13.4. UV (CH_3OH): λ_{max} (log ε) = 208 nm (4.13), 248 nm (4.36), 268 nm (3.99), 230 nm (3.91).

Ethyl 2,6-bis(1-methyl-1*H*-imidazol-2-yl)isonicotinate 15a.

A mixture of 2.97 g (9.6 mmol) of compound **14**, 1-methyl-2-tributylstannylimidazole (9.6 g, 26 mmol) and $(Ph_3P)_4Pd$ (0.29 g, 0.02 mmol) was heated under N_2 in toluene (100 ml) for 12 h. After cooling the solvent was removed and the residue was purified by column chromatography on silica gel (5% MeOH in CH_2Cl_2). Yield: 79% (2.35 g, 7.6 mmol), mp 148-150 ºC. ^{1}H NMR ($CDCl_3$): δ 1.40 (t, *J*=7.1 Hz, 3H, CH_3), 4.12 (s, 6H, NCH_3), 4.41 (q, *J*=7.1 Hz, 2H, OCH_2), 7.02 (d, *J*=1.2 Hz, 2H, CHN), 7.18 (d, *J*=1.0 Hz, 2H, CHN), 8.62 (s, 2H, aromatic H); ^{13}C NMR ($CDCl_3$): δ 14.29 (CH_3), 61.90 (OCH_2), 121.71, (2xCH), 124.53 (2xCH), 128.86 (2xCH), 139.66 (C), 144.72 (C), 150.34 (C), 164.58 (CO_2). $C_{16}H_{17}N_5O_2 \cdot 0.2H_2O$: calcd. C 61.0, H 5.6, N 22.2; found C 61.3, H

5.4, N 21.9. HRMS calcd for $C_{16}H_{17}N_5O_2$ 311.1382, found 311.1374. UV (CH_3OH): λ_{max} (log ε) = 279 nm (4.32), 341 nm (4.06).

2,6-Bis(1-methyl-1*H*-imidazol-2-yl)isonicotinic acid 16.

A mixture of compound **15a** (3.2 g,10.3 mmol), 1.15 g of KOH, dissolved in 20 ml of water and 50 ml of ethanol was refluxed for 2 hours. Ethanol was removed by evaporation and water was added to the residue. The mixture was acidified with 1 N HCl to pH~6.2, which gave compound **16** as a white solid. Yield: 79% (2.3 g, 8.1 mmol), mp 315-318 ºC. ^{1}H NMR (D_2O): δ 3.78 (s, 6H, NCH_3), 7.09 (d, *J*=1.2 Hz, 2H, CHN), 7.16 (d, *J*=1.0 Hz, 2H, CHN), 7.97 (s, 2H, aromatic H); ^{13}C NMR (D_2O/CD_3OD): δ 121.12 (2xCH), 126.27 (2xCH), 128.30 (2xCH), 139.64 (C), 144.09 (C), 150.27 (C), 164.77 (CO_2). HRMS calcd for $C_{14}H_{13}N_5O_2$ 283.1069, found 283.1059.

1,3-Propyl bis-[2,6-bis(1-methyl-1*H*-imidazol-2-yl)isonicotinate] 15b.

A mixture of 0.28 g (1.0 mmol) of compound **16** in 10 ml CH_2Cl_2, 2.2 mmol of DCC, 0.04 g (0.5 mmol) of propanediol and a catalytic amount of DMAP was stirred for 2 days at room temperature. The precipitate was removed by filtration, the filtrate was concentrated and the residue was purified by column chromatography (5% MeOH in CH_2Cl_2). The product was recrystallized from MeOH/hexane. Yield 53% (0.16 g, 0.3 mmol), mp 220-222 ºC. ^{1}H NMR ($CDCl_3$): δ 2.30 (quint, *J*=6.2 Hz, 2H, CH_2), 4.07 (s, 12H, NCH_3), 4.53 (t, *J*=6.2 Hz, 4H, OCH_2), 7.02 (d, *J*=1.2 Hz, 4H, CHN), 7.18 (d, *J*=1.0 Hz, 2H, CHN), 8.61 (s, 4H, aromatic H); ^{13}C NMR ($CDCl_3$): δ 27.82 (CH_2), 62.46 (2xOCH_2), 121.60 (4xCH), 124.72 (4xCH), 128.24 (4xCH), 139.29 (2xC), 144.21 (2xC), 150.01 (2xC), 164.34 (2xCO_2). HRMS calcd for $C_{31}H_{30}N_{10}O_4$ 606.2451, found 606.2442. UV (CH_3OH): λ_{max} (log ε)=279 nm (4.75), 342 nm (4.30).

Octadecyl 2,6-bis(1-methyl-1*H*-imidazol-2-yl)isonicotinate 15c.

A mixture of 0.30 g (1.1 mmol) of compound **16** in 10 ml CH_2Cl_2, 1.2 mmol of DCC, 0.27 g (1.0 mmol) of octadecanol and a catalytic amount of DMAP was stirred for 2 days at room temperature. The precipitate was removed by filtration, the filtrate was concentrated and the residue was purified by column chromatography (5% MeOH in CH_2Cl_2). The product was recrystallized from MeOH/hexane. Yield 89% (0.48 g, 0.9 mmol), mp 98-99 ºC. ^{1}H NMR ($CDCl_3$): δ 1.25 (t, *J*=6.5 Hz, 3H, CH_3), 1.24 (m, 30H, CH_2), 1.70 (quint, *J*=7.1 Hz, 2H, CH_2), 4.08 (s, 6H, NCH_3), 4.45 (t, *J*=6.8 Hz, 2H, OCH_2), 7.02 (d, *J*=1.2 Hz, 2H, CHN), 7.18 (d, *J*=1.0 Hz, 2H, CHN), 8.61 (s, 2H, aromatic H); ^{13}C NMR ($CDCl_3$): δ 14.15 (CH_3), 22.71-35.85 (16xCH_2), 66.15 (OCH_2), 121.74 (2xCH), 124.45 (2xCH), 128.87 (2xCH), 139.72 (C), 144.75 (C), 150.33 (C), 164.71

(CO_2). HRMS calcd for $C_{32}H_{49}N_5O_2$ 535.3886, found 535.3887. UV (CH_3OH): λ_{max} (log ε) = 280 nm (4.26), 341 nm (3.99).

5.4 References

1. Kimura, M.; Horai, T.; Muto, T.; Hanabusa, K.; Shirai, H. *Chem. Lett.* **1999**, 1129-1130.
2. Kelch, S.; Rehahn, M. *Macromolecules* **1999**, *32*, 5818-5828.
3. Velten, U.; Lahn, B.; Rehahn, M. *Macromol. Chem. Phys.* **1997**, *198*, 2789-2816.
4. Schubert, U. S.; Eschbaumer, C. *Angew. Chem. Int. Ed.* **2002**, *41*, 2892-2926.
5. Schubert, U. S.; Weidl, C. H.; Moorefield, C. N.; Baker, G. R.; Newkome, G.R. *Polymer Preprints* **1999**, *40*, 940-941.
6. Salditt, T.; An, Q.; Plech, A.; Eschbaumer C.; Schubert, U. S. *Chem. Commun.* **1998**, 2731-2732.
7. Holliday, B. J.; Mirkin, C. A. *Angew. Chem. Int. Ed.* **2001**, *40*, 2022-2043.
8. Schubert, U. S.; Eschbaumer, C.; Hien, O.; Andres, P. R. *Tetrahedron Lett.* **2001**, *42*, 4705-4707.
9. Choi, J. S.; Kang, C. W.; Jung, K.; Yang, J. W.; Kim, Y.-G.; Han, H. *J. Am. Chem. Soc.* **2004**, *126*, 8606-8607.
10. Lehmann, P.; Kurth, D. G.; Brezesinski, G.; Symietz, C. *Chem. Eur. J.* **2001**, 1646-1651.
11. Couturier, Y.; Petitfaux, C. *Bull. Soc. Chim. Fr.* **1992**, *129*, 335-342.
12. Nishiyama, H.; Yamaguchi, S.; Kondo, M.; Itoh, K. *J. Org. Chem.* **1992**, *57*, 4306-4309.
13. Jameson, D. L.; Blaho, J. K.; Kruger, K. T.; Goldsby, K. A. *Inorg. Chem.* **1989**, *28*, 4312-4314.
14. Xiaoming, X.; Haga, M.-A.; Matsumura-Inoue, T.; Ru, Y.; Addison, W.; Kano, K. *J. Chem. Soc. Dalton Trans.* **1993**, 2477-2484.
15. Yu, S. C.; Hou, S.; Chan, W. K. *Macromolecules* **1999**, *32*, 5251-5256.
16. Petoud, S.; Bünzli, J.-C. G.; Schenk, K. J.; Piguet, C. *Inorg. Chem.* **1997**, *36*, 1345-1353.
17. Beck, J. B.; Rowan, S. J. *J. Am. Chem. Soc.* **2003**, *125*, 13922-13923.
18. Heller, M; Schubert, U. S. *J. Org. Chem.* **2002**, *67*, 8269-8272.
19. de Bruin, T. J. M.; Marcelis, A. T. M.; Zuilhof, H.; Rodenburg, L. M.; Niederländer, H. A. G.; Koudijs, A.; Overdevest, P. E. M.; van der Padt, A.; Sudhölter,E. J. R. *Chirality* **2000**, *12*, 627-636.
20. Chessa, G.; Scrivanti, A. *J. Chem. Soc., Perkin Trans. 1* **1996**, 307-311.
21. Horváth, G.; Rusa, C.; Köntös, Z.; Gerencsér, J.; Huszthy, P. *Synth. Commun.* **1999**, *29*, 3719-3731.
22. Takalo, H.; Pasanen, P.; Kankare, J. *Acta Chem.Scand. B42* **1988**, 373-377.
23. Dumont, A.; Jacques, V.; Desreux, J. F. *Tetrahedron* **2000**, *56*, 2043-2052.
24. Fallahpour, R.-A. *Synthesis* **2000**, *8*, 1138-1142.
25. Jameson, D. L.; Goldsby, K. A. *J. Org. Chem.* **1990**, *55*, 4992-4994.
26. Molloy, K. C.; Waterfield, P. C.; Mahon, M. F. *J. Organometallic Chem.* **1989**, *365*, 61-73.
27. Harirchain, B.; Gormley, J. L. US Patent 5 300 657, **1993**.
28. Ulrich, G.; Bedel, S.; Picard, C.; Tisnès, P. *Tetrahedron Lett.* **2001**, *42*, 6113-6115.

Solvent effects on the reversibility of coordination polymers

Chapter 6

*The reversibility of the coordination bonds in two coordination polymers was studied in different solvents. In water, a ligand with two 2,6-bis(aminomethyl)pyridine groups as complexing groups was used (**BAMPy**). In an organic solvent (chloroform/acetonitrile), a ligand with two 2,6-bis(methylimidazolyl)pyridine groups was used (**BMIPy**). Both terdendate ligands bind to Zn^{2+} ions via three nitrogens. Viscosity measurements were used to follow the formation and breaking of the polymers as a function of the metal/ligand molar ratio for **BMIPy**. The breaking of the water-soluble **BAMPy** coordination polymers was shown by addition of monofunctional ligands. The coordination polymers in water showed fast equilibration upon changes in concentration, while in an organic solvent no changes in size of the structures of **BMIPy** were found upon dilution in viscosity measurements. ^1H NMR measurements were used to monitor the ring-chain equilibrium of the coordination polymers containing **BMIPy** ligands in a chloroform/acetonitrile mixture. The coordination polymers in the organic solvent showed some exchange, but much slower than in the water-based system.*

6.1 Introduction

In today's materials research a lot of effort is devoted to the development of supramolecular polymers. One of the main advantages of supramolecular polymers over conventional polymers is the reversibility of the bonds between the repeating units. When the reversibility of these bonds can be tuned, it could lead to "smart materials". These materials could behave as polymers, but can lose their polymeric properties, when exposed to external stimuli that break the supramolecular bonds.

Supramolecular coordination polymers can be divided into two groups with respect to the reversibility. The first group consists of coordination polymers that are usually formed in water or other coordinating solvents, such as methanol. Due to the competition between solvent molecules and ligand groups for the complexation of metal ions, the exchange of ligands is very fast. This leads to an immediate equilibration of the system, resulting in a solution containing rings and chains with an average degree of polymerization.[1,2] The second group of supramolecular polymers is usually prepared in non-polar organic solvents. Here, the solvent does not play a role as competitor in the complex formation or complex breaking. This results in polymers that reach their equilibrium state much slower than the water-based coordination polymers. The solvent may not be the only factor responsible for the rate of equilibration. The kind of metal ion also plays a role. Some metal ions form kinetically very stable complexes and display no exchange at all. Depending on the specific metal ion-ligand group interaction even polymers can be formed in coordinating solvents in which no exchange is detected at all.[3,4] So, these polymers cannot be called reversible polymers, although the bonds between repeating units are not covalent.

An example of a slowly equilibrating coordination polymer in an organic solvent is the polymer described by Sijbesma et al.[5] that consists of ligands with two diphenylphosphino groups connected by a spacer that bind to Pd^{2+}. This is a nice example because the authors showed that the coordination bonds could be broken by ultrasound.[6] After sonication the system returns to its equilibrium state with polymers of the same average length as before sonication in about 23 hours. Although the system is reversible, it is very slow.

The properties of faster equilibrating systems in water can be influenced by many external stimuli. In chapter 2, it was shown that the ring-chain equilibrium could be adjusted by changes in the metal to ligand molar ratio and the temperature.[1] In chapter 4, we saw the influence of temperature on the material properties of a water-soluble three-dimensional coordination polymer.[7] However, besides temperature increase also pH-changes can be used to break coordination polymers. Lohmeijer

and Schubert have shown that terpyridine metal complexes in water can be broken at both very high and low pH values.[8] It depends on the metal ion, whether the decomplexation is fast (Fe^{2+}, Co^{2+}, Zn^{2+}, Cd^{2+}), slow (Cu^{2+}) or "immune" (Ru^{2+}, Ni^{2+}) to pH changes.

In this chapter, the influence of the solvent on the rate of exchange of ligand groups in coordination polymers is described. Because it is difficult to synthesize a bifunctional ligand that dissolves both in water and in non-coordinating organic solvents, we used two different ligand molecules in this study. Although the ligands have different ligand groups, they both bind to metal ions via three nitrogens. To be able to compare the results as properly as possible only one kind of metal ion was used to study the complexation with both ligand molecules. Zinc is a suitable metal ion because it has shown to form fast exchanging coordination polymers in water.[1]

6.2 Results and discussion

The ligands we used for this study are **BAMPy** (Bifunctional ligand with AminoMethyl Pyridine groups) and **BMIPy** (Bifunctional ligand with MethylImidazolyl Pyridine groups) as depicted in figure 1. The syntheses of these ligands were described in chapter 5.[9] The **BAMPy** ligand is water-soluble, while the **BMIPy** ligand is soluble in various organic solvents. The metal ion used in this study is Zn^{2+}. As reported, this metal ion is capable of binding two bis-aminomethyl pyridine groups.[10,11] No direct data have been reported about the complexation of bis-methylimidazolyl pyridine groups to Zn^{2+} ions, but many structurally related compounds (mainly bis(benzimidazolyl)pyridines) are known to bind several metal ions.[12,13,14] Furthermore, bis(benzimidazolyl)pyridines groups have been used for the formation of supramolecular coordination polymers using, amongst others, Zn^{2+} as connecting metal ion.[15,16] On the basis of the results reported for the structurally related bis-benzimidazolyl pyridines, complexation of Zn^{2+} by two methylimidazolyl ligand groups is presumed. ^{1}H NMR spectroscopy also confirmed the complexation of Zn^{2+} ions to the ligands, as will be described in section 6.2.2.

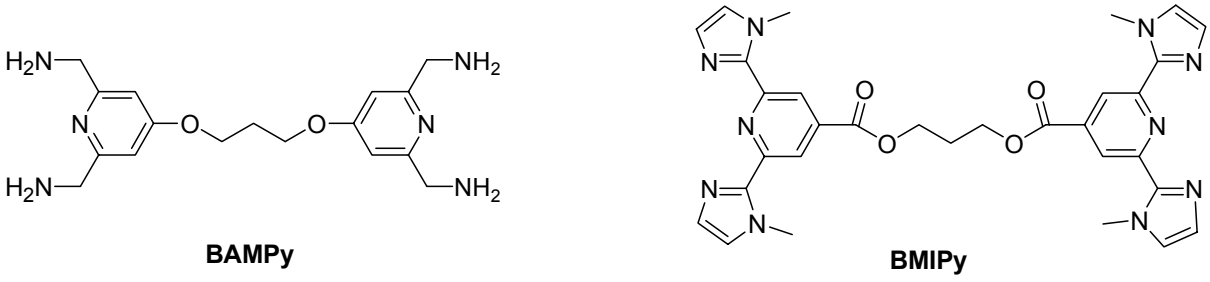

***Figure 1**: Bifunctional ligands **BAMPy** and **BMIPy**.*

6.2.1 Viscosity measurements

The first approach to look at the formation of coordination polymers is to measure the viscosity of a ligand solution upon addition of metal ions. The longest polymers and thus the highest viscosity are expected when the solution contains equimolar amounts of metal ions and bifunctional ligand molecules.

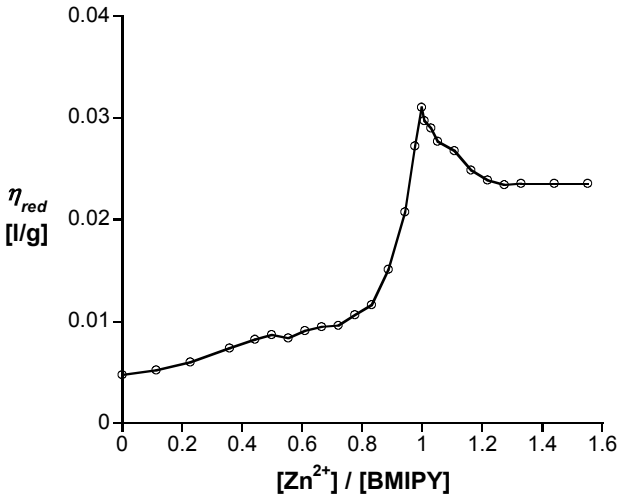

***Figure 2**: Reduced viscosity of **BMIPy** in $CHCl_3/CH_3CN$ (1:1) at a concentration of 29.3 mM as a function of molar ratio $Zn(ClO_4)_2$/**BMIPy** at 298 K.*

For the **BMIPy** ligand, a molar ratio-viscosity curve in a 1:1 mixture of chloroform and acetonitrile was measured (figure 2). Upon addition of zinc ions, an increase in the viscosity is seen, indicating an increase in the average chain length of the polymers. After the equivalence point a small decrease is found, that levels off toward a plateau value. In a completely reversible system one would expect a significant decrease in viscosity after the equivalence point, because excess of metal ions acts as chain stoppers. Since this is not the case here, the system seems not as reversible as the water-soluble coordination polymers reported in chapter 2.

For the **BAMPy** ligands in an aqueous system, we were unfortunately not able to measure such a curve. They are not very well soluble with metal ions in a reasonably concentrated buffer (100 mM PIPES, pH 7). For the measurements in water in which the metal-ligand ratio is varied a buffer is necessary, because upon addition of metal ions the pH drops significantly. At a low pH, the ligands are protonated and Zn^{2+} ions cannot bind. Fortunately, a buffer is only necessary when the molar ratio is varied. When the ratio remains constant during experiments, the pH of the solution can be set at a certain value using a NaOH solution.

Because it was not possible to perform the molar-ratio dependent experiments with **BAMPy**, another approach was used to see whether the coordination bonds in

the polymers in water are reversible on the time scale of the experiment. Not only an excess of either bifunctional ligands or metal ions can decrease the average chain length, but also monofunctional ligands can act as chain stoppers and reduce the chain length. A solution with **BAMPy** and $Zn(NO_3)_2$ at a 1:1 molar ratio in water was set at a pH of 9.2. This pH is certainly high enough to prevent protonation of the ligands and is therefore promoting the complexation of metal ions. The viscosity of this coordination polymer solution was measured after additions of small amounts of the monofunctional ligand, **MAMPy** (figure 3). The large drop in viscosity found after addition of only a small amount of monofunctional ligand shows that the polymers become shorter. The equilibration is fast and occurs within the time scale of the experiment. A similar effect was found before in reversible hydrogen-bonded polymers in organic solvents.[17,18]

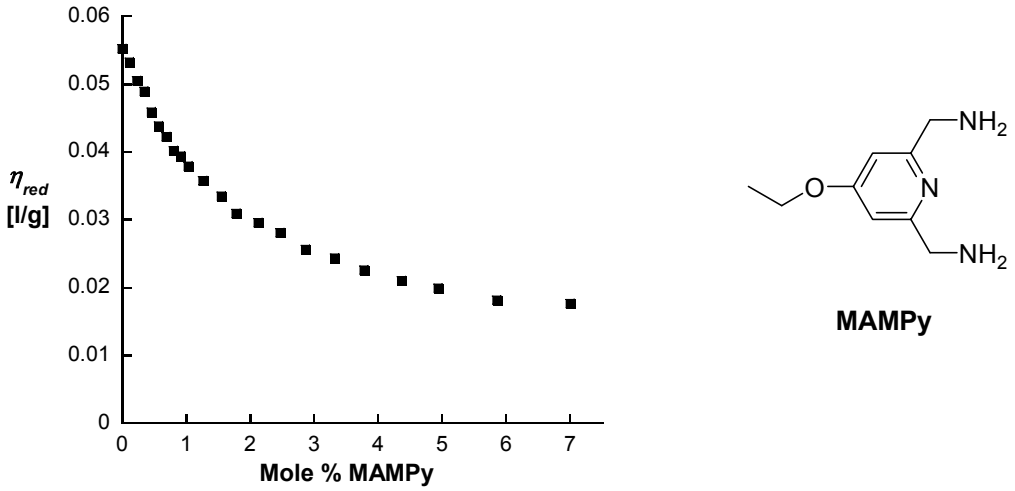

Figure 3: *Reduced viscosity of a 66 mM solution of* ***BAMPy*** *and* $Zn(NO_3)_2$ *(1:1) in* H_2O *at pH 9.2 upon addition of monofunctional ligand* ***MAMPy****.*

Concentration dependent viscosity measurements at a 1:1 metal to ligand ratio can also be used to show the reversibility of the system. In a system in equilibrium, the average chain length of the polymers is dependent on the concentration. The polymers become longer at high concentrations yielding a higher viscosity of the solution than at lower concentrations. In figure 4, the concentration dependence of the specific viscosity of solutions of **BAMPy** in water and **BMIPy** in an organic solvent with Zn^{2+} is shown. The measurements were started at the highest displayed concentration and the viscosity was measured after each dilution step. For **BAMPy** the viscosity dropped upon dilution as expected for a reversible polymer system. The curve has a slope of about 1.8. For linear reversible polymers, Cates predicted a slope of 3.5 above the overlap concentration.[19] The slope of 1.8 is considerably

smaller than 3.5, indicating that the polymers formed here are probably not very long and even the highest concentration is below the overlap concentration. For **BMIPy** a slope of 1.0 was found, which suggests that the size of the polymers does not change upon dilution. This would mean that the **BMIPy** system in an organic solvent is not reversible on the time scale of these measurements. Each dilution and viscosity measurement step took about 10-15 minutes.

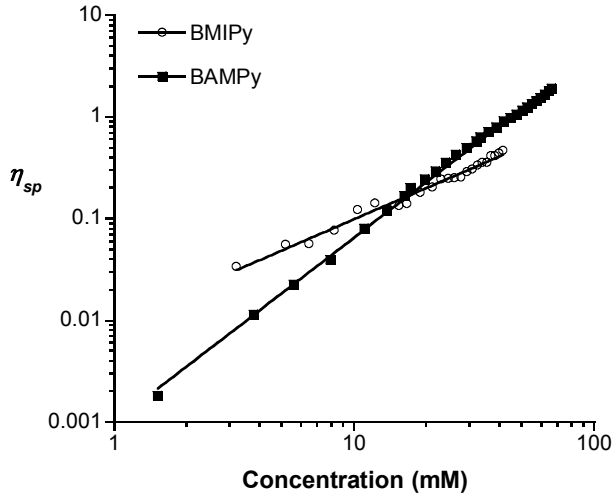

Figure 4: *Concentration dependent specific viscosity of* ***BAMPy*** *and* $Zn(NO_3)_2$ *(1:1) in* H_2O *at pH 9.2 and of* ***BMIPy*** *and* $Zn(ClO_4)_2$ *(1:1) in* $CHCl_3/CH_3CN$ *(1:1).*

6.2.2 NMR measurements

Sometimes ^{1}H NMR spectroscopy can also give information on the equilibrium state of reversible polymers. The solution can also contain rings besides linear chains as was described earlier in chapter 2.[1] The relative amount of rings is higher at low concentrations, while linear polymers dominate at high concentrations. The rings and chains sometimes give separate signals in ^{1}H NMR spectra. In that case, the contributions of rings and chains can be measured as a function of the concentration. If the system equilibrates fast enough the signals of rings should become larger upon dilution.

^{1}H NMR spectra of **BAMPy** with Zn^{2+} ions were measured at different concentrations in D_2O, but did not give any additional signals that could be attributed to rings and chains. This does not necessarily mean that rings are not present; either the exchange between rings and chains is very fast or they just do not give separate signals. In the spectra of **BMIPy** with Zn^{2+} in an organic solvent ($CDCl_3/CD_3CN$) the signals of the pyridine and imidazolyl protons are shifted a little to higher field compared to the same signals of **BMIPy** without metal ions.[9] This is additional proof that complexation takes place. Also separate signals that could be

ascribed to rings and chains are found. The singlet at 8.3 ppm belongs to the aromatic protons in the pyridine ring. The peaks at 6.85 and 6.25 ppm originate from the CH groups in the methylimidazolyl aromatic rings. Next to these larger signals several smaller peaks are found. To determine which peaks belong to protons in a ring or in a chain conformation, DOSY NMR can be used.[20] With this technique the diffusion coefficient that belongs to the different species in the solution is measured. For each peak in the NMR spectrum a diffusion coefficient can be determined. Unfortunately, a DOSY NMR measurement failed for the samples containing **BMIPy** and Zn^{2+}. A negative value for the peaks denoted with an "R" in figure 6 was obtained. Since a negative value for diffusion coefficients is impossible, some kind of artifact in the measurement method must have been present. So, it was not possible to determine which peaks belong to rings and chains using this technique.

However, the contribution of rings should increase with decreasing concentration in a reversible system. In a concentration dependent series of NMR spectra the contribution of "ring-peaks" should be smallest at the highest concentration. By measuring the integrals of the peaks denoted with "R" and "C" in all spectra, these peaks can be assigned. With increasing concentration the integrals of the peaks denoted with an "R" decrease a little compared to the integrals of the peaks denoted with a "C". As a result, the "R" peaks can be assigned to the ring structures in the solution and the "C" peaks can be assigned to the chain structures.

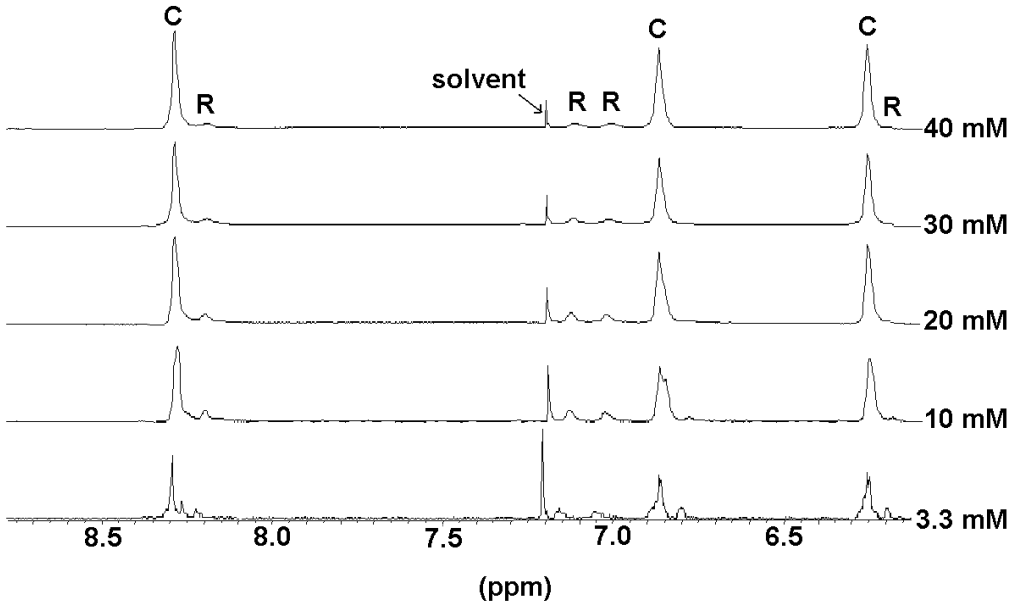

***Figure 6**: [1]H NMR spectra of **BMIPy** with $Zn(ClO_4)_2$ (1:1) in $CDCl_3/CD_3CN$ (1:1) at 298 K at different concentrations.*

The relative amounts of rings at the different concentrations are plotted in figure 7. As can be seen, the decrease in fraction of rings with increasing concentration is very small. This could be caused by the slow equilibration of the system. The samples were diluted and measured again within 30 minutes. Some exchange must have occurred on this time scale, because small peaks at 6.80 and 8.27 ppm appear at the lowest concentrations. The absence of these peaks at higher concentrations indicates that some shift in the ring-chain equilibrium must have taken place upon dilution.

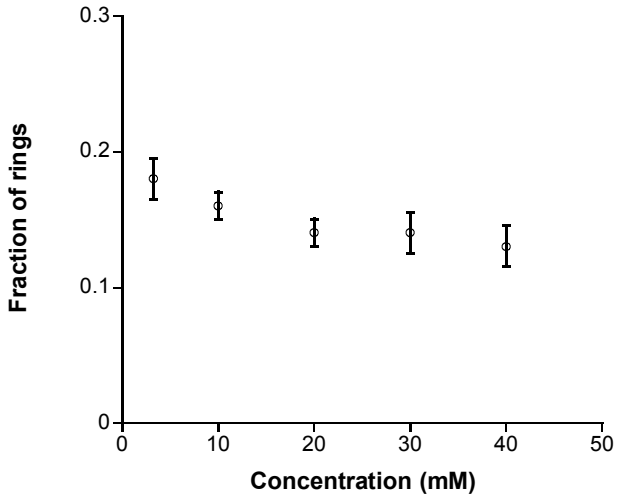

***Figure 7**: Fraction of rings of **BMIPy** and $Zn(ClO_4)_2$ (1:1) in $CDCl_3/CD_3CN$ (1:1) at 298 K as a function of concentration, determined from the integrals of the peaks in ^1H NMR spectra.*

6.3 Concluding remarks

In this chapter, it was shown that the reversibility of coordination polymers is highly dependent on the solvent used. When a coordinating solvent such as water is used to prepare coordination polymers with **BAMPy** ligands and Zn^{2+} ions, the exchange of ligands was demonstrated by a drop in the solution viscosity upon addition of monofunctional ligands. The exchange of **BMIPy** ligands with Zn^{2+} ions in a 1:1 mixture of $CHCl_3/CH_3CN$ is much slower. The ^1H NMR measurements showed that some exchange occurs. However, the molar ratio dependent viscosity measurements showed that after the equivalence point the viscosity did not drop as much as expected for a reversible system. This is probably a time related effect. If the system would have had much more time to equilibrate after each addition of metal ion, the viscosity is expected to drop further.

In conclusion, when the aim is to prepare "smart materials", whose properties can be tuned rapidly upon external stimuli, water-soluble reversible coordination

polymers seem more useful than coordination polymers in organic solvents. In addition, water is obviously a much better biocompatible solvent than most organic solvents.

6.4 Experimental section

^{1}H NMR (200 MHz) spectra were recorded on a Bruker AC-E 200 spectrometer at room temperature. Viscosity measurements were performed on a Schott AVS 360 capillary viscosimeter. The reduced viscosity is defined as the specific viscosity divided by the ligand concentration C in grams per liter, i.e., $\eta_{red} = \eta_{sp}/C = (\eta_s - \eta_0)/(\eta_0.C)$ with η_s being the viscosity of the sample and η_0 the viscosity of the solvent.

6.5 References

1. Vermonden, T.; Van der Gucht, J.; De Waard, P.; Marcelis, A. T. M.; Besseling, N. A. M.; Sudhölter, E. J. R.; Fleer, G. J.; Cohen Stuart, M. A. *Macromolecules* **2003**, *36*, 7035-7044.
2. Van der Gucht, J.; Besseling, N. A. M.; Van Leeuwen, H. P. *J. Phys. Chem. B* **2004**, *108*, 2531-2539.
3. Knapp, R.; Schott, A.; Rehahn, M. *Macromolecules* **1996**, *29*, 478-480**.**
4. Kelch, S.; Rehahn, M. *Macromolecules* **1997**, *30*, 6185-6193**.**
5. Paulusse, J. M. J.; Sijbesma, R. P. *Chem. Commun.* **2003**, 1494-1495.
6. Paulusse, J. M. J.; Sijbesma, R. P. *Angew. Chem. Int. Ed.* **2004**, *43*, 4460-4462.
7. Vermonden, T.; Van Steenbergen, M. J.; Besseling, N. A. M.; Marcelis, A. T. M.; Hennink, W. E.; Sudhölter, E. J. R.; Cohen Stuart, M. A. *J. Am. Chem. Soc.* **2004**, *126*, 15802-15808.
8. Lohmeijer, B. G. G.; Schubert, U. S. *Macromol. Chem. Phys.* **2003**, *204*, 1072-1078.
9. Vermonden, T.; Branowska, D.; Marcelis, A. T. M.; Sudhölter, E. J. R. *Tetrahedron* **2003**, *59*, 5039-5045.
10. Bonhôte, P.; Ferigo, M.; Stoeckli-Evans, H.; Marty, W. *Acta Cryst.* **1993**, *C49*, 2102-2107.
11. Couturier, Y.; Petitfaux, C. *Bull. Soc. Chim. Fr.* **1992**, *129*, 335-342.
12. Yu, S. C.; Hou, S.; Chan, W. K. *Macromolecules* **1999**, *32*, 5251-5256.
13. Haga, M.; Kato, N.; Monjushiro, H.; Wang, K.; Hossein, M. D. *Supramolecular Science* **1998**, *5*, 337-342.
14. Carina, R. F.; Williams, A. F.; Piguet, C. *Helv. Chim. Acta* **1998**, *81*, 548-557.
15 . Beck, J. B.; Rowan, S. J. *J. Am. Chem. Soc* **2003**, *125*, 13922-13923.
16 . Zhao, Y.; Beck, J. B.; Rowan, S. J.; Jamieson, A. M. *Macromolecules* **2004**, *37*, 3529-3531.
17. Lange, R. F. M.; Van Gurp, M.; Meijer, E. W. *J. Polym. Sci.: Part A: Polym. Chem.* **1999**, *37*, 3657-3670.
18. Sijbesma, R. P.; Beijer, F. H.; Brunsveld, L.; Folmer, B. J. B.; Hirschberg, J. H. K. K.; Lange, R. F. M.; Lowe, J. K. L.; Meijer, E. W. *Science* **1997**, *278*, 1601-1604.

19. Cates, M. E. *Macromolecules* **1987**, *20*, 2289-2296.
20. Johnson Jr., C. S. *Prog. Nucl. Magn. Spectrosc.* **1999**, *34*, 203-256.

Trifunctional ligands in coordination polymers

Chapter 7

*Two trifunctional ligands were synthesized consisting of three pyridine-2,6-dicarboxylate groups connected by a phenyl (**TPh**) or triazine (**TTr**) spacer. These trifunctional ligands can act as cross-linkers in the formation of coordination polymers. They were mixed in small percentages with a bifunctional ligand with the same coordinating groups connected by a tetra ethylene oxide spacer (**C4**) in water to study the polymer and network formation. An increasing percentage of **TPh** yielded an increasing solution viscosity at a Zn^{2+}/ligand ratio close to unity, while increasing the percentage of **TTr** yielded a decrease in viscosity. **TTr** has shorter arms and is more rigid than **TPh**. **C4** is probably able to form chain-stopping rings with two arms of **TTr** and therefore a decrease in viscosity is found here.*

7.1 Introduction

The synthesis and characterization of novel soluble supramolecular polymers has been a major goal in research in the past ten years because of their reversible character. There is a lot of confidence that this trend continues and leads to the development of novel materials. Nowadays, most attention is paid to hydrogen-bonded polymers. Hydrogen bonds are very interesting molecular interactions because of their directionality. Unfortunately, these interactions are generally not strong enough to be used for supramolecular polymers in aqueous systems.

To construct reversible polymers in water, coordination polymers are a good alternative. The type of metal ion, the nature of the ligands and the solvent can be used to tune the strength of the bonds between ligand molecules and metal ions. A disadvantage of these kinds of polymers is that always two components in a specific ratio should be present. If either ligand molecules or metal ions are present in excess, it is impossible to construct very long polymers (chapters 2 and 6). This molar ratio problem can be circumvented somewhat by using metal ions that can bind to three ligand groups instead of two. Branching or network formation is possible now, and in those systems the size of the polymers is less influenced by small deviations from the ideal stoichiometric molar ratio (chapters 3 and 4).

In chapters 3 and 4, we saw that the coordination polymers in water that are capable of branching gave much better material properties than the linear coordination polymers. So, it seems sensible to extend further research in that direction in view of possible applications in materials industry. Still a lot has to be done to understand how the three-dimensional polymers look like on a molecular level. In chapter 4, rheological experiments gave an indication about the structure, but morphological proof is still lacking. A theoretical prediction of the behavior of reversible three-dimensional polymers is much more complicated than for linear coordination polymers. However, it might be one of only few options to gain more insight into the system.

The most simple method for making branch points in coordination polymers is the use of lanthanide ions as described in chapters 3 and 4. However, lanthanide ions are generally not compatible with biological applications. For those applications metal ions such as Ca^{2+} and Fe^{3+} are more beneficial. To make branching possible with these metal ions, ligands with more functional groups should be introduced. In principle, there are several ways to accomplish this. One option is the synthesis of trifunctional ligands. Two trifunctional ligands have been synthesized that could act as branch points in three-dimensional polymers analogous to the polymers described in chapters 3 and 4. The main problem for designing new functional

ligand molecules is the solubility of both the ligands and their complexes with metal ions. To obtain ligands that are water-soluble over a broad pH range, a rather polar spacer is needed. The best water-soluble complexating group described in this thesis is 2,6-pyridine-dicarboxylic acid. This complexing group is able to bind strongly to a large variety of metal ions under neutral to slightly acidic conditions, and is therefore a good choice for further research.[1]

7.2 Results and discussion

Trifunctional ligands **TPh** (trifunctional ligand with a phenyl spacer) and **TTr** (trifunctional ligand with a triazine spacer) are depicted in figure 1. They were synthesized starting from 1,3,5-tri(bromomethyl)benzene and 2,4,6-trichloro-1,3,5-triazine, respectively. Although these ligands are very well soluble in water, their complexes with Zn^{2+} ions in buffer (100 mM PIPES, pH 5.4) precipitate. The ligands are probably not polar enough.

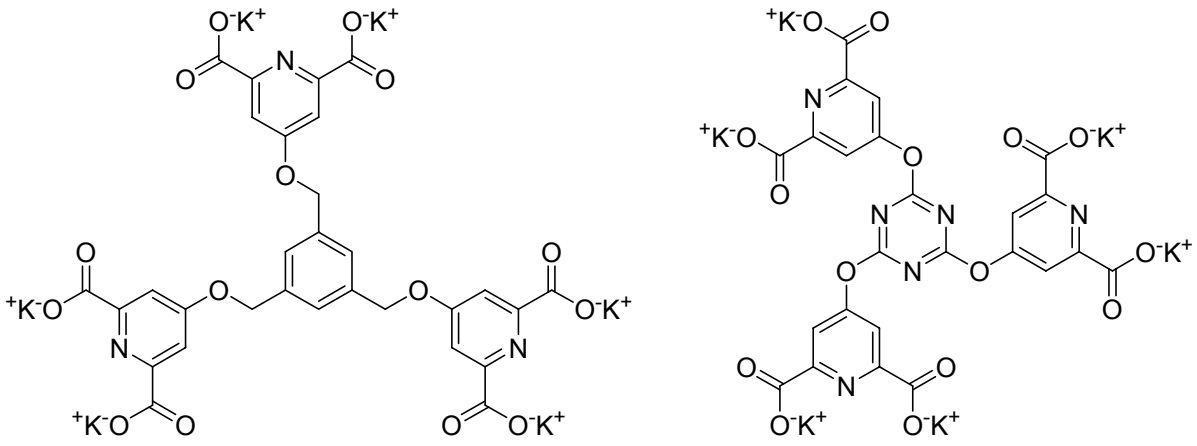

TPh **TTr**

***Figure 1*:** Trifunctional ligands **TPh** and **TTr**.

The trifunctional molecules can, however, be mixed with bifunctional molecules and upon addition of metal ions, linear polymers with branch points can be formed. A maximum of 18% **TTr** with 82% of the bifunctional **C4** (two 2,6-pyridine-dicarboxylic acid groups connected by a tetra ethylene oxide spacer) can be dissolved with Zn^{2+}. For **TPh**, the maximum percentage that dissolves in water is only 8% with 92% **C4**. The spacer of **TTr** is obviously more polar than the spacer of **TPh** and therefore **TTr** is soluble in higher percentages when mixed with bifunctional ligands and Zn^{2+}. The influence of different percentages of trifunctional ligand on the solution viscosity was studied. For these measurements mixtures of

bifunctional **C4** and trifunctional ligands were prepared and the viscosity was measured upon titration with $Zn(NO_3)_2$. The results are shown in figures 2a (for **TPh**) and 2b (for **TTr**).

a) b)

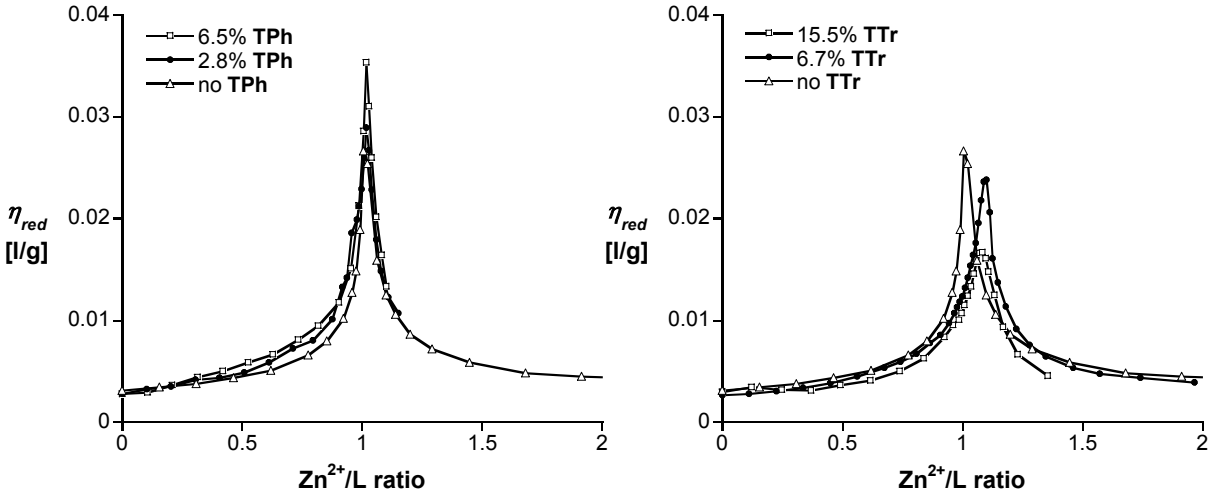

***Figure 2**: Reduced viscosity of **C4** as a function of the molar ratio Zn^{2+}/ligand with different percentages of trifunctional ligands **TPh** (a) and **TTr** (b) in 0.1 M PIPES buffer pH 5.4 at 298 K at a total ligand concentration of 35-38 mM.*

The viscosity of solutions with trifunctional **TPh** is larger than when only bifunctional ligands are present. The higher the relative amount of **TPh** the higher the maximum viscosity is. After a molar ratio of about 1.2 the polymers start to precipitate and no further measurements were possible. The maximum of the viscosity would be expected at a molar ratio of 1.5 when 100% trifunctional ligands are used. With only a small percentage of trifunctional ligand, the maximum in viscosity is expected at a ratio only a little above 1. The maximum in the case of 6.5% trifunctional ligand is expected at a ratio of 1.03 and is found to be 1.02. Both the small shift and the increase in viscosity upon increasing percentage of trifunctional ligands indicate that cross-links are formed. This would mean that if better water-soluble trifunctional ligands are used, material properties could be obtained at high concentrations.

However, the water-solubility is not the only prerequisite. When **TTr** is used in small percentages with **C4**, it was found that the maximum viscosity of the solution decreases. This puzzling behavior could be explained by the fact that besides being more polar than **TPh**, **TTr** is also more rigid. This rigidity in combination with the short "arms" of the molecule make it possible that rings are formed with bifunctional ligands as displayed in figure 3. These kinds of structures are also

possible with **TPh**, but this is less favorable for entropic reasons. The ring formation seems to be the most logical explanation why **TTr** decreases the viscosity. Also a larger shift in the maximum of the viscosity with respect to the molar ratio is found for **TTr** (For 6.7% the maximum is expected at a molar ratio of 1.03 and found at a ratio of 1.10). A similar shift was found in chapter 3 for neodymium coordination polymers and this shift was also attributed to the presence of ring-like structures acting as chain-stoppers.[2] Using trifunctional ligands with longer arms might decrease the possibility of formation of chain-stopping rings.

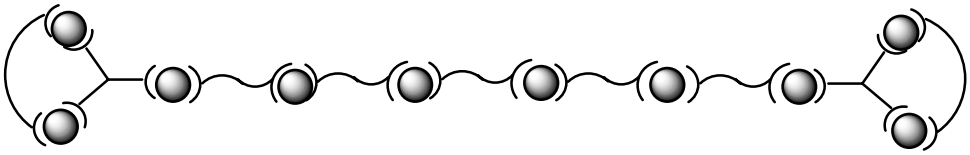

***Figure 3**: Schematic representation of chain stopping rings in a mixture of bifunctional and trifunctional ligands when the trifunctional ligand has short rigid arms.*

7.3 Conclusions and recommendations

Trifunctional ligands are a new group of compounds that may give very interesting coordination polymers with metal ions. The first synthetic problems that need to be dealt with are the polarity and the length/flexibility of the arms. The ligands should be very well soluble in water and the trifunctional spacer should not be too rigid. Triazine as building block for the spacer may be an appropriate group, because it is more polar than phenyl groups. To solve the rigidity problem, di- or tri-ethylene oxides could be coupled on one side to the triazine and on the other side to the ligand group. But many other promising structures can be envisioned as a challenge for synthetic chemists.

Other possibilities are the incorporation of ligand groups on oligomer or polymer backbones.[3,4] Oligosaccharides might be useful molecules to link ligand groups, because of their good water solubility. Further ideas are to prepare block-copolymers in which on both ends of the polymer a block with multiple coordination groups is linked by a long oligoethylene oxide block. The oligoethylene oxide block is then responsible for good water solubility (figure 4).

***Figure 4**: Schematic representation of block-copolymer, with ethylene oxide block in the middle and ligand group rich blocks at the ends.*

To recapitulate, further research towards soluble coordination polymers is expected to lead to new tunable materials. Both coordination polymers and hydrogen-bonded polymers have many possibilities for future applications in nanoscience. For water-based systems the coordination polymers seem to have the best properties at the moment. The main problems that need to be solved are the solubility of the ligands and the need for an exact molar ratio of metal ions to ligands. With the suggestions mentioned above and the results shown in section 7.2, these problems are expected to be solved in the near future.

7.4 Experimental section

All commercial chemicals were obtained form Acros or Aldrich and were used as received. ^{1}H NMR (200 MHz) and ^{13}C NMR spectra were recorded on a Bruker AC-E 200 spectrometer. Viscosity measurements were performed in a 100 mM 1,4-piperazinebis(ethanesulfonic acid) buffer (PIPES) pH 5.4, on a Schott AVS 360 capillary viscosimeter. The reduced viscosity is defined as the specific viscosity divided by the ligand concentration *C* in grams per liter, $\eta_{red} = \eta_{sp}/C = (\eta_s - \eta_0)/(\eta_0.C)$ with η_s the viscosity of the sample and η_0 the viscosity of the solvent.

Synthesis of 1,3,5-tris(2,6-dicarboxypyridin-4-yloxymethyl)benzene, TPh.
1,3,5-Tris(bromomethyl)benzene was synthesized according to a literature procedure and used as a spacer for the **TPh** ligand.[5] Diethyl 4-hydroxypyridine-2,6-dicarboxylate[6] (9.28 g, 38.84 mmol), 12.95 mmol of 1,3,5-tris(bromomethyl)benzene and 11 g K_2CO_3 were refluxed in 2-butanone for 4 days under N_2 atmosphere. The reaction can be followed by TLC analysis using a few percent of MeOH in CH_2Cl_2 as eluent. The solvent was removed and CH_2Cl_2 was added. The salt was filtered over Celite and the filtrate was concentrated and purified using column chromatography with 1-3% MeOH in CH_2Cl_2 as eluent to give the hexa ethyl ester of **TPh**. Yield: 34% (3.62 g, 4.35 mmol), mp 161-163 ºC. ^{1}H NMR ($CDCl_3$): δ 1.44 (t, 18H, CH_3), 4.46 (q, 12H, CH_2), 5.27 (s, 6H, CH_2), 7.55 (s, 3H, aromatic H), 7.88 (s, 6H, aromatic H). ^{13}C NMR ($CDCl_3$): δ 14.21 (CH_3), 62.53 (CH_2), 70.02 (CH_2), 114.53 (CH), 127.00 (CH), 136.43 (C), 150.38 (C), 164.61 (CO_2), 166.33 (CO).
Hydrolysis of 3.6 g of this ester was performed by heating it in a mixture of 50 ml H_2O, 50 ml EtOH and 6 g KOH for 12 h at 60 ºC. The product could be precipitated in a mixture of EtOH and H_2O. Yield: 95% (3.67 g, 4.11 mmol), mp > 300 ºC. ^{1}H NMR (D_2O): δ 5.14 (s, 6H, CH_2), 7.41 (s, 6H, aromatic H), 7.50 (s, 3H, aromatic H). ^{13}C NMR ($CDCl_3$): δ 72.42 (CH_2), 114.08 (CH), 130.35 (CH), 139.34 (C), 157.45 (C), 168.95 (CO), 175.26 (CO_2).

Synthesis of 2,4,6-tris(2,6-dicarboxypyridin-4-yloxy)-[1,3,5]triazine, TTr.

Cyanuric chloride (2,4,6-trichloro-1,3,5-triazine) was used as a spacer. Diethyl 4-hydroxypyridine-2,6-dicarboxylate (5 g, 20.9 mmol), 6.8 mmol (1.25 g) of 2,4,6-trichloro-1,3,5-triazine and 5 g K_2CO_3 were refluxed in 2-butanone for 7 days under N_2 atmosphere. The reaction can be followed by TLC analysis using 10% MeOH in CH_2Cl_2 as eluent. The solvent was removed and CH_2Cl_2 and H_2O were added. The product was extracted into CH_2Cl_2. The organic layer was washed with brine and dried over Na_2SO_4. The product was purified using column chromatography with 3% MeOH in CH_2Cl_2 as eluent yielding the hexa ethyl ester of **TTr** as a slightly yellow oil. Yield: 30% (1.62 g, 2.04 mmol), ^{1}H NMR ($CDCl_3$): δ 1.37 (t, 18H, CH_3), 4.38 (q, 12H, CH_2), 7.93 (s, 6H, aromatic H). ^{13}C NMR ($CDCl_3$): δ 14.10 (CH_3), 62.94 (CH_2), 121.18 (CH), 149.45 (C), 161.47 (CO_2), 163.91 (CO), 171.27 (C).

Hydrolysis of 1.60 g of this ester was accomplished by heating it in a mixture of 30 ml H_2O, 30 ml EtOH and 1 g KOH for 12 h at 60 ºC. The product could be purified using size exclusion chromatography (Sephadex G15). Yield: 93% (1.60 g, 1.88 mmol), mp > 300 ºC. ^{1}H NMR (D_2O): δ 7.66 (s, 6H, aromatic H). ^{13}C NMR ($CDCl_3$): δ 120.78 (CH), 157.11 (C), 163.30 (CO), 173.91 (CO_2), 174.15 (C).

7.5 References

1. Anderegg, G. *Helv. Chim. Acta* **1960**, *43*, 414-424.
2. Vermonden, T.; De Vos, W. M.; Marcelis, A. T. M.; Sudhölter, E. J. R. *Eur. J. Inorg. Chem.* **2004**, 2847-2852.
3. Calzia, K. J.; Tew, G. N. *Macromolecules* **2002**, *35*, 6090-6093.
4. El-ghayoury, A.; Hofmeier, H.; De Ruiter, B.; Schubert, U. S. *Macromolecules* **2003**, *36*, 3955-3959.
5. Spino, C.; Clouston, L. L.; *Can. J. Chem.* **1997**, *75*, 1047-1054.
6. Chessa, G.; Scrivanti, A. *J. Chem. Soc., Perkin Trans. 1* **1996**, 307-311.

Summary

Supramolecular polymers are polymers in which the monomers are held together by non-covalent interactions. In solution these polymers can break and recombine reversibly yielding polymers with an average degree of polymerization. This thesis is devoted to water-soluble coordination polymers, in which the bonds between the monomers are based on metal ion coordination. The most successful ligands used in this research project to construct reversible coordination polymers are based on pyridine-2,6-dicarboxylate groups connected by oligoethylene oxide spacers of different lengths. These ligands were used for the research described in chapters 2, 3 and 4.

Chapter 2 deals with the formation of water-soluble reversible coordination polymers of Zn^{2+} ions with bifunctional ligands that differ in spacer length. Besides linear chains also rings are formed. Viscosity measurements were used to follow the formation of chains and rings as a function of the ratio between metal ions and ligands, the total ligand concentration, and the temperature. To explain the experimental results a theoretical model was developed that accounts for the formation of both chains and rings. At low concentrations and at a 1:1 metal to ligand ratio, a large fraction of the ligand monomers is incorporated in small rings, with a small contribution to the viscosity. Rings are less important at higher concentrations, or if one of the two components is in excess. Also the length of the bifunctional ligands determines the amount of rings that are formed. The largest fraction of rings is found for bifunctional ligands that are just long enough to form a monomer ring around one metal ion. The fractions of monomers in chains and rings could be estimated from ^{1}H NMR measurements and they are in good agreement with the model predictions. With increasing temperature, the fraction of monomers in rings decreases. As a result, the reduced viscosity increases with increasing temperature.

In chapter 3, the formation of soluble supramolecular three-dimensional coordination polymers with Nd^{3+} and La^{3+} in aqueous solution is described for two bifunctional ligands that differ in spacer length. Neodymium(III) ions can bind three terdendate ligand groups. Viscosity measurements were used to monitor the network formation as a function of the ligand concentration and the ratio between metal ions and ligands. For corresponding conditions, solutions containing Nd^{3+} and ligands with short spacers gave always much higher viscosities than solutions containing Nd^{3+} and ligands with longer spacers. The ligand with the longer spacer is flexible enough to bind with both chelating groups to only one metal ion (ring-formation). This causes the polymers to stop growing, resulting in smaller average

sizes of the three-dimensional polymers. The ring-structures could be demonstrated by ^{1}H NMR spectroscopy using La^{3+} at low concentrations.

At very high concentrations of the three-dimensional polymers, viscoelastic materials are obtained. The rheology of these reversible coordination polymer networks in aqueous solution is described in chapter 4. The polymers are formed by neodymium(III) ions and bifunctional ligands. The rheological properties of the viscoelastic materials can be described with the Maxwell model. The scaling of the elastic modulus, relaxation time and zero-shear viscosity with concentration are in good agreement with the predictions of Cates' model that describes the dynamics of linear equilibrium polymers. This indicates that the networks have only few cross-links and can be described as linear equilibrium polymers. The gels are also thermo-reversible. At high temperatures, fast relaxation was found, resulting in liquid-like behavior. Upon cooling, the viscoelastic properties returned immediately. From the temperature dependence of the relaxation time, an activation energy of 49 kJ/mol was determined for the breaking and reptation of the polymers.

In chapter 5, the syntheses of four different ligand derivatives are described. These ligands are potential candidates for the construction and study of coordination polymers. The different 4-functionalized pyridine-based ligands were synthesized with aminomethyl, oxazolinyl, pyrazolyl and methylimidazolyl groups at the 2- and 6-position, respectively. The nitrogens of these groups together with the pyridine nitrogen can act as terdendate ligands for metal ions. Synthetic handles on the 4-position of the pyridine group were introduced via ether or ester bonds leading to monofunctional, bifunctional and amphiphilic ligands.

From the four synthesized bifunctional ligands described in chapter 5, only two were stable and soluble enough to study the coordination polymer properties with Zn^{2+}. In water, a bifunctional ligand with two 2,6-bis(aminomethyl)pyridine groups as complexing groups was used. In an organic solvent (chloroform/acetonitrile), a bifunctional ligand with two 2,6-bis(methylimidazolyl)pyridine groups was used. The reversibility of the coordination bonds in these two coordination polymers was compared in the solvents mentioned. Viscosity measurements were used to follow the formation and breaking of the polymers as a function of the molar ratio for the ligands with 2,6-bis(methylimidazolyl)pyridine groups in an organic solvent. The breaking of the polymers made of the water-soluble ligands with 2,6-bis(aminomethyl)pyridine groups was shown by addition of monofunctional ligands. Viscosity measurements of the coordination polymers in water showed fast equilibration upon changes in concentration. In an organic solvent no changes in the size of the structures were found upon dilution. ^{1}H NMR measurements were used to monitor the ring-chain equilibrium of the coordination polymers containing the

ligands with 2,6-bis(methylimidazolyl)pyridine groups in a chloroform/acetonitrile mixture. The coordination polymers in the organic solvent showed some exchange, but much slower than in the water-based system. Therefore, to prepare coordination polymers whose properties can be tuned rapidly by means of external changes, water is a more appropriate solvent than non-coordinating organic solvents.

Since the best material properties for water-soluble coordination polymers in this thesis are obtained by using metal ions that can act as branch points, further research may be directed to the use of multifunctional ligand molecules as alternative. A first attempt in that direction is described in chapter 7. Two trifunctional ligand molecules with pyridine-2,6-dicarboxylate groups are synthesized and the viscosity of solutions containing mixtures of bifunctional and trifunctional ligands was studied as a function of molar ratio. To increase the viscosity in water by increasing the percentage of trifunctional ligand a very polar but also rather flexible trifunctional ligand is necessary.

Samenvatting

Polymeren zijn lange moleculen die zijn opgebouwd uit kleinere moleculen die als een ketting aan elkaar zijn geregen. De kleinere eenheden worden ook wel monomeren genoemd (de kralen in de ketting). Polymeren zijn heel belangrijke moleculen, zowel in de natuur als in moderne materialen zoals plastics. Een voorbeeld van polymeren in de natuur is DNA. Dit polymeer is opgebouwd uit vier soorten monomeren en de volgorde waarin deze monomeren aan elkaar zitten, bepaalt de genetische code van een organisme. Behalve DNA zijn er nog meer voorbeelden te noemen van polymeren in de natuur, zoals eiwitten en zetmeel. Naast natuurlijke polymeren, is er ook een belangrijke rol weggelegd voor synthetische polymeren. Deze polymeren worden tegenwoordig gebruikt in allerlei materialen. Veelgebruikte polymeren in de industrie zijn polyethyleen en polyesters. Polyethyleen kan men in het dagelijks leven bijvoorbeeld terugvinden in plastic zakken. Polyesters worden veel gebruikt als vezels in kleding en ook in de zogenaamde PET-flessen voor frisdrank. Deze en vele andere soorten polymeren komen ook voor in allerlei andere kunststoffen en spelen dus een belangrijke rol in de huidige maatschappij.

Zoals al genoemd bestaan polymeren uit kleinere eenheden (monomeren). Als men in het productieproces de monomeren met elkaar laat reageren ontstaan de polymeren. De eigenschappen van deze polymeren hangen af van het soort monomeer dat wordt gebruikt maar ook van de uiteindelijke lengte van de polymeren. Als de reactie is afgelopen, kan er niets meer veranderd worden aan de lengte van de polymeren. Die ligt dan vast. Dit kan een nadeel zijn als men de polymeren na gebruik wil regenereren en voor een ander doel wil gebruiken. Daarom wordt nu onderzoek gedaan naar het synthetiseren van polymeren, waarbij de bindingen tussen de monomeren reversibel zijn; d.w.z dat de bindingen kunnen breken en weer opnieuw gevormd worden. De lengte van de polymeren kan dan gevarieerd worden naar gelang de gevraagde eigenschappen voor een bepaalde toepassing. Dit soort polymeren worden ook wel supramoleculaire polymeren genoemd.

Het doel van dit onderzoek is het synthetiseren van reversibele coördinatie polymeren (zie figuur 1) en het bestuderen van hun eigenschappen in oplossing. De bindingen tussen de monomeren worden hier gevormd door reversibele metaalcoördinatie bindingen. De monomeren hebben bindingsplaatsen aan beide uiteinden voor metaalionen. Deze bindingsplaatsen worden ligandgroepen genoemd. Worden deze twee componenten met elkaar gemengd dan worden de metaal-ligand bindingen spontaan gevormd.

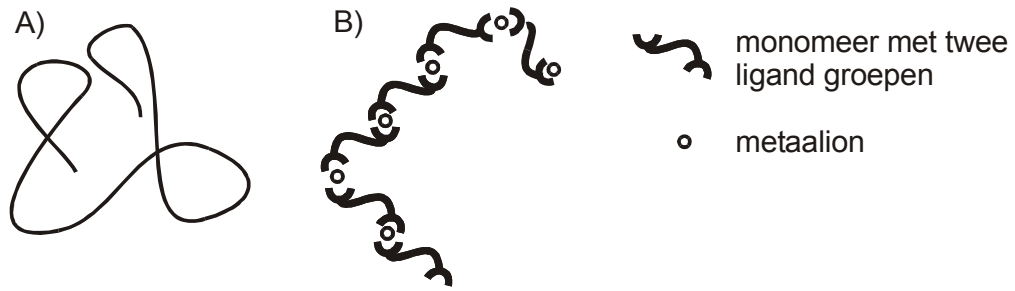

***Figuur 1**: A) Schematische voorstelling van een polymeer. B) Schematische voorstelling van een supramoleculair coördinatie polymeer.*

In hoofdstuk 2 staat beschreven wat de invloed is van de verhouding waarin de metaalionen (zinkionen) en monomeren worden gemengd op de lengte van de polymeren. Zoals al te voorspellen is uit figuur 1, worden de langste polymeren gevormd als metaalionen en monomeren in een 1:1 verhouding bij elkaar worden gedaan. Dit is bestudeerd met viscositeitmetingen. De viscositeit van een oplossing geeft aan hoe makkelijk die stroomt (bv. honing heeft een hogere viscositeit dan water). Een oplossing met lange polymeren zal een hogere viscositeit hebben dan een oplossing met korte polymeren. Er treedt echter nog een nevenreactie op. Naast lange ketens kunnen de monomeren ook ringen vormen rond metaalionen zoals weergegeven in figuur 2. De gemiddelde ketenlengte van de polymeren is een stuk kleiner als er veel van dit soort ringen aanwezig zijn. Om de hoeveelheid ringen te kunnen beperken is het nodig om te weten welke factoren de ringvorming beïnvloeden. De bijdrage van ringen bleek minder belangrijk te zijn bij hoge concentratie, bij hoge temperatuur en als de verhouding tussen metaalionen en monomeren afwijkt van 1:1. Ook de lengte van de monomeren speelt een rol in de hoeveelheid en soort ringen die worden gevormd. Sommige monomeren bleken te kort om monomeer ringen te kunnen vormen. Doordat in dat geval alleen dimeer en grotere ringen gevormd kunnen worden, is het totaal aan ringen kleiner bij de korte monomeren. Het evenwicht tussen ringen en ketens is ook voorspeld met een theoretisch model en alle experimenten kwamen overeen met dit model.

***Figuur 2**: Schematische weergave van ringvorming in coördinatie polymeren.*

In hoofdstuk 3 is gewerkt met een heel ander metaalion. Het ion neodymium is veel groter dan het zinkion en daardoor kunnen er drie ligand groepen binden aan

dit metaalion. Hierdoor kunnen netwerken worden gevormd in plaats van lineaire ketens zoals is weergegeven in figuur 3. Ook in dit hoofdstuk is met behulp van viscositeitmetingen de grootte van de netwerkpolymeren bestudeerd. De monomeren kunnen ook rond neodymium ionen ringen vormen. Alleen blijft er dan nog een bindingsplaats over voor een ligand groep van een ander monomeer. De gevonden viscositeiten voor de netwerken zijn bij vergelijkbare concentraties dan ook vele malen hoger dan bij de lineaire ketens die beschreven zijn in hoofdstuk 2.

***Figuur 3**: Schematische weergave van 3-dimensionaal netwerkpolymeer met het "grote" neodymium als metaalion.*

In hoofdstuk 4 is eigenlijk hetzelfde systeem bekeken als in hoofdstuk 3, alleen bij veel hogere concentraties. Er zijn hier samples gemaakt die voor 50-70% uit water bestaan en voor de rest uit monomeren en neodymium ionen. Deze samples zijn nauwelijks meer vloeibaar te noemen. Ze zijn zo visceus dat ze kunnen worden vastgehouden en in elke willekeurige vorm kunnen worden gekneed. Als er een balletje van wordt gemaakt, kun je dat laten stuiteren op een tafel. Het gaat hier dus duidelijk in de richting van een materiaal. In dit stuk onderzoek zijn dan ook de materiaaleigenschappen bestudeerd. Het materiaal bleek visco-elastisch te zijn. Dit betekent dat het zowel vloeistof als vaste stof eigenschappen heeft. De vaste stofeigenschappen zijn hierboven al geïllustreerd (stuiteren). Maar als de samples in buisjes worden gedaan dan vloeit het in enkele uren naar de bodem als een vloeistof.

Hoofdstuk 5 is een heel ander hoofdstuk dan de rest. In dit hoofdstuk komen geen eigenschappen van supramoleculaire coördinatie polymeren ter sprake. De synthese van vier verschillende monomeren wordt hier beschreven. Drie van deze monomeren lossen niet op in water maar wel in organische oplosmiddelen.

In hoofdstuk 6 wordt de invloed van het soort oplosmiddel bekeken op de vorming en reversibiliteit van de polymeren. Hiervoor worden twee monomeren die zijn beschreven in hoofdstuk 5 met elkaar vergeleken. De eerste vormt polymeren met zinkionen in water en de ander in een mengsel van de vloeistoffen chloroform en acetonitril. De vorming en het breken van de polymeren is bestudeerd met onder andere viscositeitmetingen. De polymeren die gevormd worden in water reageren veel sneller op veranderingen in concentratie en veranderingen in de verhouding

van metaalionen en monomeren dan de polymeren in het organische oplosmiddel. Dit komt omdat water een rol speelt in het breken van de metaal-ligand binding. Water kan tijdelijk de plaats van de ligandgroep overnemen, totdat er weer een nieuwe ligandgroep in de buurt is die kan binden. Dus als reversibiliteit een belangrijke eigenschap is voor het materiaal dat gemaakt wordt, dan zijn wateroplosbare coördinatiepolymeren geschikter dan degene die alleen oplosbaar zijn in organische oplosmiddelen.

In hoofdstuk 7 wordt een analogie voor de polymeernetwerken uit hoofdstuk 3 en 4 beschreven. Zoals hiervoor al genoemd kunnen netwerken worden gemaakt door een metaalion te gebruiken met drie bindingsplaatsen. Maar het principe kan ook worden omgedraaid en er kunnen monomeren gesynthetiseerd worden met drie ligandgroepen in plaats van twee. In hoofdstuk 7 staat de synthese van twee van deze trifunctionele monomeren beschreven (zie figuur 4).

***Figuur 4**: Schematische weergave van een trifunctioneel monomeer.*

De invloed van het toevoegen van deze monomeren aan een systeem met bifunctionele monomeren en zinkionen op de viscositeit is bestudeerd. Om de viscositeit van de oplossing te laten toenemen met toenemend percentage trifunctioneel monomeer is een monomeer nodig dat vrij flexibele “armen” heeft.

Dankwoord

Met het schrijven van dit dankwoord komt er écht een einde aan een leuke en drukke periode als AIO. Er wordt altijd gezegd dat dit het leukste gedeelte van het hele proefschrift is om te schrijven. En ik denk dat het ook wel klopt. Als ik terugkijk naar de inhoud van dit boekje dan is er toch meer van het onderzoek terechtgekomen dan ikzelf ooit had durven dromen. Dit was niet mogelijk geweest zonder de hulp van een aantal mensen die ik op deze plaats wil bedanken.

Als eerste wil ik Ton Marcelis bedanken. Als directe begeleider was je altijd beschikbaar voor het bespreken van ideeën en resultaten. Vooral op het synthetisch gebied van mijn onderzoek hebben jouw adviezen een belangrijke rol gespeeld. Verder was je altijd heel snel met het lezen van mijn artikels en hoofdstukken, wat ik zeer op prijs heb gesteld. Als tweede wil ik mijn promotor Ernst Sudhölter bedanken. Jij zag altijd alleen de zonnige kanten van dit onderzoeksproject. Toen ik zelf wat meer moeite had om de positieve dingen te zien was jouw optimisme heel belangrijk, en mede dankzij jou heb ik uiteindelijk toch de moed gehad om verder te gaan.

Dat er in dit boekje ook enkele theoretische en fysische resultaten beschreven staan is te danken aan de goede samenwerking met de vakgroep Fysische Chemie en Kolloïdkunde. In het kader van die samenwerking wil ik graag Jasper van der Gucht, Klaas Besseling, Martien Cohen Stuart en Gerard Fleer bedanken. Ik had al veel respect voor mensen die met formules kunnen toveren en dat is zeker niet minder geworden in de afgelopen jaren. Jasper, zonder jou was het “dipje” in hoofdstuk 2 misschien altijd onverklaard gebleven en de verklaring zeker niet zo mooi bewezen. In mijn laatste jaar was Jasper al vertrokken naar Parijs en toen kon ik voor alle hulp op fysisch-chemisch gebied aankloppen bij Klaas. Jouw bijdrage in het reologieverhaal is van essentieel belang geweest. Ik was heel blij met het enthousiasme waarmee je iedere keer bij me kwam met nieuwe suggesties en ik heb er dan ook heel veel van geleerd.

Verder heb ik nog hulp gehad van drie studenten en een postdoc. Danuta, I would like to thank you for the synthetic work you did in the period you were in Holland. I wish you all the best for your career in Poland. Petra, jij had de ondankbare taak om een afstudeervak te doen toen ik zelf nog maar amper wist waar het onderzoek over ging. Hoewel jouw resultaten niet direct zijn terug te vinden in dit boekje, heb je wel een belangrijke bijdrage geleverd aan de basis. Michelle, ook jij had geen makkelijk opdracht als afstudeervak. Je was wat onzeker over je eigen kunnen, maar dat was echt nergens voor nodig. De synthese van de liganden was heel moeilijk, maar het is je wel gelukt. Wiebe, jij hebt vanaf het begin

heel zelfstandig gewerkt en de resultaten stroomden binnen. Soms kon ik amper bijhouden waar je mee bezig was. Het werk leverde je uiteindelijk zelfs de Unilever-prijs op.

De prettige werksfeer bij OC heeft op veel manieren bijgedragen aan dit proefschrift. Alle collega's hebben wel op een of andere manier geholpen met grote en kleine dingen en zijn ook verantwoordelijk voor de gezelligheid. Ik heb het dan over de pauzes, borrels (borrelcie met Louis), labuitjes, sportdagen (skaten met Floor en Gabriëlle), tourtoto en de AIO-reizen (Chicago en Zwitserland). Een paar mensen wil ik toch nog apart noemen. Uiteraard als eerste Arie. Jij hebt me op het lab ontelbaar veel handigheidjes geleerd als het om synthese gaat. Mijn kamergenoten, Hendra, Ioan en Ganesan, zorgden voor veel gezelligheid en ook eerste hulp bij computerproblemen. Ik denk ook nog met veel plezier terug aan het uitstapje met Hendra naar Autrans en Lyon. Op het gebied van NMR-metingen ben ik dank verschuldigd aan Beb, Barend en natuurlijk aan Pieter voor de DOSY-NMR's. Verder wil ik de dames van het secretariaat bedanken; Elbert voor de elementenanalyses; Maarten voor de massa's; Ronald voor het verstrekken van chemicaliën en Simon voor het herhaaldelijk repareren van de vriesdroger.

Van buiten OC wil ik graag Mies van Steenbergen en prof. Wim Hennink van Universiteit Utrecht bedanken voor het bieden van de mogelijkheid om reologiemetingen te doen met hele kleine volumina. Mies, bedankt voor de eerste uitleg over reologie en de werking van het apparaat. Bij Fysco wil ik verder nog Anton Korteweg bedanken voor de hulp met het ITC apparaat en Ronald Wegh voor de hulp met de oude en nieuwe viscosimeter.

Maar ook buiten het werk om waren er vele mensen die mij hebben gesteund en voor de nodige afleiding hebben gezorgd. In het bijzonder Sandra en Sacha, jullie zijn al zolang mijn vriendinnen. We zien elkaar niet zo vaak, maar het is altijd heel gezellig, zoals o.a. tijdens de weekendjes weg (Parijs, Milaan). Ik wens jullie allebei veel geluk met de gezinsuitbreiding. Cécile, Chrit en Juul wil ik bedanken voor de altijd hartelijke ontvangst in Roermond en Birmingham. En verder wil ik Leo bedanken voor vele ontspannende uurtjes te paard. Op Chester kon ik mijn onderzoek even vergeten en alleen maar genieten van het rijden.

Als laatste wil ik mijn familie bedanken voor het grenzeloze vertrouwen in mij. Papa en mama, ik kan helaas niet alles opnoemen dat jullie voor mij hebben gedaan. Dat varieert van het samen op vakantie gaan (Canada, Costa Rica, Curaçao), het aanhoren van mijn frustraties tot en met hulp bij de lay-out van dit boekje en alles daartussenin, dus dank je wel voor alles. Kim, voor het feit dat je mijn zusje bent en ik het superfijn vind dat je weer zo dichtbij woont, want ik heb je tijdens je stages echt gemist. Ik wens je veel succes met je eigen promotieonderzoek in Nijmegen. En

mijn laatste woorden gaan natuurlijk naar Remko. Door jouw steun en relativeringsvermogen kon ik de frustraties van het werk thuis makkelijk van me af zetten. Dank je wel voor de leuke tijd en alvast veel succes met het afronden van je proefschrift.

Tina

Curriculum Vitae

Tina Vermonden werd geboren op 9 november 1975 in Terheijden. Zij behaalde haar VWO diploma in 1995 aan het Newmancollege in Breda en begon in datzelfde jaar aan de studie Moleculaire Wetenschappen aan de Wageningen Universiteit. In 2000 studeerde zij af na een afstudeervak bij de leerstoelgroep Organische Chemie en een afstudeervak bij de leerstoelgroep Fysische Chemie en Kolloïdkunde. Van januari 2000 tot december 2004 was zij werkzaam als promovendus bij de leerstoelgroep Organische Chemie van Wageningen Universiteit. Onder leiding van prof. dr. E. J. R. Sudhölter en dr. A. T. M. Marcelis werkte zij aan het onderzoek dat in dit proefschrift staat beschreven.

List of Publications

N-Cholyl Amino Acid Alkyl Esters- A Novel Class of Organogelators.
H. M. Willemen, T. Vermonden, A. T. M. Marcelis, E. J. R Sudhölter
Eur. J. Org. Chem. **2001**, 2329-2335.

Reversibility of Structural Rearrangements in Bovine Serum Albumin during Homomolecular Exchange from AgI Particles.
T. Vermonden, C. E. Giacomelli, W. Norde
Langmuir **2001**, *17*, 3734-3740.

Alkyl Derivatives of Cholic Acid as Organogelators: One-Component and Two-Component Gels.
H. M. Willemen, T. Vermonden, A. T. M. Marcelis, E. J. R. Sudhölter
Langmuir **2002**, *18*, 7102-7106.

Aggregation of Different Amino Acid Conjugates of Cholic Acid in Aqueous Solution.
H. M. Willemen, T. Vermonden, A. Koudijs, A. T. M. Marcelis, E. J. R. Sudhölter
Colloids and Surfaces A **2003**, *218*, 59-64.

Synthesis of 4-Functionalized Terdendate Pyridine-Based Ligands.
T. Vermonden, D. Branowska, A. T. M. Marcelis, E. J. R. Sudhölter
Tetrahedron **2003**, *59*, 5039-5045 (chapter 5)

Water-Soluble Reversible Coordination Polymers: Chains and Rings.
T. Vermonden, J. van der Gucht, P. de Waard, A. T. M. Marcelis, N. A. M. Besseling, E. J. R. Sudhölter, G. J. Fleer, M. A. Cohen Stuart
Macromolecules **2003**, *36*, 7035-7044 (chapter 2).

3-D Water-Soluble Reversible Neodymium(III) and Lanthanum(III) Coordination Polymers.
T. Vermonden, W. M. de Vos, A. T. M. Marcelis, E. J. R. Sudhölter
Eur. J. Inorg. Chem. **2004**, 2847-2852 (chapter 3).

Linear Rheology of Water-Soluble Reversible Neodymium(III) Coordination Polymers.
T. Vermonden, M. J. van Steenbergen, N. A. M. Besseling, A. T. M. Marcelis, W. E. Hennink, E. J. R. Sudhölter, M. A. Cohen Stuart
J. Am. Chem. Soc. **2004**, *126*, 15802-15808 (chapter 4)

This research project was financially supported by the Dutch Polymer Institute.